



Power Electronics to Improve the Performance of Modern Power Systems: Case Study on Partially Rated SST

Final Project Report

T-58

Power Systems Engineering Research Center
*Empowering Minds to Engineer
the Future Electric Energy System*



Power Electronics to Improve the Performance of Modern Power Systems: Case Study on Partially Rated SST

Final Project Report

Project Team

Ali Mehrizi-Sani, Project Leader
Washington State University

Gerald Heydt
Arizona State University

Maryam Saeedifard
Georgia Institute of Technology

Graduate Students

Armin Teymouri
Washington State University

Qichen Yang
Georgia Institute of Technology

PSERC Publication 18-07

September 2018

For information about this project, contact:

Ali Mehrizi-Sani
Washington State University
School of Electrical Engineering and Computer Science
EME 35 – 355 NE Spokane St
Pullman, WA 99164
Tel: +1 (509) 335-6249
Fax: +1 (509) 335-3818
Email: mehrizi@wsu.edu

Power Systems Engineering Research Center

The Power Systems Engineering Research Center (PSERC) is a multi-university Center conducting research on challenges facing the electric power industry and educating the next generation of power engineers. More information about PSERC can be found at the Center's website: <http://www.pserc.org>.

For additional information, contact:

Power Systems Engineering Research Center
Arizona State University
527 Engineering Research Center
Tempe, Arizona 85287-5706
Phone: 480-965-1643
Fax: 480-727-2052

Notice Concerning Copyright Material

PSERC members are given permission to copy without fee all or part of this publication for internal use if appropriate attribution is given to this document as the source material. This report is available for downloading from the PSERC website.

© 2018 Washington State University. All rights reserved.

Acknowledgements

We express our appreciation for the support provided by PSERC industry members: Shaun Mann (Tri-State), Jay Caspary (SPP), Harvey Scribner (SPP), Joe Schatz (Southern Co), Reynaldo Nuqui (ABB), Bob Malek (AEP), Eduard Muljadi (NREL), Sudipta Chakraborty (NREL), Vahan Gevorgian (NREL), Daniel Arjona (Idaho Power), Orlando Ciniglio (Idaho Power), Giuseppe Stanciulescu (BC Hydro), Ram Adapa (EPRI), Naim Logic (Salt River Project), Xiaoming Feng (ABB), Kathleen O’brein (GE), Miaolei Shao (GE), Dale Osborn (MISO), Alan Ettlinger (NYPA), Saman Babaei (NYPA), Neil Kirby (GE), Deepak Konka (GE), Terry Oliver (BPA), Ziyuan Zhang (BPA), Andres Johnson (BPA), Chetan Mishra (Dominion Virginia Power), Matt Gardner (Dominian Virginia Power), Venkat Kolluri (Entergy), and Alan Engelman (Exelon).

Special thanks are also due to Harvey Scribner (SPP) for his comments on improving this report.

Executive Summary

As the power industry updates distribution and transmission assets as needed, it is prudent to consider the alternatives and new applications that may become available due to advances in the technology and material science. Among these technologies is power electronics. Power electronics have been in the technical vocabulary for a few decades and can offer significant advantages in stability, speed, and power flow control. However, their applications are still limited due to factors such as limited ratings, relatively high cost, high losses, potential problems in meeting basic impulse level requirements, and lack of operational experience. In this project, we discuss a two-pronged research effort: (i) an explorative study on the requirements of power electronics (e.g., ratings, basic impulse level, lifetime, and maintenance) and necessary improvements in this technology to enable its use in power systems and (ii) an application design study of partially rated power electronics-enabled transformers for load tap changer applications. The goal of this project is not to apply power electronics to every task in power engineering; rather, it is to: (i) identify which tasks and applications (and to what extent) can benefit from power electronic solutions and (ii) explore the technologies that would accomplish the identified task.

Part I: Study on the Available Technologies and Identification of their Advantages and Shortcomings

Power electronics can offer significant advantages in stability, speed, and power flow control. However, their applications are still limited due to factors such as limited ratings, relatively high cost, high losses, potential problems in meeting basic impulse level requirements, and lack of operational experience. Even with these challenges, in recent years, the industry has commissioned several new power electronics-based projects. A recent example is the modular multilevel converter (MMC) high-voltage DC (HVDC) 200 kV, 400 MW underwater line completed by Siemens and the California ISO as the Trans Bay Cable project in San Francisco in Nov. 2010. Several other new HVDC lines and flexible AC transmission system (FACTS) installations are also underway. In recent years, power electronics devices have received significant renewed attention as an enabling technology due to several breakthroughs with the promise of wide bandgap (WBG) devices, especially high-voltage Silicon carbide (SiC) switches. These advances have the potential to improve the efficiency, power density, and thermal management of power electronics devices. Additionally, these advances can make future power electronics superior to their legacy power system counterparts in certain applications. This part provides a compendium of required/recommended specifications, characteristics, and necessary improvements for power electronics devices and a survey of available technologies, broken down by different power system applications. Emerging technologies such as wide bandgap devices as well as niche and unconventional applications such as mobile and truck-mounted FACTS devices are also studied. It is discussed that while power electronics are limited in their blocking voltage, switching frequency, efficiency, and workforce and cost-effectiveness, there are applications for which power electronics are the only (or the most dominant) application. These applications include integration of renewables and power routing. Several areas for further research, including operation of an all-converter power system as well as use of solid-state transformers (SST) for power transfer limit improvement are also discussed.

Part II: The Role of Basic Impulse Insulation Level in the Application of Power Electronics at the Distribution Level

Basic Impulse Insulation Level (BIL), also termed Lightning Impulse Withstand Level (LIWL) is discussed in this part. The application area is in power electronic controls and devices in power distribution systems (e.g., 15 kV class). The topical coverage includes the following:

- A literature survey of this topic
- Identification of the BIL requirements and the connection with the applicable codes and standards
- Methods to attain the BIL requirements
- A discussion of safety.

Part III: Partially-Rated Solid-State Transformers Based on the Modular Multilevel Converter

The increasing penetration rate of dynamic sources such as renewable energy resources together with the emergence of new dynamic loads such as electric vehicles, necessitate more flexible, efficient, and economical operation of the power grid. To maximize utilization of the power system infrastructure in an efficient and economical way, significant efforts have been made to actively control real and reactive power flows, compensate voltage sag/swell, and filter current harmonics based on power electronics. To this end, among the proposed power electronics-based solutions, solid-state transformer (SST) has become one of the emerging technologies. However, the application/deployment of SST has been limited due to high cost and reliability issues. To combine the flexibility provided by the power electronics and reliability of the conventional magnetic transformer, an alternative method, i.e., partially-rated solid-state transformer (PSST), has emerged, in which a power electronics converter is integrated into the conventional magnetic transformer. Even if the power electronics part of the PSST fails, the conventional magnetic transformer is still able to transfer power, thereby preserving the reliability aspect. Furthermore, since the majority portion of power in a PSST is still transferred by the main magnetic part, the power electronics part does not need to be fully rated. The power electronics part of a PSST can be realized by a DC-AC or an AC-AC converter. Since the AC-AC converter, including the back-to-back connected AC-DC-AC converter, has two AC ports, it is capable of simultaneously adjusting the voltage and current of the grid. Therefore, an AC-AC converter-based PSST can provide most functionalities including power flow control, voltage sag/swell compensation, and current harmonics filtering. In this report, two PSSTs based on the emerging Modular Multilevel Converter (MMC) topology along with their supporting control strategies are proposed and investigated for power flow control and active power filtering. The proposed PSSTs borrow the features of the MMC and combine them with new control strategies to enable the MMC-based PSSTs. Simulation studies in the PSCAD/EMTDC software environment are carried out to validate the performance and effectiveness of the proposed MMC-based PSSTs and their supporting control methods.

Project Publications:

- [1] Q. Yang and M. Saeedifard, “An AC-AC Modular Multilevel Converter-based Partially-Rated Solid-State Transformer for Power Flow Control,” *IEEE IECON*, 2018.
- [2] Q. Yang and M. Saeedifard, “An AC-AC Modular Multilevel Converter-based Partially-Rated Solid-State Transformer,” Submitted to *IEEE Journal of Emerging and Selected Topics in Power Electronics* (under review), 2018.
- [3] A. Teymouri, A. Mehrizi-Sani, and C.-C. Liu, “Cyber security risk assessment of solar PV units with reactive power capability,” in *IEEE Ind. Electron. Soc. Annu. Conf. (IECON)*, Washington, DC, Oct. 2018.

Student Theses:

- [1] Armin Teymouri, *Power electronics converters for renewables applications under sensor malfunctions*, PhD, Washington State University, May 2020 (expected).
- [2] Qichen Yang, *Control of the DC-AC and AC-AC Modular Multilevel Converters under Abnormal Conditions*, PhD, Georgia Institute of Technology, December 2018 (expected).

Part I

Study on the Available Technologies and Identification of Their Advantages and Shortcomings

Ali Mehrizi-Sani
Armin Teymouri, Graduate Student

Washington State University

For information about this project, contact:

Ali Mehrizi-Sani
Washington State University
School of Electrical Engineering and Computer Science
EME 35 – 355 NE Spokane St
Pullman, WA 99164
Tel: +1 (509) 335-6249
Fax: +1 (509) 335-3818
Email: mehrizi@wsu.edu

Power Systems Engineering Research Center

The Power Systems Engineering Research Center (PSERC) is a multi-university Center conducting research on challenges facing the electric power industry and educating the next generation of power engineers. More information about PSERC can be found at the Center's website: <http://www.pserc.org>.

For additional information, contact:

Power Systems Engineering Research Center
Arizona State University
527 Engineering Research Center
Tempe, Arizona 85287-5706
Phone: 480-965-1643
Fax: 480-727-2052

Notice Concerning Copyright Material

PSERC members are given permission to copy without fee all or part of this publication for internal use if appropriate attribution is given to this document as the source material. This report is available for downloading from the PSERC website.

© 2018 Washington State University. All rights reserved

Table of Contents

1. Introduction.....	1
2. Power Electronics Applications.....	2
2.1 Wind Energy Systems	2
2.1.1 Wind power resources.....	2
2.1.2 Power electronics topologies for wind energy systems	3
2.1.3 Penetration of wind turbine sources in the network.....	4
2.1.4 Challenges and issues in wind turbine systems with power electronics	6
2.2 Solar Systems	9
2.2.1 Different Topologies of Solar Photovoltaic Systems.....	10
2.2.2 Benefits and challenges of PV power electronics	11
2.3 Solid-State Transformers.....	12
2.3.1 Basics	12
2.3.2 Variability of prices	13
2.3.3 SST realization and application challenges.....	14
2.4 Solid-State Circuit Breakers	21
2.4.1 Solid-state switch topologies	22
2.4.2 Cost of different topologies.....	23
2.4.3 Reliability of different topologies	23
2.4.4 Challenges and advantages of solid state circuit breaker technology	24
2.5 Storage.....	25
2.6 Flexible AC Transmission Systems (FACTS)	26
2.6.1 Topologies.....	26
2.6.2 Planning Perspective	27
2.7 High-Voltage DC (HVDC) Transmission	28
2.8 Microgrids	28
2.8.1 DC Microgrids	29
2.8.2 HFAC Microgrids	29
2.8.3 LFAC Microgrids.....	30
2.8.4 Hybrid Microgrids.....	30
2.8.5 Electronically coupled DER units	31
3. Technology Trends	32

3.1	Wide Band Gap (WBG) Semiconductors.....	32
3.1.2	SiC.....	33
3.1.3	GaN	34
3.1.5	Applications	35
3.2	Multilevel Converters	36
4.	New and Commercial Applications	38
4.1	NR Electric DC De-icer.....	38
4.2	Siemens SVC Plus.....	39
4.3	Mitsubishi HVDC Diamond.....	41
4.4	ABB DC Circuit Breaker.....	42
4.5	ABB Plug and Play Microgrid	42
4.6	Siemens Mobile STATCOM.....	43
5.	Conclusions and Future Trends	45
5.1	Notion of Inertia with Converter-Rich Power Systems.....	46
5.2	Solid-State Transformers for Power Transfer Limit Improvement	47
	References	48

List of Figures

Fig. 1 Worldwide wind power capacity [7].	2
Fig. 2. Market shares between different wind power manufacturers [8].	3
Fig. 3. Trends of wind turbine sizes from 1980 to 2018 [7].	3
Fig. 4. Doubly-fed induction generators for wind applications [7].	4
Fig. 5. Wind turbine system with fully rated power conversion system [7].	4
Fig. 6. Available power versus frequency [11].	5
Fig. 7. Real and reactive powers curves [12].	5
Fig. 8. LCOE of different sources of energy [14].	7
Fig. 9. Multidisciplinary approaches for reliability analysis of wind systems [7].	7
Fig. 10. Cascaded converters equipped with medium frequency transformers [7].	8
Fig. 11. Material cost of three consecutive generations of PV-inverters, solely silicon power semiconductor designs [18].	10
Fig. 12. PV topology without (left) and with (right) transformer and the coupling capacitor leading to leakage currents (marked in red) [18].	10
Fig. 13. Topologies of single string photovoltaic systems (top), photovoltaic systems with DC-DC converters (middle), and photovoltaic systems with ac micro-inverters (bottom) [20].	11
Fig. 14. A multi-string photovoltaic installation [20].	11
Fig. 15. I-V curves of different PV topologies [21].	12
Fig. 16. Medium frequency (MF) transformers with choppers on sides.	13
Fig. 17. Power losses of different transformers.	13
Fig. 18. Historical Copper and Steel price from 2000 to 2013.	14
Fig. 19. Power conversion partitioning.	15
Fig. 20. Medium voltage modularity.	15
Fig. 21. Partitioning of medium voltage.	16
Fig. 22. Classification of SST structures.	16
Fig. 23. Current semiconductor technology limits.	17
Fig. 24. H-bridge converter cells.	18
Fig. 25. Switching losses comparison.	18
Fig. 26. Protection schemes of SST and conventional transformers [35].	20
Fig. 27. Medium voltage solid state transformer (a) weight breakdown (b) cost breakdown [36].	21
Fig. 28. SST technology hype cycle.	21

Fig. 29. Solid state circuit breaker topologies.....	23
Fig. 30. Rectifier solutions for solid state circuit breakers.	23
Fig. 31. An example of an electronic circuit breaker [3].	24
Fig. 32. Annual worldwide ESS capacity [45].	25
Fig. 33. Implementations of FACTS devices.....	26
Fig. 34. SVC and STATCOM [60].	26
Fig. 35. TCSC and SSSC [60].	27
Fig. 36. TCPR and UPFC [60].	27
Fig. 37. A microgrid based on power electronic devices [68].	28
Fig. 38. Different categories of microgrids [68].	29
Fig. 39. An LVDC microgrid [68].	29
Fig. 40. A high frequency ac microgrid based on power electronics devices [72].	30
Fig. 41. A low frequency ac microgrid based on power electronics devices [68].	30
Fig. 42. Summary of Si, SiC, and GaN properties [75].	33
Fig. 43. On-resistance of different Si, SiC, GaN, unipolar and bipolar devices with respect to the blocking voltage [78].	34
Fig. 44. SiC high voltage switches voltage-frequency capability [88].	35
Fig. 45 Single phase converters and output waveforms (a) two level, (b) three level, (c) nine level [93].	36
Fig. 46 Multilevel converter classification [93].	37
Fig. 47 Melting configuration with DC de-icer [103].	38
Fig. 48 Fixed DC de-icer topology [103].	39
Fig. 49 Relocatable DC de-icer topology [103].	39
Fig. 50 Space requirement of an SVC plus compared with a classic SVC [104].	40
Fig. 51 Harmonics content of SVC plus versus SVC classic [104].	41
Fig. 52 A VSC-based HVDC configuration [104].	41
Fig. 53 The structure of Mitsubishi HVDC-Diamond [104].	42
Fig. 54 ABB DC circuit breaker footprint compared to other technologies [105].	42
Fig. 55 ABB modular microgrid [106].	43
Fig. 56 Details on ABB Plug and Play microgrid [106].	43
Fig. 57 The Mobile STATCOM by Siemens [107].	44
Figure 58 Example FACTS devices for power routing and control (from EPRI).	46

Figure 59. (a) A system with an unlimited grid-forming unit; (b) a system with a limited grid-forming unit. In both systems, the load at bus 6 increases by 15 MW at $t = 1$ s and the load at bus 5 increases by 80 MW at $t = 3$ s. 47

List of Tables

Table 1. Comparison between different features of a conventional generation unit and wind turbine systems [7]	6
Table 2 Semiconductors for wind applications [7].	9
Table 3 Performance characteristics overview [36].	20
Table 4. Reliability of the topologies [40].	24
Table 5 Major ESS manufacturers and their solutions [53].	25
Table 6 Physical properties of various semiconductors for power devices [76].	33
Table 7 Increased power transfer in the IEEE 9-bus system	47

Nomenclature

Abbreviations

<i>AC</i>	Alternating Current
<i>CAGR</i>	Compounded Annual Growth Rate
<i>DC</i>	Direct Current
<i>DER</i>	Distributed Energy Resource
<i>DFIG</i>	Doubly Fed Induction Generator
<i>DG</i>	Distributed Generation
<i>D-STATCOM</i>	Dynamic Static Compensator
<i>EMI</i>	Electro Magnetic Interference
<i>EPRI</i>	Electric Power Research Institute
<i>ESS</i>	Energy Storage System
<i>FACTS</i>	Flexible Alternating Current Transmission Systems
<i>FET</i>	Field Effect Transistor
<i>FIT</i>	Failure In Time
<i>GCT</i>	Gate Commutated Thyristor
<i>GTO</i>	Gate Turn-off Thyristor
<i>HEMT</i>	High Electron Mobility Transistor
<i>HV</i>	High Voltage
<i>HVDC</i>	High Voltage Direct Current
<i>IEEE</i>	Institute of Electrical and Electronics Engineers
<i>IGBT</i>	Isolated Gate Bipolar Transistor
<i>IGCT</i>	Integrated Gate Commutated Thyristor
<i>ISOP</i>	Input Series Output Parallel
<i>LCC</i>	Line Commutated Converter
<i>LCOE</i>	Levelized Cost of Energy
<i>LED</i>	Light Emitting Diode
<i>LF</i>	Low Frequency
<i>LFT</i>	Low Frequency Transformer
<i>LV</i>	Low Voltage

<i>MTBF</i>	Mean Time Before Failure
<i>MF</i>	Medium Frequency
<i>MISFET</i>	Metal Insulator Semiconductor Field Effect Transistor
<i>MOSFET</i>	Metal-Oxide Semiconductor Field Effect Transistor
<i>MV</i>	Medium Voltage
<i>MPPT</i>	Maximum Power Point Tracking
<i>NREL</i>	National Renewable Energy Laboratory
<i>O&M</i>	Operation and Maintenance
<i>PV</i>	Photovoltaic
<i>R&D</i>	Research and Development
<i>SG</i>	Synchronous Generator
<i>SSCB</i>	Solid State Circuit Breaker
<i>SSSC</i>	Static Synchronous Series Compensator
<i>SST</i>	Solid State Transformer
<i>STATCOM</i>	Static Compensator
<i>SVC</i>	Static Var Compensator
<i>TCPR</i>	Thyristor Controlled Power Controller
<i>TCSC</i>	Thyristor Controlled Series Capacitor
<i>UPFC</i>	Unified Power Flow Controller
<i>VSC</i>	Voltage Source Converter
<i>WBG</i>	Wide Band Gap

1. Introduction

Power electronics plays an important role in high voltage DC (HVDC), flexible AC transmission systems (FACTS), drive systems, and distribution system integration of renewables. Specifically, in transmission and distribution grids, there has been a growth in the number of power electronic converters that can control the power flow (e.g., FACTS devices), improve system stability (e.g., STATCOM (STATic COMpensator)), and increase power quality (e.g., D-STATCOM and active filters). Although power electronics devices can provide several advantages and enable new applications, their penetration level in the grid is still low. This low proliferation level stems from generally high cost, concerns about reliability, lack of expertise and experience, and low ratings. Simultaneously, modern grid requirements and priorities, such as integration of renewables, higher flexibility requirements, and power quality metrics can benefit significantly from the availability of power electronics devices.

This report aims at (i) investigating different applications of power electronic devices in power system, (ii) analyzing their benefits, shortcomings, and challenges, and (iii) studying the application-specific requirements for these devices.

This report is structured as follows. Section 2 investigates different applications of power electronics systems, e.g., solar photovoltaic (PV) systems, wind power system, solid-state transformers, and circuit breakers. It also studies energy storage systems, FACTS devices, and microgrids. Section 3 investigates the technology. Section 4 surveys several commercial power electronic solutions and analyzes their applications and features. Section 5 provides concluding remarks.

2. Power Electronics Applications

2.1 Wind Energy Systems

Among different renewable energy resources (except for hydro), wind power has the highest capacity. In 2016, 5.5% of the electrical energy in the United States was supplied by wind generators. The rating of a single wind turbine was merely a few tens of kilowatts in the 80s, while now most common wind turbines provide about 2 MW of power. This change in power rating was accompanied with a change in the topology and integration of power electronics in wind systems [1]-[4]. In the technology used in 1980s, power electronic devices were merely used as soft starters to connect the squirrel-cage induction generators to the power grid (Type I) [1]. Power electronics was used to control the rotor resistance of wound-rotor induction generators during the 90s (Type II) [2]. In 2000, more sophisticated back-to-back power converters in the rotor circuit were introduced that provide partial speed control (30%) (Type III). Type IV converters provide complete decoupling between the mechanical and electrical frequency by utilizing a back-to-back power electronics converters in the stator circuit. This converter can also provide ancillary services such reactive power compensation [5], [6].

2.1.1 Wind power resources

Fig. 1 shows the worldwide wind power generation capacity from 1999 to 2020 [7]. According to [8], the cumulative global wind power generation is expected to reach 760 GW in 2020. The growth of wind power generation is at a higher rate than any other renewable source. As an example, Denmark has over 30% of its power generation from wind with the goal of complete independence from fossil fuels by 2050 [9].



Fig. 1 Worldwide wind power capacity [7].

Fig. 2 compares the global market shares between different wind turbine manufacturers around the world.

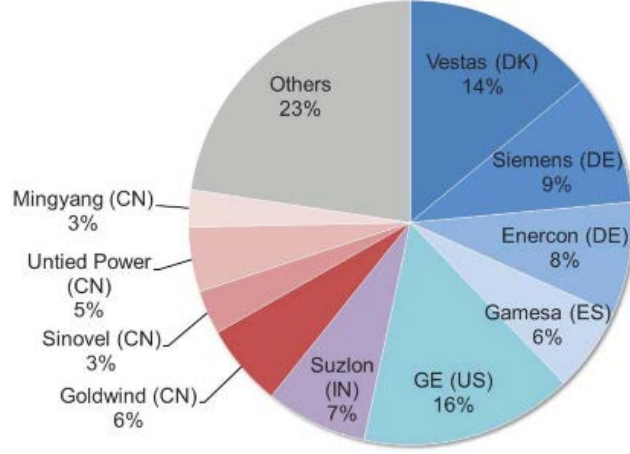


Fig. 2. Market shares between different wind power manufacturers [8].

In addition to the fast increase in the installed wind capacity, the power generation capacity of the individual wind turbines is also increasing, causing a decline in the price of the electricity generated by wind turbines. The trends of different turbine sizes over a four-decade time frame from 1980 to 2018 is shown in Fig. 3. This figure also illustrates the rating of power electronics in wind turbines and its development trends [10].

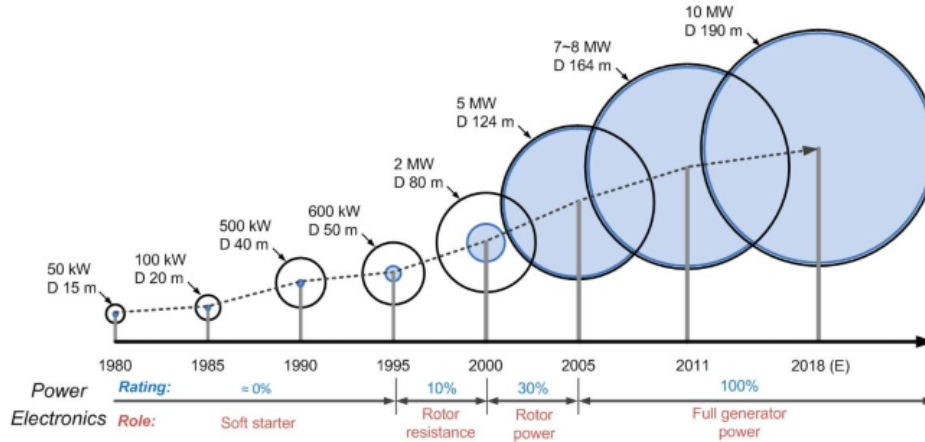


Fig. 3. Trends of wind turbine sizes from 1980 to 2018 [7].

2.1.2 Power electronics topologies for wind energy systems

Generator types, power electronics, speed control systems, and aerodynamic power limits are the degrees of freedom in designing wind turbines [3]. Today, doubly-fed induction generators (DFIG) and synchronous generator (SG)-based wind turbines with partial or fully rated power electronics (Type III and Type IV, respectively) are dominant, with Type IV eventually taking over.

A. DFIG with partially rated power conversion systems (Type III)

Fig. 4 shows the most commonly installed wind power system topology today that includes a DFIG connected to a power electronic conversion system. In this configuration, the stator windings are connected directly to the while the rotor is connected via a power electronics converter. This

topology can have a variable speed range (within 30% of rated speed). However, slip rings and difficulties in control of power during faults are the challenges with this topology.

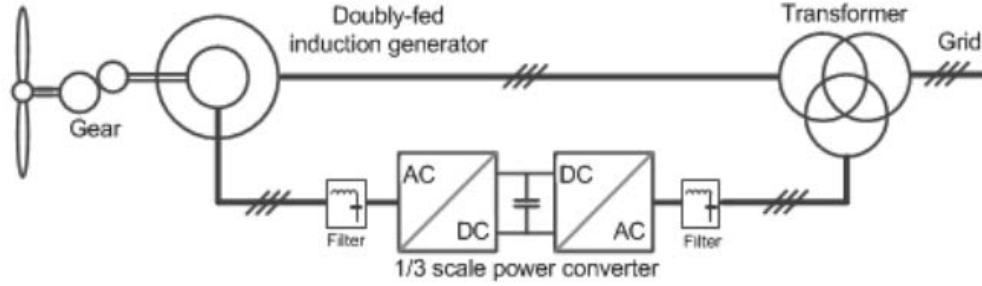


Fig. 4. Doubly-fed induction generators for wind applications [7].

B. A/SG with fully-rated power electronics converter (Type IV)

Fig. 5 shows the Type IV wind power system. In this system, the stator is connected to the grid via a fully rated power electronics converter. Therefore, the generator speed can be fully controlled to ensure maximum power extraction. Slip ring elimination, simpler gearbox, complete power and frequency control, and superior grid support capability are the benefits of this topology over the Type III topology. However, higher costs of power electronic devices, higher ratings, and higher losses in power components are the disadvantages of this configuration.

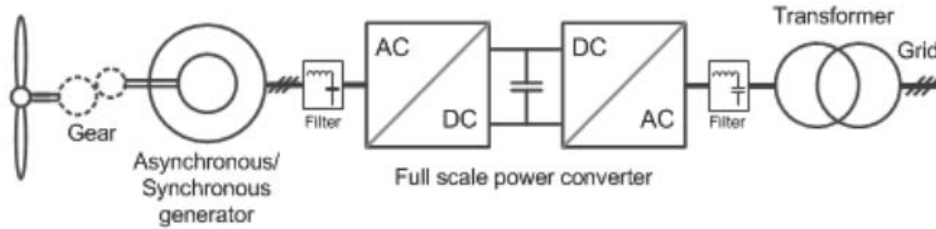


Fig. 5. Wind turbine system with fully rated power conversion system [7].

2.1.3 Penetration of wind turbine sources in the network

The intermittent and variable nature of wind power generation is perhaps the most important issue in the integration of wind sources to the power system. Different countries have instituted appropriate grid codes to ensure stable and appropriate interactions between wind turbines and other dynamical devices in the power system, including providing voltage/frequency regulation with reactive power support. Fig. 6 shows an example of frequency support through real power control of the wind turbine—the real power output is adjusted when the frequency passes 49.85 or 50.15 Hz (in a 50 Hz system). Wind turbines are also expected to compensate for the reactive power in some grid codes. An example of the reactive power support with respect to real power outputs is shown in Fig. 7.

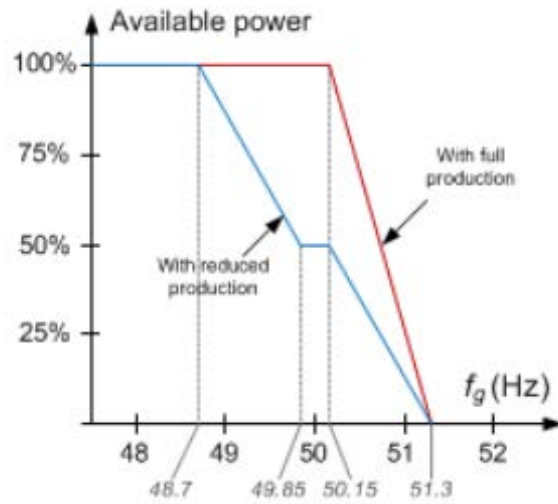


Fig. 6. Available real power versus frequency [11].

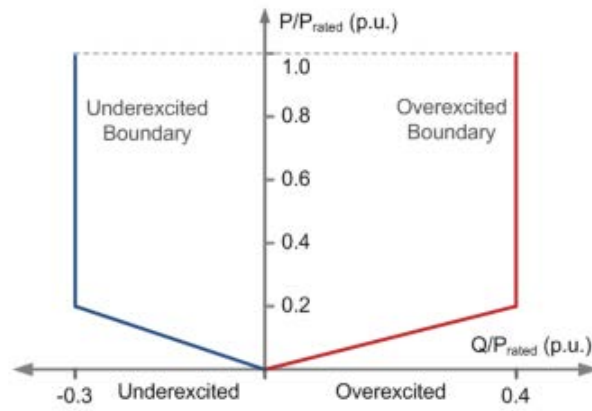


Fig. 7. Real and reactive powers curves [12].

Table 1 compares the characteristics of conventional power plants, wind turbine systems without power electronic converters, and wind turbine generation systems with power electronics converters [7].

Table 1. Comparison between different features of a conventional generation unit and wind turbine systems [7].

Grid integration Features	Conventional power plant	WTG in the past (without/few PEC)	WTG nowadays/future (With PEC)
Active power control	+	0	+
Reactive power control	+	0 / -	++
Short circuit capability	++	+	++
Voltage backup	++	-	+
Power output Inertia	++	-	+
Frequency control	++	-	++
Black start capability	+	-	+

++ : highest performance level, - : lowest performance level.

2.1.4 Challenges and issues in wind turbine systems with power electronics

Despite the potential benefits of power electronic devices, there are several challenges caused by these devices as follows.

A. Lower Levelized Cost of Energy

To compare the cost of different sources of energy, levelized cost of energy (LCOE) is utilized [13]. LCOE captures the overall cost of a system during lifetime and includes initial investment, developing cost, capital investment, O&M cost, and fuel cost [7]. LCOE is defined as

$$LCOE = \frac{C_{Dev} + C_{Cap} + C_{O\&M}}{E_{Annual}} \quad (1)$$

Fig. 8 compares the LCOE of different renewable resources connected at the high voltage transmission level, in the U.S. The capital cost accounts for the largest portion of the costs and is expected to remain so within the next decade [7]. On-shore wind power is the most economically reasonable renewable source compared to other promising renewable resources. Power electronic devices used in wind turbine systems make up a dominant part of the system costs. Choosing the right power electronic topology depends on the technology of the wind turbine systems. To increase power rating of the wind energy system, higher rated power electronics, better cooling systems, and higher grade insulation material are required. Remote locations of the wind power farms increases the costs of the system. In these conditions, power electronic devices have to be designed to be highly reliable, modular, and redundant.

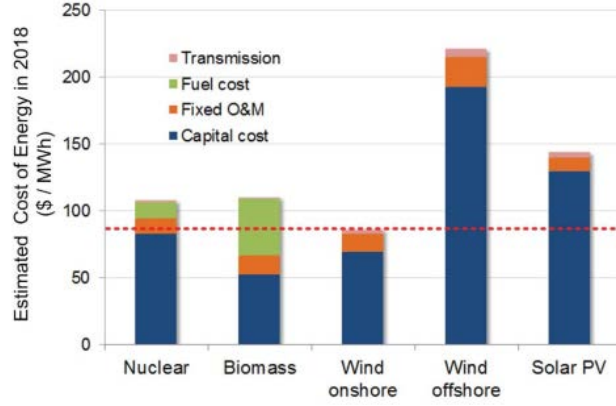


Fig. 8. LCOE of different sources of energy [14].

B. Increased reliability

The global increase in wind power generation and the increase in the individual wind turbine sizes cause the failure of these systems to have a significant impact on the power system, e.g., stability issues and cost of maintenance especially in remote areas. Furthermore, the outage of wind power generation decreases the annual generated energy of these units and results in a higher LCOE. According to [15], among various components of wind turbine systems, power electronic accounts for the highest failure rates. Thus, an increase in the reliability of power electronic converters causes a drop in wind power LCOE. The reliability of power electronic devices has been a subject of research for decades. Fig. 9 shows different possible solutions for reliability analysis and improvement in power electronic devices. Multi-disciplinary approaches are used to increase the reliability of power electronic devices. These approaches involve stress analysis, probability and statistics, monitoring and control, and strength modeling of power electronic converters [16].

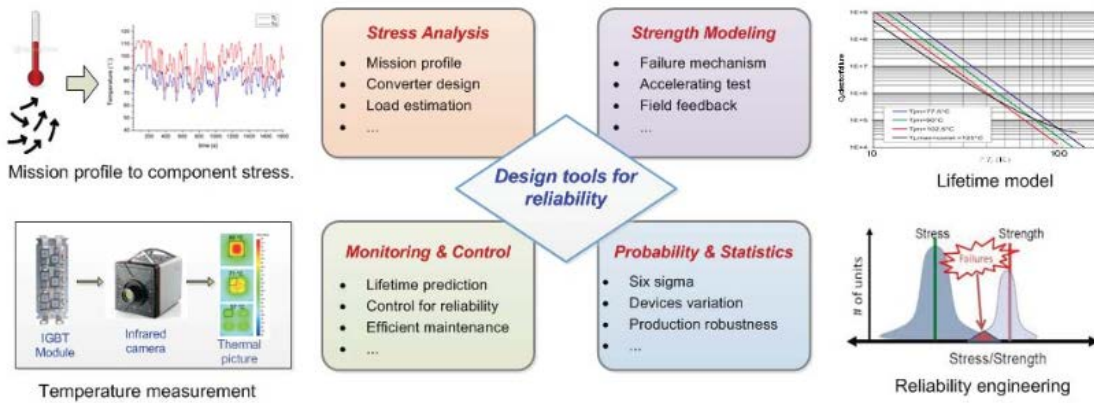


Fig. 9. Multidisciplinary approaches for reliability analysis of wind systems [7].

Strength modeling is a discipline that tries to identify, model, and test the failure mechanisms in power electronic devices to find connections between the stress and failure in a system for critical components. Monitoring and control focuses on lifetime monitoring, temperature control, and intelligent maintenance [17]. Probability and statistics attempts to estimate the failure rate of power electronic devices and the wind turbine system within its lifetime.

C. Advanced grid integration features

Protection and islanded system operation of wind power systems needs them to operate differently from the traditional centralized. Thus, the protection schemes of wind power units should be changed to a more distributed scheme able to make the islanded operation of wind power stations possible. Wind turbines today rely on power electronic devices to convert the power at low voltage levels. However, to comply with the increasing wind power integration, it is needed to introduce more advanced technologies that can operate at higher voltages (1-10 kV). Fig. 10 shows a topology as an H-bridge converter with medium-frequency DC-DC transformers with a reduced size as a result of their higher frequency. Cascaded converters allow wind turbines to have a direct connection to the network. This topology is based on the topologies used in traction applications and leads to a higher power quality and redundancy without any filters.

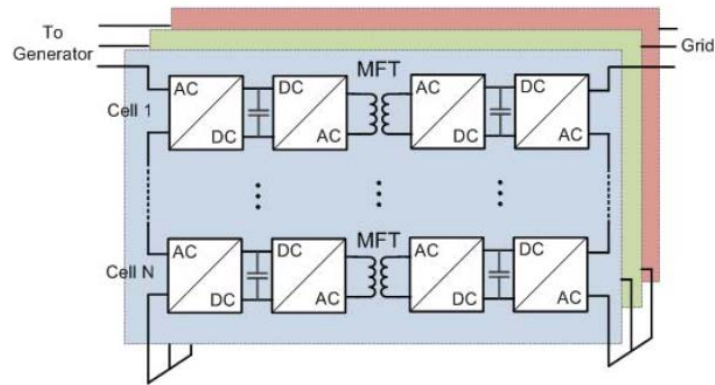


Fig. 10. Cascaded converters equipped with medium frequency transformers [7].

Semiconductor devices are important in reducing the cost of wind turbine systems. They increase the system reliability, efficiency, and modularity. There are four types of semiconductors used in wind power applications that are modular insulated-gate bipolar transistor (IGBT), press-pack modular IGBT, press-pack packaged IGCT, and SiC modules. Different features of these devices are shown in Table 2.

Table 2. Semiconductors for wind applications [7].

	<i>IGBT module</i>	<i>IGBT Press-pack</i>	<i>IGCT Press-pack</i>	<i>SiC MOSFET module</i>
Power Density	Low	High	High	Low
Reliability	Moderate	High	High	Unknown
Cost	Moderate	High	High	High
Failure mode	Open circuit	Short circuit	Short circuit	Open circuit
Easy maintenance	+	-	-	+
Insulation of heat sink	+	-	-	+
Snubber requirement	-	-	+	-
Thermal resistance	Large	Small	Small	Moderate
Switching loss	Low	Moderate	Moderate	Low
Conduction loss	Moderate	Moderate	Moderate	Large
Gate driver	Moderate	Moderate	Large	Small
Major manufacturers	Infineon, Semikron, Mitsubishi, ABB, Fuji	Westcode, ABB	ABB	Cree, Rohm, Mitsubishi
Medium voltage ratings	3.3 kV / 4.5 kV / 6.5 kV	2.5 kV / 4.5 kV	4.5 kV / 6.5 kV / 10 kV	1.2 kV / 10 kV
Max. current ratings	1.5 kV / 1.2 kA / 750 A	2.3 kA / 2.4 kA	3.6 kA / 3.8 kA / 2 kA	180 A / 120 A

2.2 Solar Systems

There are several advantages for using PV systems over other sources of energy. However, a main drawback in the development of PV units is their high costs. According to [18], in 1991, the PV electricity cost was 120 cents/kWh while this number reached 14 cents/kWh in 2014 (and 5 cents in 2017). This report shows that a great part of this reduction, 41 cents/kWh, was because of the increased efficiency and reduced losses. The developments in power electronic systems made up for 30 cents/kWh reductions that was a result of increased reliability, efficiency, failure management, and communication capability. The worldwide PV generating capacity was 302 GW by the end of 2016 [19]. There were several reasons for the cost reductions in PV inverters over the years:

- Increase in inverter rated power.
- Reduction of component costs as a result of higher number of components.
- Reduced production time due to automation.

Fig. 11 shows a comparison between the costs of 5 main components of PV inverters for three successive generations. Components such as safety functions and communication have experienced a gradual reduction in costs while housing and inductors had a rapid cost reduction throughout the three generations. However, the cost of semiconductor devices are increased.

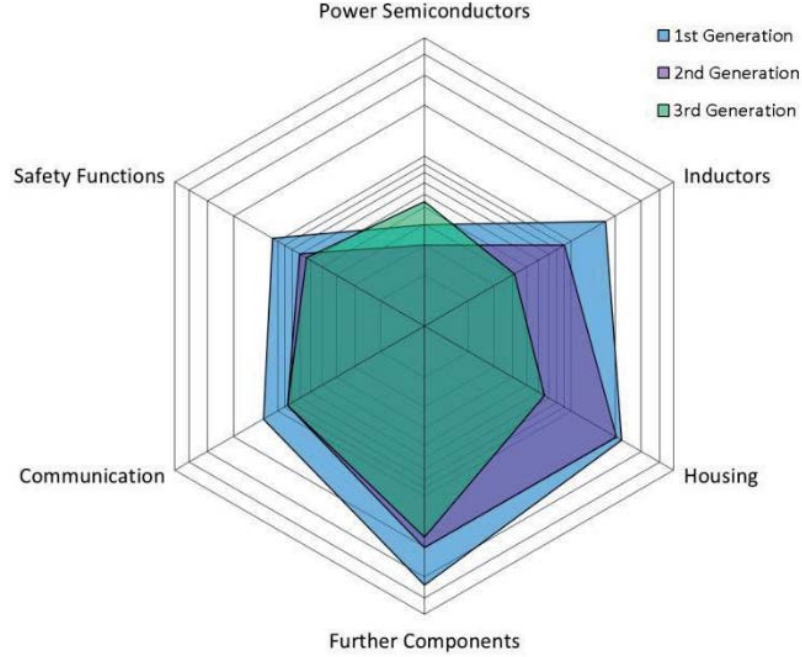


Fig. 11. Material cost of three consecutive generations of PV-inverters, solely silicon power semiconductor designs [18].

2.2.1 Different Topologies of Solar Photovoltaic Systems

Many different PV inverter topologies are proposed by researchers and manufacturers. These topologies aim at reducing the PV generation costs and increasing the efficiency. The first introduced concepts for PV inverters included transformers for safety and galvanic isolation. These transformers were later replaced by reliable power electronic solutions that caused an increased efficiency and a decrease in size, weight, and cost. PV topologies with and without transformers are shown in Fig. 12. Transformer-less topologies are categorized into three main groups:

1. Topologies with grounded PV generator,
2. Topologies with stationary potential against ground,
3. Topologies with non-stationary potential against ground with grid frequency.

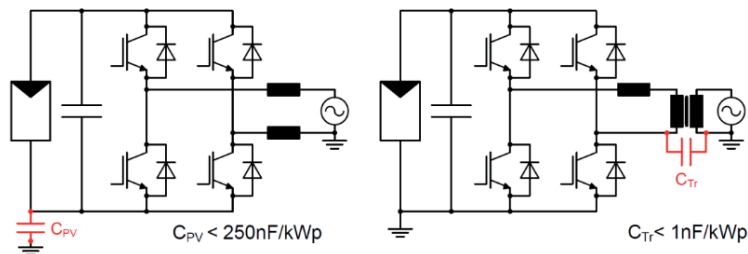


Fig. 12. PV topology without (left) and with (right) transformer and the coupling capacitor leading to leakage currents (marked in red) [18].

To decrease the effects of module mismatch or partial shading in PV units, power electronic devices used in string or modular topologies are utilized. The use of string inverters instead of the centralized increases the number of modules doing MPPT independently and causes the system to avoid power generation reduction caused by a module mismatch.

Micro-inverters, for which each panel is individually connected to the grid, can avoid power mismatch issues between different modules resulting in an improved performance. Different topologies of PV strings are shown in Fig. 13. In larger PV installations, power mismatch is not addressed in panel levels. A possible way is to use DC-DC converters in the strings that can be placed within string boxes and followed by a centralized inverter (Fig. 14).

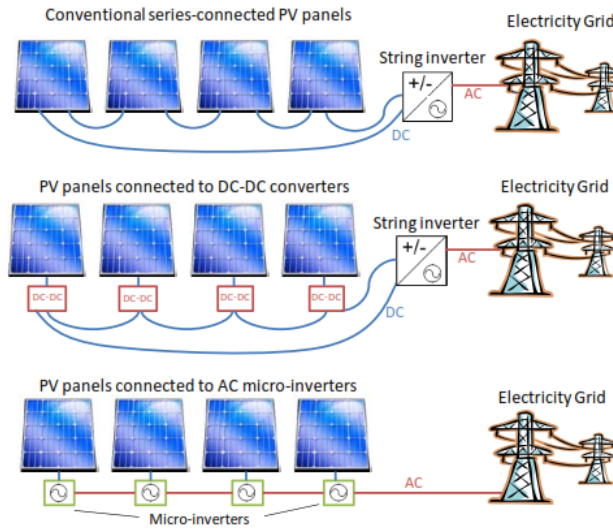


Fig. 13. Topologies of single string photovoltaic systems (top), photovoltaic systems with DC-DC converters (middle), and photovoltaic systems with ac micro-inverters (bottom) [20].

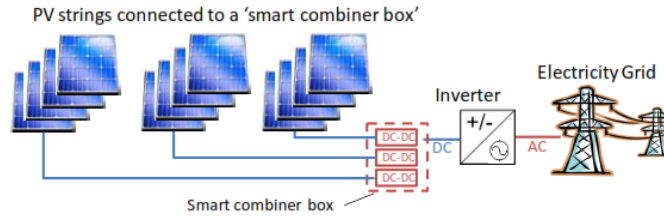


Fig. 14. A multi-string photovoltaic installation [20].

2.2.2 Benefits and challenges of PV power electronics

Fig. 15 compares the I-V curves of different types of PV systems. The lost power in conventional units is the highest but they are the least complex.

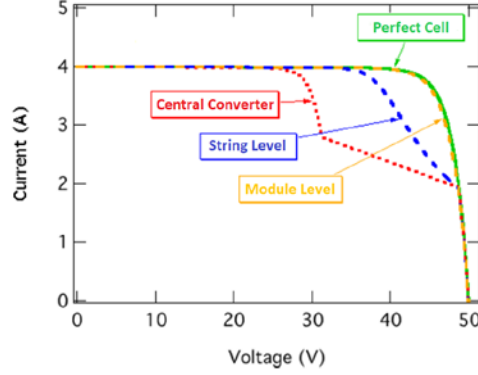


Fig. 15. I-V curves of different PV topologies [21].

PV manufacturers may choose to use thinner Silicon cells in their PV systems to reduce costs. However, thinner Silicon cells are more vulnerable to cracking. Cell cracking can cause partial changes in the output power of the PV units and is undesirable. To solve this problem, DC-DC conversion units can be utilized to mitigate the impact of cracked cells on the output voltage. DC-DC converters can also solve the problem of hot spots in PV cells caused by partial shading that makes a reverse bias in each diode of the cells.

There are some other concerns in using power electronics in PV system design and operation. The DC-DC converters used in PV systems may require a certain range of voltages and currents and the inverters connected afterwards may need specific values of voltages and currents based on the output voltage and the MPPT algorithm. According to several tests done by NREL [20], certain combinations of DC-DC converters and inverters have voltage instability issues because of the input voltage variability.

There is not enough data from test results illustrating the lifetime of power electronic devices used in distributed PV systems. Datasheets for individual DC-DC converters shows they have about 25 years of lifetime. Long-term reliability of distributed power electronics and its impacts on the lifetime of other devices needs to be investigated more. Moreover, the interoperability of power electronic devices has to be taken into account. There are some times when the individual parts of the system need to be replaced. However, due to the lack of interoperability in electronic components, the system owner is forced to change all the components, leading to high costs.

2.3 Solid-State Transformers

2.3.1 Basics

To have a better comparison between classical and solid state transformers, this section reviews their fundamentals. Classical or traditional transformers are based on magnetic cores that are constructed from material like Silicon steel. Windings are mainly made up of Copper and Aluminum. Further, there is a system for the cooling of these transformers that uses mineral oil. Fig. 16 (a) shows a purely passive low-frequency-isolated conventional transformer. Figs. 16(b) and 16(c) work with a low frequency (LF). Fig. 1 (b) uses series voltage compensation and Fig.

16(c) has a central series AC chopper on its secondary side. Fig. 16(d) shows a medium-frequency-isolated transformer with two AC choppers on both sides.

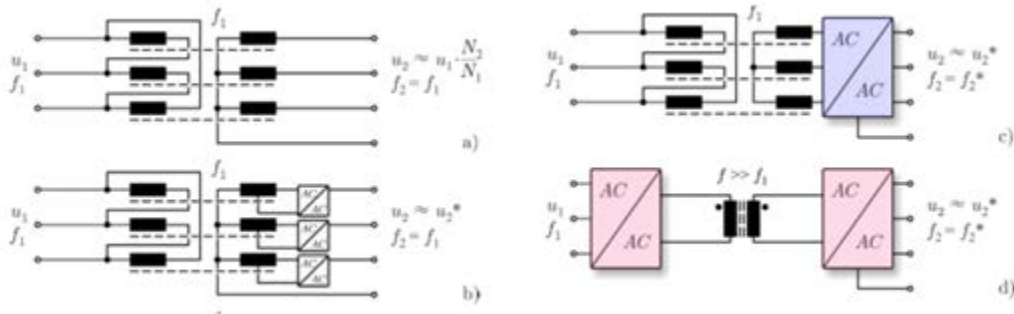


Fig. 16. Medium frequency (MF) transformers with choppers on sides.

Fig. 17 shows the power loss for different structures of power converters. The power loss in the medium frequency (MF) transformer is lower than the conventional transformer. However, MF transformers need series converters on both sides. This increases the overall power loss of these structures. As a result, the LF transformer has a higher efficiency than the other three structures. While the LF transformer has higher efficiency the higher-frequency transformer may allow for significant volume savings due to the reduced capacitance required in the cell stacks of the converters.

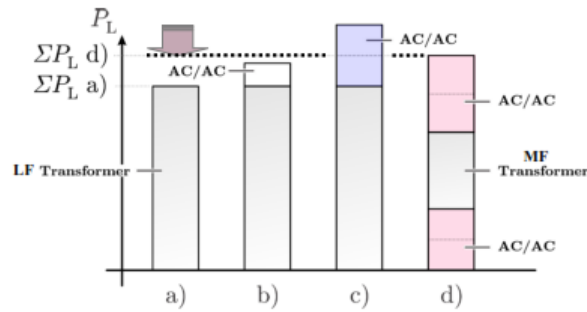


Fig. 17. Power losses of different transformers.

2.3.2 Variability of prices

Since 2004, both Steel and Copper global markets experienced large price fluctuations as a result of the increasing demand from emerging economies. Statistics show that the average price of Copper has quadrupled between 2003 and 2013.

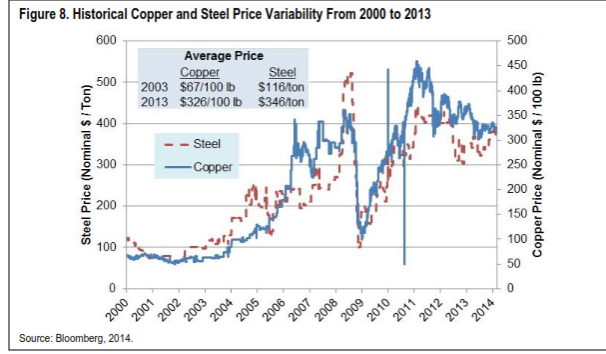


Fig. 18. Historical Copper and Steel price from 2000 to 2013.

The global power transformer market is mature. Power transformer prices experienced a depression for most of the 1990s. However, transitory raw material market, unprecedented market demand, and changes in manufacturing bases have reversed the constant price situation since 2002.

According to a recent industry analysis, the compound annual growth rate (CAGR) of the power transformer market was about 13% from 2000 to 2009 and reached a total revenue of \$11B in 2009 [22]. Another report published in 2013 indicates that the global power transformer market is expected to be worth \$29 billion by 2019, with a CAGR of 8% from 2013 to 2019.

2.3.3 SST realization and application challenges

A. SST topologies

There are three degrees of freedom in selecting the topology of an SST as follows.

1. Partitioning of the AC/AC power conversion

Considering MF isolation, there are 4 types of partitioning options for different applications. These four groups are shown in Fig. 19 and are as follows.

- 1-stage matrix type topologies
- 2-stage with low voltage DC link
- 2-stage with medium voltage DC link
- 3-stage with medium voltage and low voltage DC link

The two-stage topologies with low voltage DC links are used for energy storage applications while those with medium voltage DC links are used for HVDC applications.

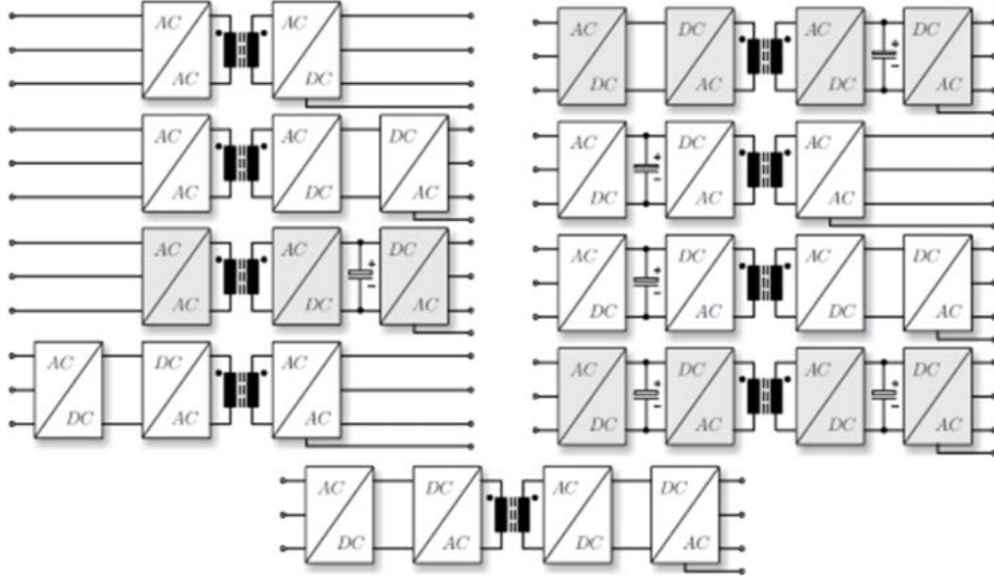


Fig. 19. Power conversion partitioning.

2. Partial or full phase modularity

The modularity concept stems from the use of several smaller converters instead of a bigger central converter. As shown in Fig. 20, there are different possible structures for solid state transformers. These structures are different in the number of components in each level of the electric and the magnetic circuits.

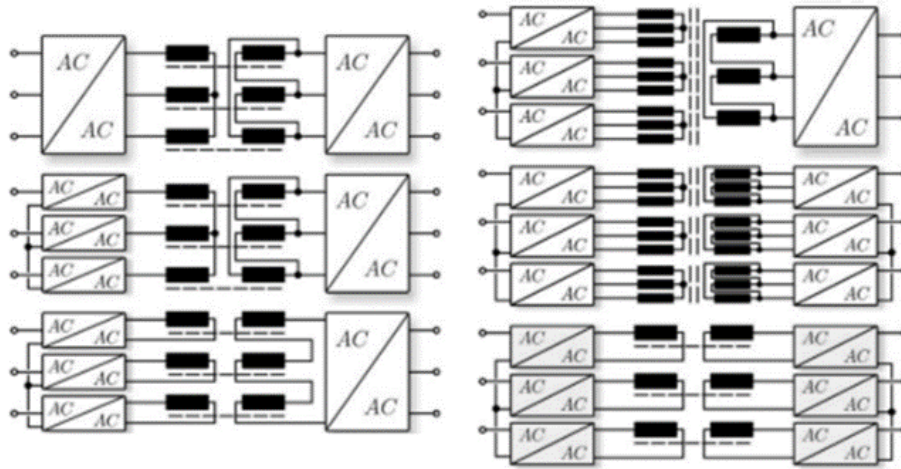


Fig. 20. Medium voltage modularity.

3. Partitioning of medium voltage

The last degree of freedom in topology selection is the partitioning of medium voltage. The medium voltage level can be treated in multi-cell and multilevel approaches. Different possible input series/ output parallel (ISOP) structures are seen in Fig. 21. The potential benefits of using multi-cell approaches are low input voltage and output current harmonics, low input/output filter requirement, and low blocking voltage requirements.

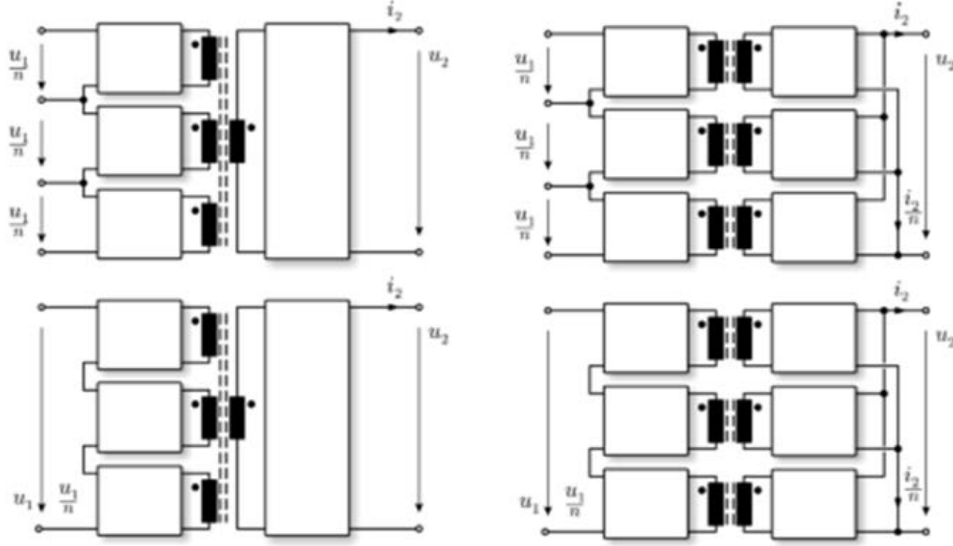


Fig. 21. Partitioning of medium voltage.

Fig. 22 shows a classification of SST structures with regard to the three degrees of freedom discussed earlier. As phase modularity increases, a three phase system tends to be split into individual phases. Power conversion partitioning leads the system towards matrix and DC link topologies. Finally, the increased number of levels causes the medium operating voltage to split into low partial voltages, resulting in multilevel/cell approaches.

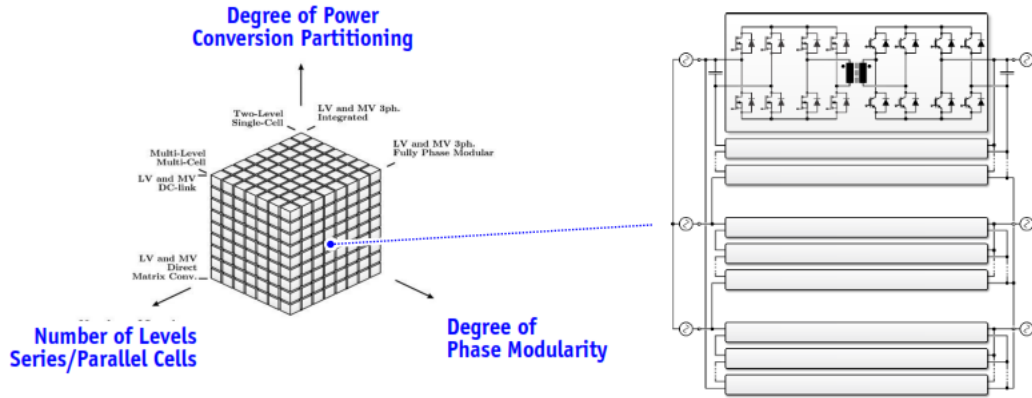


Fig. 22. Classification of SST structures.

B. Availability and selection of power semiconductors

Conversion, control, and processing of electric power in power electronics is performed with the use of solid state devices. Silicon (Si) is the best known semiconductor material. Wide bandgap (WBG) semiconductors have the potential to make significant changes in the system's operating voltage, temperature, frequency, and efficiency. SiC and GaN are the two major materials expected to replace Silicon in power applications and reduce the system costs. WBG semiconductors are covered in the next sections of this report. The biggest challenge for the widespread use of WBG semiconductors is cost. Cooling and insulation levels are also important issues to be considered

while designing WBG devices [23]. The availability of Si for high voltage applications with respect to different frequencies is shown by ABB and plotted in Fig. 23.

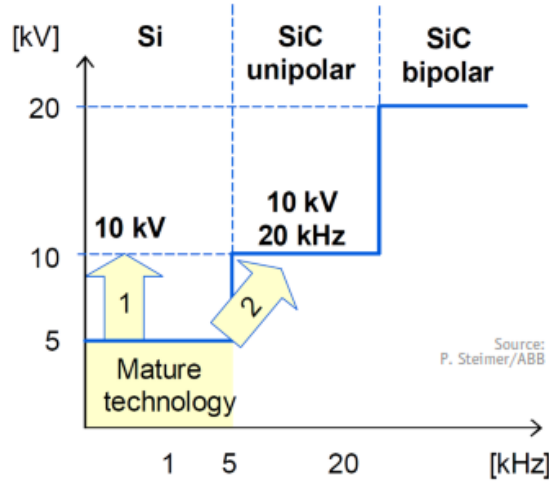


Fig. 23. Current semiconductor technology limits.

C. Single-cell and multi-cell converter concepts

To decrease costs, different voltage levels may be used. The voltage level selection is ruled based on an underlying tradeoff between the system cost and efficiency. The cost of insulation and conductors together with the cost of losses make up for the total costs. To calculate the efficiency, three quantities are involved. The maximum voltage is multiplied by the maximum possible current and then divided by the losses [24]. The general topology of a series connected multi-cell converter is shown in Fig. 24. The switching losses for equal $\Delta i/I$ and dv/dt is illustrated in Fig. 25. The interleaved series connection of converters reduces the switching losses. Further, using multi-cell series converters allows the operation of the system at lower frequencies (e.g. 5 kHz).

The challenge is to choose the optimum number of converter cells. As this number goes up, the conduction losses of the system grow. However, increasing the number of cells decreases the switching frequencies and switching losses. Thus, choosing the right number of cells in a multi-cell topology is a trade-off between switching and conduction losses. Ideally, inductive components are designed such that efficiency and power density are in a Pareto optimum where an increase in power density causes a decrease in efficiency. In designing an MF transformer, there is a certain frequency that maximizes the power density and efficiency. Apart from the power losses, factors such as mean-time-to-failure, power density, junction temperature, and the number of redundant cells should be considered when selecting the suitable topology for multi-cell converters.

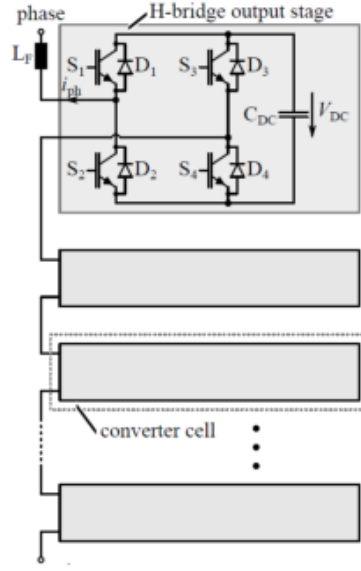


Fig. 24. H-bridge converter cells.

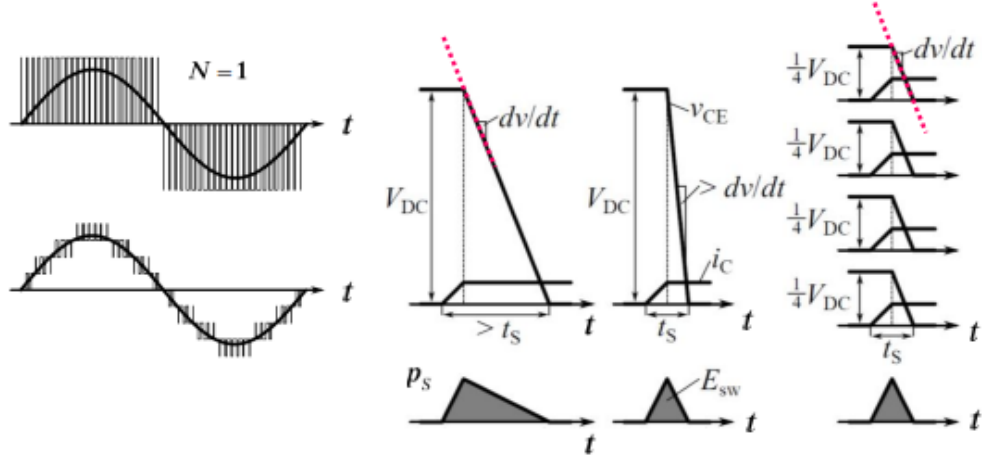


Fig. 25. Switching losses comparison.

D. SST noise emissions

Transformers vibrate as a result of the electromagnetic excitation, fans, and oil pumps and produce acoustic waves in the air. The main sources of vibration in medium frequency transformers are as follows.

- The core magnetostriction;
- The core Maxwell force;
- The winding Lorentz force.

The details for these sources of vibration are found in [26].

E. SST protection

SST is the interface between a medium voltage AC grid and a low voltage AC or DC grid. Faults in the grid influence the application of solid state transformers. Likewise, faults in these transformers affect the utility grid. Therefore, it is necessary to pay attention to the design of protection devices for solid state transformers. To deal with this issue, SST structures can be divided into several categories as follows.

- SSTs used in traditional distribution grids as alternatives for low frequency transformers. Traditional distribution grids have a unidirectional flow of power and there is no control on the loads [26].
- SSTs used in industrial distribution grids that are directly connected to medium voltage levels [27].
- SSTs used in traction systems. This category does not have any interface with utility grids and is not in the scope of this report. The increased complexity of solid state transformers leads to more challenging protection schemes because a wider variety of faults are possible. Examples of faults in SSTs are semiconductor failures, thermos-mechanical failures, error in control systems, error in measurements, and insulation breakdown. Although SSTs have overload capabilities, their semiconductors limit their current and voltage capabilities [28]. Power semiconductor switches have thermal time constants of several seconds while time constants of the range of milliseconds apply for semiconductor chips. As a result, the duration of overcurrents is significantly limited by the thermal limits of semiconductors. According to [29], the maximum allowable overcurrent ratio for a solid state transformer is 1.5x for several minutes and 5x for several milliseconds.

Regarding the overvoltage capability of SSTs on the MV side, pulses such as lightning, that are of a short duration, are allowed and can increase the breakdown voltages (dielectric breakdown and flashover in air) [30]. However, semiconductors have a high sensitivity to long lasting overvoltages that are more than their maximum blocking capability. To deal with this issue, filters are used to make surges smooth [31]. When designing SSTs, the breakdown voltages of semiconductors should be able to withstand the maximum voltages of the surges for longer periods, without considering the smoothing effects of filters. Thus, voltage utilization is determined by transient overvoltages. Based on the research study done in [32] and [33], voltage utilization for MV IGBTs is between 40% and 60% while it is around 80% for SiC FETs at the nominal operating point.

Overvoltage capabilities of solid state transformers can be increased by introducing redundancy in the system. Multi-cell SSTs are good examples of increased redundancy. Also, the DC link in SSTs can be used to isolate the MV and LV networks to not let disturbances from one grid affect the other. Further, using the measurement equipment in SSTs, they are able to order a shutdown command when necessary [34].

Fig. 26 shows a comparison between a low frequency transformer protection scheme and a protection scheme for solid state transformers [35]. Because semiconductors are too fragile to be able to trigger medium voltage fuses, breakers are used at the MV side of the SST. Also, the inrush

current produced during the startup procedure of the SST should be limited. The charging resistors at the MV side are used for this purpose and are bypassed after the startup.

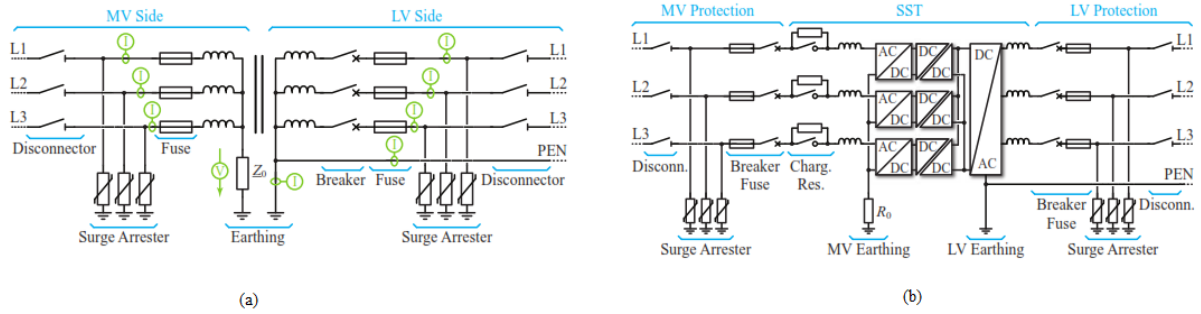


Fig. 26. Protection schemes of SST and conventional transformers [35].

F. SST efficiency, size, and costs

This section compares efficiency, size, and cost of solid-state and low frequency transformers. This comparison is based on the research done by Power Electronic Systems Laboratory at the Swiss Federal Institute of Technology in Zurich [36]. Table 3 shows a comparison between the mentioned factors for 100 kVA LFT, low voltage SST, and medium voltage SST [36].

The conventional low frequency transformers have lower power loss and thus higher efficiency. The difference between the efficiency of an LFT and an SST is not considerable. However, regarding the volume and weight, the size of solid state transformers is largely decreased compared to low frequency transformers. This is because of the higher frequency in solid state transformers. As a result, solid state transformers are more convenient choices for applications in which the transformers are mobile, such as traction and truck-mounted applications. Fig. 27(a) shows the weight breakdown diagram for medium voltage solid state transformers. The filter has the largest weight among all the elements. Frames and MF transformers are the second heaviest parts and semiconductors are the lightest elements.

Table 3. Performance characteristics overview [36].

	SST MV	SST LV	LFT
efficiency	98.2 %	98.2 %	98.7 %
volume	1.751 m ³	0.211 m ³	3.427 m ³
weight	1262 kg	1036 kg	2591 kg
cost	49.3 kUSD	27.7 kUSD	16 kUSD

Based on the research study done in [36], the estimated cost for solid state transformers is very high, especially for MV SST, compared to the traditional low frequency transformers. Higher costs may be a discouraging factor for utilities to use solid state transformers. However, it is a trade-off between the importance of the application and costs. Fig. 27(b) shows the cost breakdown for the average medium voltage solid state transformers. Filters account for a large portion of the costs. They cost higher than the medium frequency transformer, semiconductors, and capacitors.

Capacitors, semiconductors, and MF filters make up for around 60% of the costs. The lowest portions of the costs belong to control systems and heatsinks.

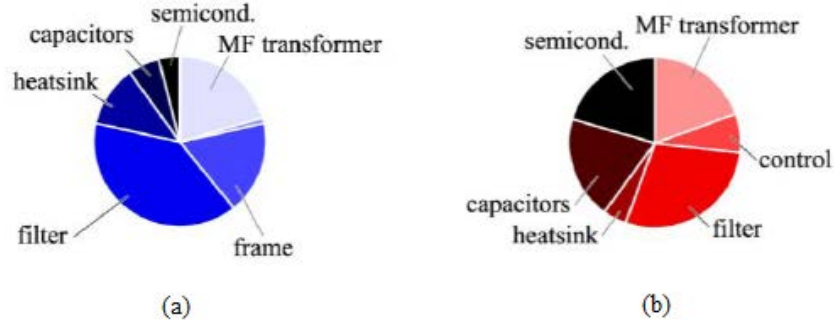


Fig. 27. Medium voltage solid state transformer (a) weight breakdown (b) cost breakdown [36].

The different states of development of solid state transformers are shown in Fig. 28. There has been an inflated peak of expectations from solid state transformers after the technology was introduced. This peak was followed by a sudden drop in the visibility of SSTs and then a slope of enlightenment after the appearance of traction applications [36].

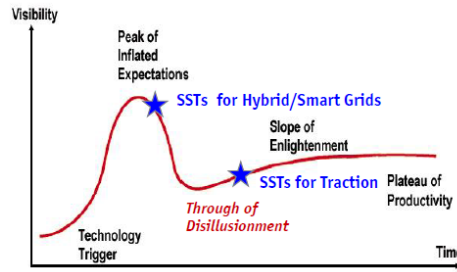


Fig. 28. SST technology hype cycle.

Besides all the advantages of solid state transformers, there are still limitations in this area. They have relatively 2-6% higher losses compared to conventional transformers. Their cost-performance ratio should still be clarified and their overload capability is limited. Furthermore, their reliability is not higher than conventional transformers. Solid state transformers are not a 1:1 replacement for conventional distribution transformers. Further, solid state transformers are not able to replace all conventional distribution transformers, even in a mid-term future.

2.4 Solid-State Circuit Breakers

To increase the availability and quality of the delivered power to the customers, it is crucial to handle faults. The problem of short circuits is even more severe if the short circuit level of the system is increased as a consequence of distributed energy resources in medium voltage networks. A traditional AC grid has generators that can sustain high fault currents for about one second. This gives the mechanical circuit breakers some time to isolate faults. Because the overload capability of systems that utilize power electronics is constrained by the thermal-electrical capability of semiconductor devices, and because these semiconductors are not able to sustain currents higher than their ratings for more than a few milliseconds, in case these limits are exceeded, power converters face a self-shutdown or fatal failure [37].

Mechanical circuit breakers are the currently used to address the problem of short circuits in the grids. These devices are not fast and it takes them several fundamental periods to open after the short circuit detection. This delay causes an arc and because the current can only be stopped when it passes zero, it takes around 100 ms for the current to stop. The current mechanical circuit breakers have several shortcomings as follows.

- 1) Mechanical circuit breakers are not able to affect the peak current. As a result, all the components in the grid have to endure the peak current, which can be around 20 times the peak of operating current. This increased current puts the equipment in the grid under stress and leads to component oversizing and increased costs.
- 2) The short circuit current rating of mechanical circuit breakers is limited. As a result, the grid designers should try to decrease the short circuit levels in the network by introducing more inductance. However, this results in a decreased power transfer capacity of the lines.
- 3) When a short circuit happens in the medium voltage network, the grid experiences a sag. Because mechanical circuit breakers have some delays breaking the fault currents, certain sensitive loads may be damaged by this voltage sag. There is a need for uninterruptable power supplies (UPS) for some loads to be able to survive these sags. This might not be cost effective for some units.

Unlike mechanical circuit breakers, solid state circuit breakers are fast and can switch in a few microseconds. This higher speed potentially results in different advantages for solid state circuit breakers over mechanical ones.

2.4.1 Solid-state switch topologies

To operate in various voltage and current levels, a breaker should be modular, which is less expensive than changing the whole device for a new voltage or current level [38]. Since the power loss in the available semiconductors today is high, most topologies are asymmetric and have a series connection of diodes. The turn off voltage in solid state circuit breaker modules should be limited. To do this, varistors are utilized in these modules. Further, solid state circuit breaker modules take advantage of semiconductors like GCTs and GTOs working beside the aforementioned rectifier diodes. Because it is not possible to turn off the GTOs without the help of an auxiliary circuit, capacitors and resistors are connected in parallel with them. In some cases such as modules with a single GCT, capacitor and resistor snubber circuits are not needed. Thus, varistors can be connected in parallel with each semiconductor [39]. These technical specifications lead to solid state circuit breaker topologies shown in Figs. 29(a) and (b) [40].

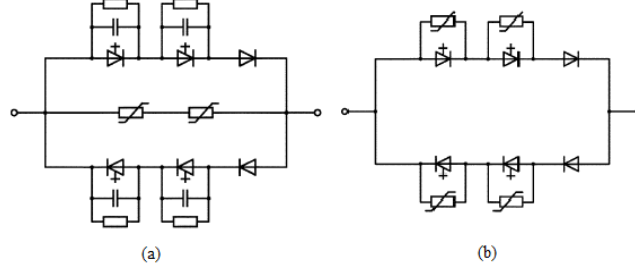


Fig. 29. Solid state circuit breaker topologies.

Fig. 29(a) shows a topology with 4 GTOs and 2 diodes. These GTOs use resistor-capacitor snubber circuits. Fig. 29(b) shows a GCT based breaker that does not use any capacitor snubber circuits. These topologies can be modified to lower the costs by reducing the number of active semiconductors. Fig. 30 shows the rectifier solutions for solid state circuit breakers [41]. The GTO based solution, Fig. 30(b), utilizes resistor-capacitor snubber circuits while the GCTs in the module shown in Fig. 30(a) use varistors in parallel with their semiconductors.

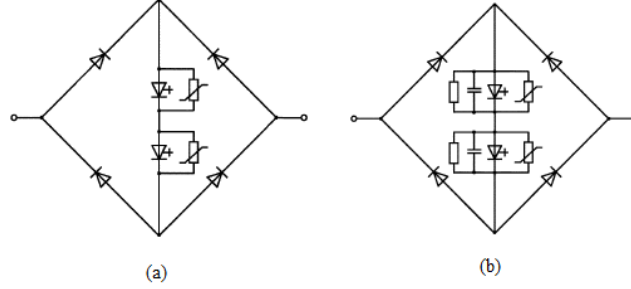


Fig. 30. Rectifier solutions for solid state circuit breakers.

The number of semiconductors in Figs. 29 and 30 is the same. Two of the active semiconductors in Fig. 29 are replaced by diodes. This reduces costs but on-state losses are increased.

2.4.2 Cost of different topologies

To compare the costs of different topologies, the costs of the switches and the cost of power losses should be considered. Despite having the same number of semiconductors, these topologies are different in the number of active semiconductors. At the first glance, it is concluded that topologies with more active semiconductors cost more. However, topologies with diodes have more power loss in each cycle. This necessitates more detailed analysis. Reference [40] performs analytical calculations to determine the costs of different solid state circuit breaker topologies.

2.4.3 Reliability of different topologies

A feature that plays an important role in choosing different topologies is reliability. In solid state circuit breakers, even if a single component of a redundant device fails to operate, although the switch can still be utilized, it usually has to be replaced because of safety issues [40]. As a result, costs of the system are increased.

There are two parameters for measuring and comparing system reliability: failure in time (FIT) and mean time between failures (MTBF). FIT shows the number of failures in 10^9 operation hours of the device and is determined by the manufacturer. MTBF considers the additional costs imposed to the system due to any kind of need for the replacement of the switches, although redundant modules may still be working. Table 4 shows the statistics for the reliability of different mentioned topologies. The failure ratio of the topologies that utilize GTO is greater because of the added snubber circuits. Semiconductors have the same reliability, but the capacitors decrease the reliability of the module because failure of one may affect the whole module.

Table 4. Reliability of the topologies [40].

Topology	FIT	MTBF
GTO (series)	9840	11.6 years
GCT (series)	5040	22.6 years
GCT (rectifier)	2880	39.6 years
GTO (rectifier)	5280	21.6 years

2.4.4 Challenges and advantages of solid state circuit breaker technology

Solid state circuit breakers have a higher voltage drop compared with mechanical circuit breakers. A higher voltage drop leads to higher power dissipations and need for heat sinks, which in turn means higher weight and volume and naturally cost. Solid state circuit breakers also suffer from leakage currents during their off states and need EMI protection. Unlike mechanical circuit breakers, the off-state in solid state circuit breakers is not a 100% physical disconnection from the power source [42]. The semiconductors used in solid state circuit breakers, such as MOSFETs and IGBTs, use high impedance inputs for turning on the conduction. This high impedance input is sensitive to electromagnetic fields and consequently requires filters for a reliable operation.

Fig. 31 shows a solid state circuit breaker for low frequency AC systems that utilizes a TRIAC for load switching. The control block is isolated from the load. In some topologies, to ensure a 100% physical isolation in the off state, mechanical contacts are used in series with the load.

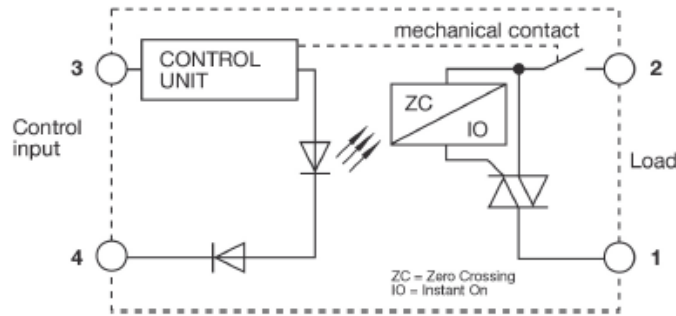


Fig. 31. An example of an electronic circuit breaker [3].

Developments in the solid state technology naturally benefit circuit breakers too. Among these are the improvement of the on state resistance and decreased saturation voltage. Unlike mechanical breakers, solid state breakers do not need auxiliary circuits or permanent magnets and vacuum switching chambers to deal with arcs. Furthermore, the life-cycle of solid state circuit breakers is much longer than mechanical breakers. It is possible to program solid state circuit breakers for features such as the nominal current, tripping curve for overcurrents, undervoltage limits, and thresholds for overcurrents [43].

2.5 Storage

The intermittent nature of the power generated by many renewable sources necessitates the use of storage devices. Energy storage systems (ESS) have the ability to smoothen the output of these sources. The key to this technology is the power electronics. Power electronics can provide a controllable connection point between the ESS, DER, and the network [39]. The high response speed of energy storage systems makes them capable of providing frequency and voltage support in the grid. Furthermore, ESS can be a good help for the system when trying to black-start the network [41]. Fig. 32 shows the trend in the use of energy storage systems since 2010.

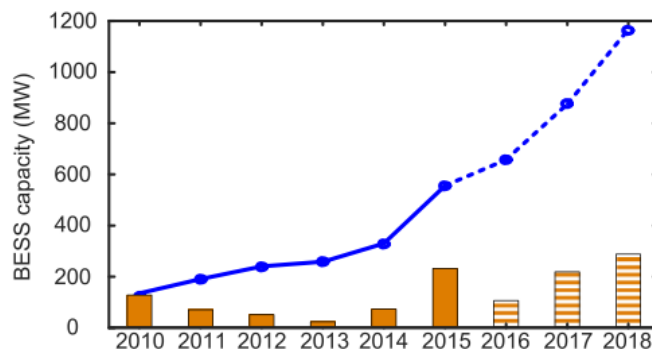


Fig. 32. Annual worldwide ESS capacity [45].

Table 5 shows examples of ESS products. According to [45], ABB has a 200 kW storage unit operating with semiconductors connected in series. DynaPeaQ uses only one monolithic converter and can work in a power rating of 50 MW [52].

Table 5. Major ESS manufacturers and their solutions [53].

PE Provider	Power/Energy (MW/MWh)	Topology	Battery Technology	DC-DC Stage	AC/DC Voltage (V)	Module Power Level
ABB	20/6.67	2L/3L	Li-Ion	No	415–690 V_{ac} ; 975–1200 V_{dc}	72 kW–1 MW
DynaPower	11/4.4	2L/3L	Li-Ion	–	750–1150 V_{dc}	1 MVA
Enercon	10/10	2L/3L	Li-Ion	Yes	–	300 kW
Extreme Power	10 / 7.5	2L	Advanced Lead Acid	–	480 V_{ac} ; 750–1200 V_{dc}	1.5 MVA
General Electric	21/14	2L/3L	Lead Acid	–	480 V_{ac} ; 431–850 V_{dc}	1.25 MW
Mitsubishi	20/6.33	2L/3L	Li-Ion	–	300 V_{ac}	0.5 MW
Nidec	12/96	2L	NaS	Yes	–	1.2–2.5 MW
Parker SSD	12/4	2L/3L	Li-Ion	No	400–480 V_{ac} ; 720–1200 V_{dc}	1.2–2.2 MW
S&C Electric	10/0.14	2L/3L	Lead Acid	Yes	480 V_{ac} ; 460–800 V_{dc}	1 MW/1.25 MVA
Yunicos	36/24	2L/3L	Advanced Lead Acid	–	415–690 V_{ac} ; 975–1200 V_{dc}	250 kVA

2.6 Flexible AC Transmission Systems (FACTS)

The IEEE working group on FACTS devices defines FACTS as “alternating current transmission systems incorporating power electronic-based and other static controllers to enhance controllability and increase power transfer capability” [60]. FACTS devices can be an alternative for new transmission line construction because of their lower infrastructure investment cost, environmental impact, and construction time. Power electronic solutions, specifically voltage sourced converters (VSC), are widely used in FACTS. These converters are used in topologies such as static synchronous compensators (STATCOM) [54], unified power flow controllers (UPFC) [55], convertible series compensators (CSC) [56], back-to-back DC ties (VSC-BTB) [53], and VSC HVDC transmission [57], [58], [59]. FACTS devices can be used in series, shunt, or series-shunt connections as shown in Fig. 33.

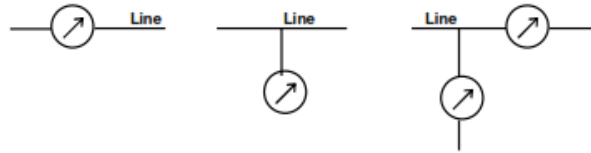


Fig. 33. Implementations of FACTS devices.

2.6.1 Topologies

SVC and STATCOM are two examples of shunt FACTS devices. These devices are shown in Fig. 38 with their corresponding characteristics.

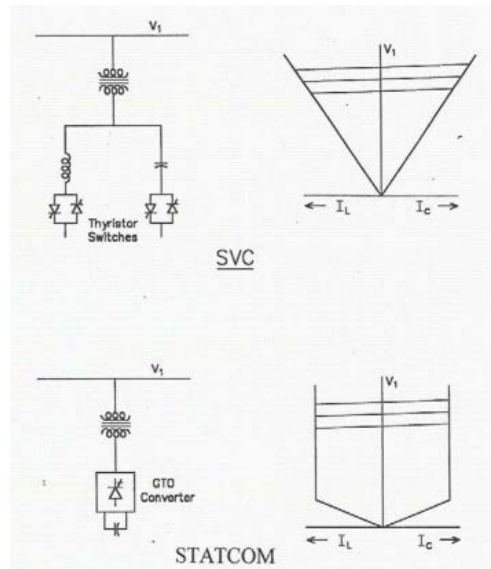


Fig. 34. SVC and STATCOM [60].

Two other topologies for FACTS devices are shown in Fig. 35: thyristor controller series capacitor (TCSC) and static synchronous series compensator (SSSC) that are used for the compensation of series reactive voltage. SSSC directly injects the desirable voltage into the system while TCSC controls a variable impedance. Performance characteristics of these devices are shown in Fig. 36 [60]. According to [60], TCSC is more cost effective than SSSC. A thyristor controlled phase angle

controller (TCPR) and a unified power flow controller (UPFC) are shown in Fig. 36. These devices are combinations of series and shunt controllers and are able to control both the real and reactive power flow and the voltage of the lines.

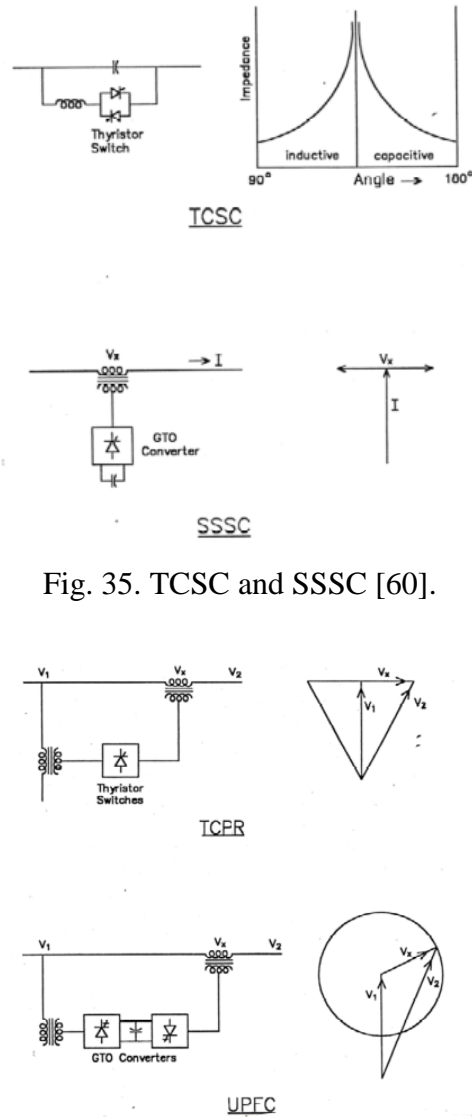


Fig. 35. TCSC and SSSC [60].

Fig. 36. TCPR and UPFC [60].

2.6.2 Planning Perspective

To include FACTS in transmission planning, it is necessary to have a thorough investigation on their effects on the dynamic/transient voltage stability, load flow, sub synchronous oscillations, dynamic voltage violations, voltage collapse, steady state voltage, and reactive power flows [61].

2.7 High-Voltage DC (HVDC) Transmission

HVDC has well-established advantages for long-distance or underwater transmission of bulk power. Another application is as a tie-line between asynchronous regions due to phase angle mismatch (e.g., western and eastern interconnects in the US) or frequency mismatch (Japan and Brazil-Paraguay). There are two main technologies for HVDC: line commutated converter (LCC) and voltage-sourced converter (VSC). LCC systems operate based on thyristor and hence are an earlier technology. They cannot provide reactive power (always consume reactive power) but are able to operate at higher voltage and power ratings. More than 100 such systems are in service with voltages reaching $\pm 800\text{kV}$ and transmission power capacity of up to 10GW.

In contrast, VSC-based topologies can independently control both real and reactive power and are hence suitable for weaker grids. Availability of multilevel power electronics converter topologies, especially MMC, has enabled application of VSC-HVDC in the power system. More than 30 such systems are in service with voltages up to $\pm 320\text{ kV}$ and the transmission capacity up to 1 GW.

2.8 Microgrids

A microgrid is a collection of loads, distributed generations (DG), and energy storage devices that operate in a reliable manner to provide electricity in both grid-connected and islanded modes of operation. This concept allows for an increased flexibility in the control of DER units, improves the power quality, and results in a more reliable electricity supply and higher efficiency [62], [63], [64]. The general configuration of a microgrid based on power electronic solutions is shown in Fig. 37. Fig. 38 shows different categories of microgrids based on their DC vs. AC systems.

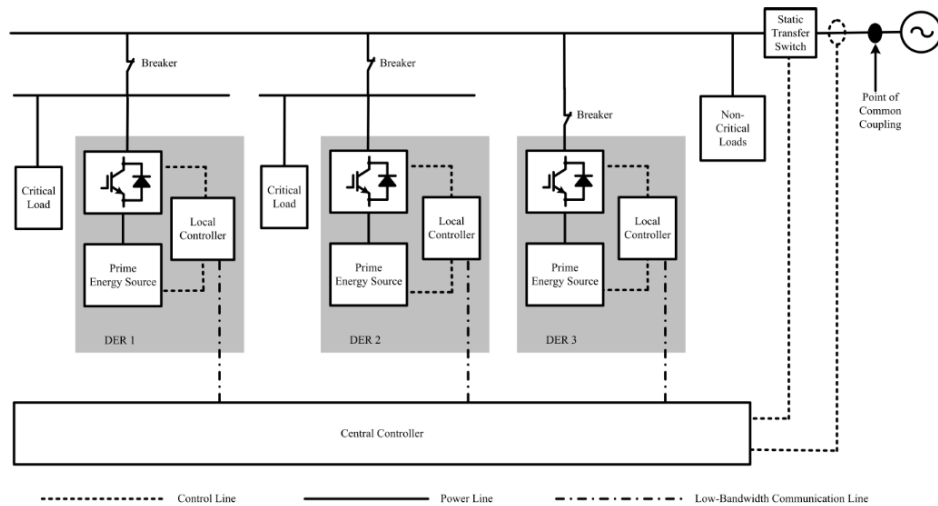


Fig. 37. A microgrid based on power electronic devices [68].

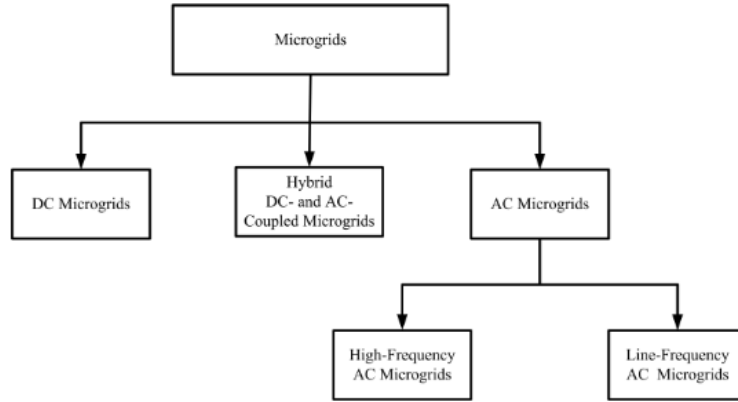


Fig. 38. Different categories of microgrids [68].

2.8.1 DC Microgrids

Fig. 39 shows the generic block diagram of an LVDC microgrid [69]-[71]. LVDC microgrids can significantly outperform LVAC microgrids with regard to cost and efficiency [72] with applications in electric vehicles, communication systems, load centers, and PV systems.

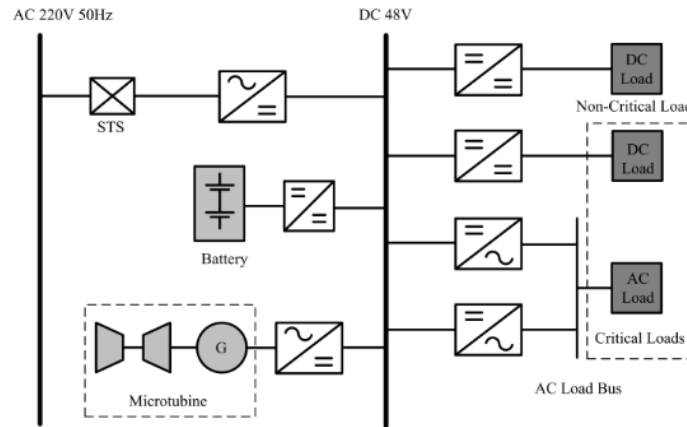


Fig. 39. An LVDC microgrid [68].

2.8.2 HFAC Microgrids

Higher frequency power networks have been used for a long time in military applications. The utilization of higher frequencies lowers the size and weight of the system. However, these systems are mostly suitable for small scales because the increased distances increase their power loss. The schematic diagram of a power electronic based high frequency AC microgrid is shown in Fig. 40.

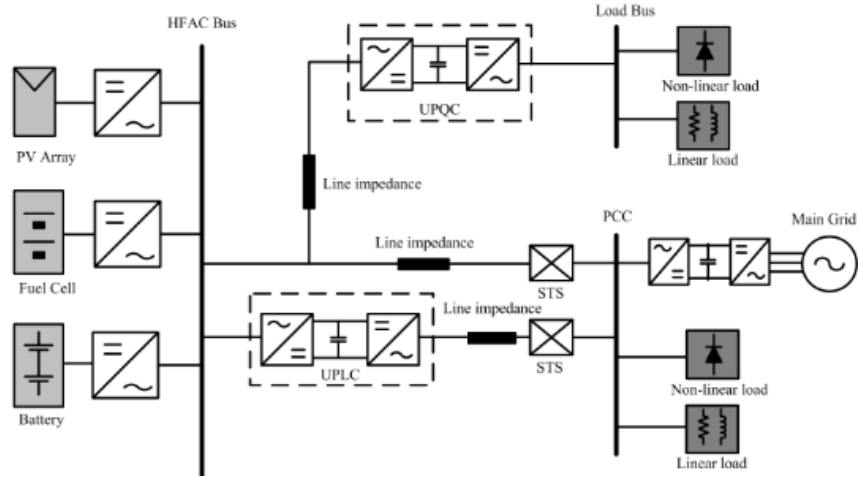


Fig. 40. A high frequency ac microgrid based on power electronics devices [72].

2.8.3 LFAC Microgrids

The typical topology for these types of microgrids is shown in Fig. 41.

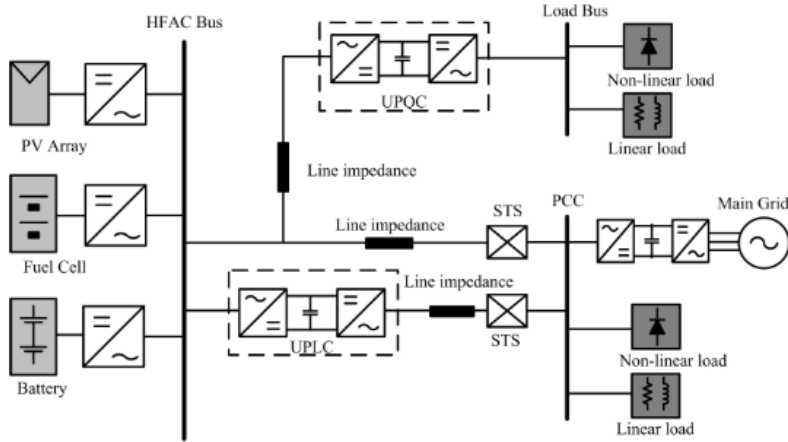


Fig. 41. A low frequency ac microgrid based on power electronics devices [68].

2.8.4 Hybrid Microgrids

Hybrid microgrids provide effective means to connect both DC and AC power sources. DC sources such as fuel cells and photovoltaic units are attached to DC-DC conversion systems and then DC-AC inverters to connect to an AC system. Rectifiers are also used to connect AC sources such as microturbines to DC links. The control structures of the DC and AC parts are decoupled. Hybrid microgrids provide a more flexible platform to connect different types of DERs. However, they need updated protection schemes and study on their stability issues.

2.8.5 Electronically coupled DER units

In a microgrid, DER units that are connected to the point of common coupling through power electronic devices are categorized into three groups as follows.

A. Grid-forming units

The application of grid-forming units is mostly for islanded microgrids because these units control the frequency and voltage of the system by controlling the flow of power and load.

B. Grid-feeding units

Grid-feeding units can control the flow of real and reactive power within the network and follow the dispatching requirements. These units can follow variations of load [73].

C. Grid-supporting units

Grid-supporting units can provide ancillary services to the grid. These units are expected to extract as much real power as possible from their primary sources of energy and provide power quality improvements through different ancillary services.

3. Technology Trends

3.1 Wide Band Gap (WBG) Semiconductors

3.1.1 Introduction

Currently, Si-based technologies are dominantly used in power electronic systems, despite several drawbacks: limited voltage, temperature, and frequency rating. Si-based technologies cannot have a temperature higher than 200 °C and the highest voltage allowed on them is 6.5 kV. There are some unavoidable physical limits that result in decreased efficiencies and increased costs. Wide band gap (WBG) semiconductors can be a solution for the problem of limited voltage, temperature, and frequency. They result in increased efficiencies, decreased size and cost, and improved robustness of the system. Their application is expected to become more widespread and lead to a transformative change in the power electronics industry.

There are several reasons why miniaturization of power electronic devices is important. The first reason is that there are many applications where size and weight are very important. The other reason is the impact of an increased power density on the possibility of introducing new design architectures. Further, the higher density of integrated circuits results in a revolution in mobile communication. Supplies, communication, and energy conversion systems are big parts of power systems. However, their thermal management is a limiting factor. Thermal considerations are very important in systems that have higher power densities. Wide band gap devices can perform their duties in higher temperatures and as power electronic devices become smaller and smaller, they become more dominant.

Blocking voltage, switching frequency, operation temperature, commercial availability, and maturity of the technological processes are the features that are important in choosing semiconductors. Considering these factors, Silicon-Carbide (SiC) and Gallium Nitride (GaN) show promising features. Fig. 42 compares the properties of these candidate WBG semiconductors and Silicon [74]. Among all wide band gap devices, GaN and SiC have the most well developed manufacturing lines for high power electronics. Although GaN has a better performance in high voltages and frequencies, factors such as thermal conductivity lead to a more widespread use of SiC devices in high power electronics. SiC devices have already begun their competition with their Si counterparts. GaN devices are gradually gaining attention from the industry in fields such as light emitting diodes.

WBG devices bring their own challenges, e.g., nonoptimized designs, technology limitations, reliability, and not exploiting the full material quality [75]. However, with the future developments expected for drivers, electro-thermal operation, designs and packaging, and controllers, wide band gap devices will be a real breakthrough. Table 6 compares the physical features and performance indices of different semiconductors and wide band gap devices [76].

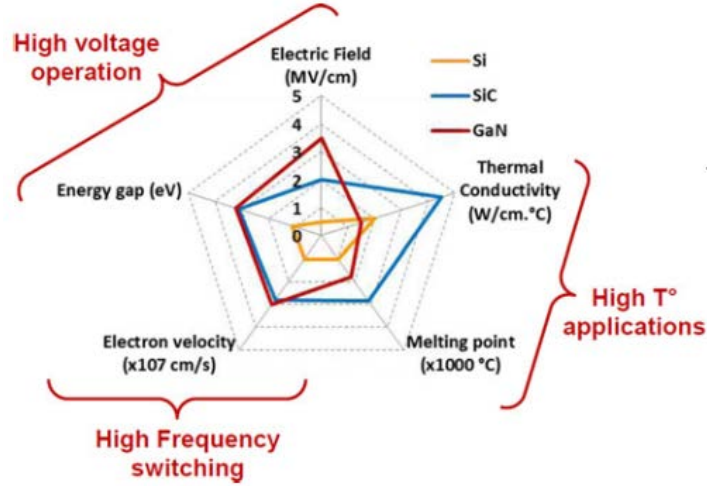


Fig. 42. Summary of Si, SiC, and GaN properties [75].

Table 6. Physical properties of various semiconductors for power devices [76].

Material	E_g at 300 K, eV	μ_n , $\text{cm}^2/\text{V s}$	μ_p , $\text{cm}^2/\text{V s}$	v_{sat} , cm/s	E_c , V/cm	λ , W/cm K	ϵ_r
Si	1.12	1450	450	10^7	3×10^5	1.3	11.7
GaAs	1.4	8500	400	2×10^7	4×10^5	0.54	12.9
3C-SiC	2.3	1000	45	2.5×10^7	2×10^6	5	9.6
6H-SiC	2.9	415	90	2×10^7	2.5×10^6	5	9.7
4H-SiC	3.2	950	115	2×10^7	3×10^6	5	10
GaN	3.39	1000	350	2×10^7	5×10^6	1.3	8.9
GaP	2.26	250	150	10^7	10^7	1.1	11.1
diamond	5.6	2200	1800	3×10^7	5.6×10^7	20	5.7

3.1.2 SiC

Currently, the price for an SiC wafer is about 50 times higher than the price of an equivalent Si wafer. However, this higher cost of material is not the biggest factor comprising cost compared with the other costs of a full system such as fabrication and packaging. Moreover, this extra cost is expected to be paid back in forms of higher efficiency, smaller size, lower weight, or rudimentary requirements for cooling systems. Yet, to be cost competitive in today's market, SiC wafer sizes and the yield per wafer should increase [77].

There is a trade-off between the blocking voltage and the on resistance in any power device that is a result of the drift phenomenon [78]. At higher operating voltages, the drift region resistance dominates the on resistance. Thus, the increased attraction of SiC or GaN for a manufacturer stems from the larger unipolar limits shown in Fig. 48. Wide band gap devices can be designed to have thinner drift regions and a higher critical electric field. Still, when the voltage is decreased below 1200 V, the channel resistance of the SiC devices increases and the carrier mobility remains an unresolved problem. The mobility problem in channels stops SiC from approaching its material limit within the MOSFET semiconductors manufactured to work at lower voltages, Fig. 43.

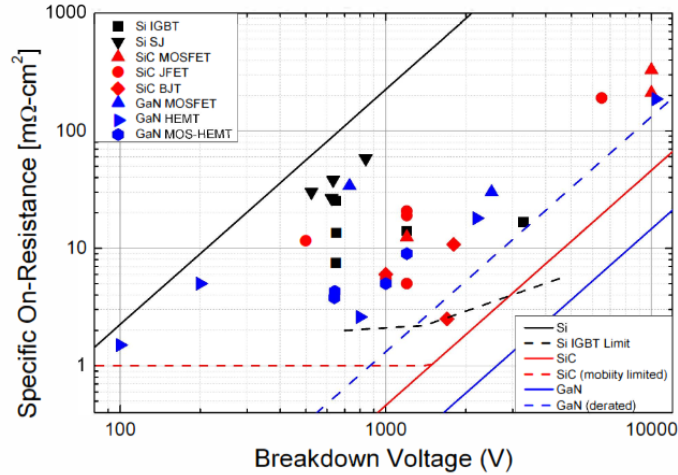


Fig. 43. On-resistance of different Si, SiC, GaN, unipolar and bipolar devices with respect to the blocking voltage [78].

BJTs do not depend on any kind of channels. As a result, there is no resistance problem limiting their operation. Thus, they have better gains and higher speeds. A negative aspect of BJT devices is that, in contrast to voltage driven MOSFETs, they are driven by current. This increases the losses and increases the complexity of the drive system [79].

What stands out in the performance of SiC compared to Si is its thermal conductivity. The wide band gap features cause the level of carriers in Si that are triggered by temperature to enter the semi-metal mode at 200 °C. This is not activated in SiC until after 1000 °C [76]. This results in a higher thermal conductivity and easier dissipation of the heat produced by losses due to high frequency switching.

3.1.3 GaN

GaN devices have larger band gaps (3.4 eV) than Si (1.1 eV) and SiC (2.36, 3.05, or 3.23 eV depending on their polytype) devices. These devices are mainly used as epitaxial layers on other wafers made up of Si or SiC materials and not independently. One of the first such combinations was employed in LED [76]. However, there is still a question of which material to use with GaN for the best result. Si is deemed the most popular choice due to its low price. However, it has some problems such as significant thermal mismatch [80]. The other option is SiC that offers the lowest mismatch and high thermal conductivity, however it has a higher cost. Low thermal conductivity of GaN means a poor performance at high temperatures and consequently at high powers. Self-heating has different effects on a device such as thermal runaways and the derating of GaN devices [81], as seen in Fig. 44.

Despite all the issues with GaN materials, they are gaining interest because of the improvements in high electron mobility transistors (HEMTs). These transistors that were first introduced in RF systems use the band-bending influences of AlGaIn on GaN materials. This leads to high charge densities, easy electron movements, and very low on state resistances [80].

3.1.4 Diamond

Diamond is a wide band gap device with near ideal properties, as seen in Table 6. It has a wide band gap of 5.6 eV that makes it appealing for unipolar devices. Diamond has some fabrication difficulties regarding the deep carrier activation energy that is high and difficult to reach at room temperature [76]. Reference [82] proposes a method for the development of high quality single-crystal diamond that can control the concentration of dopant atoms within a CVD process. This approach can potentially enable the remarkable properties of diamond for high power applications. Reference [83] demonstrates diamond based Schottky diodes with breakdown voltages of up to 2500 V. References [84] and [85] report several structures of diamond metal-insulator-semiconductor FETs (MISFETs). These MISFET structures have cut-off frequencies of 30 GHz and the maximum oscillation frequency of 60 Hz reported for a $0.35\ \mu\text{m}$ gate. They have power densities as high as 2.14 W/mm at 1 GHz [76].

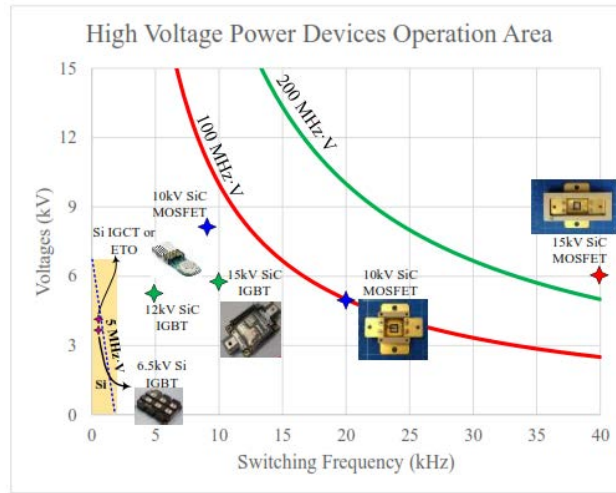


Fig. 44. SiC high voltage switches voltage-frequency capability [88].

3.1.5 Applications

As of today, wide band gap technology does not have any known commercialized applications in high voltage networks. High voltage power systems, such as HVDC and FACTS systems, use Silicon based power switches such as thyristors and IGBTs. However, high blocking voltages and frequencies of wide band gap devices can make significant changes in high voltage power systems. High blocking voltages provided by SiC devices can benefit the HVDC systems. Although the frequency of switching does not need to be large in HVDC applications, the ratings of current and voltage need to be high. SiC-based GTO technology is capable of providing high voltages of 15 kV or more with high current capabilities.

The voltage level for wide band gap devices in renewable applications is from 1200 V to 6500 V with a high level of current rating. There are some studies to develop SiC devices for renewable energy markets [78]. The promising feature of these devices for renewable systems is a higher reliability including avalanche capability and the linearity of the relationship between current and

voltage; in other words, a linear resistive characteristic [78]. Recent development examples of wide band gap devices for renewable and traction applications can be found in [89] including 900 V/1.25 mΩ modules introduced by Wolfspeed.

3.2 Multilevel Converters

The technology of multilevel converters is a significant breakthrough in high power electronics and systems that need a high quality power [90], [91]. Today, the multilevel technology is a dominant technology in high power quality demanding [92] due to their higher operating voltage capability, reduced dV/dt , reduced voltage harmonics, reduced current harmonics, smaller filter (if necessary), higher efficiency, and possible fault tolerant operation [92], [93]. Fig. 45 shows three example topologies of single phase converters with different number of voltage levels [94].

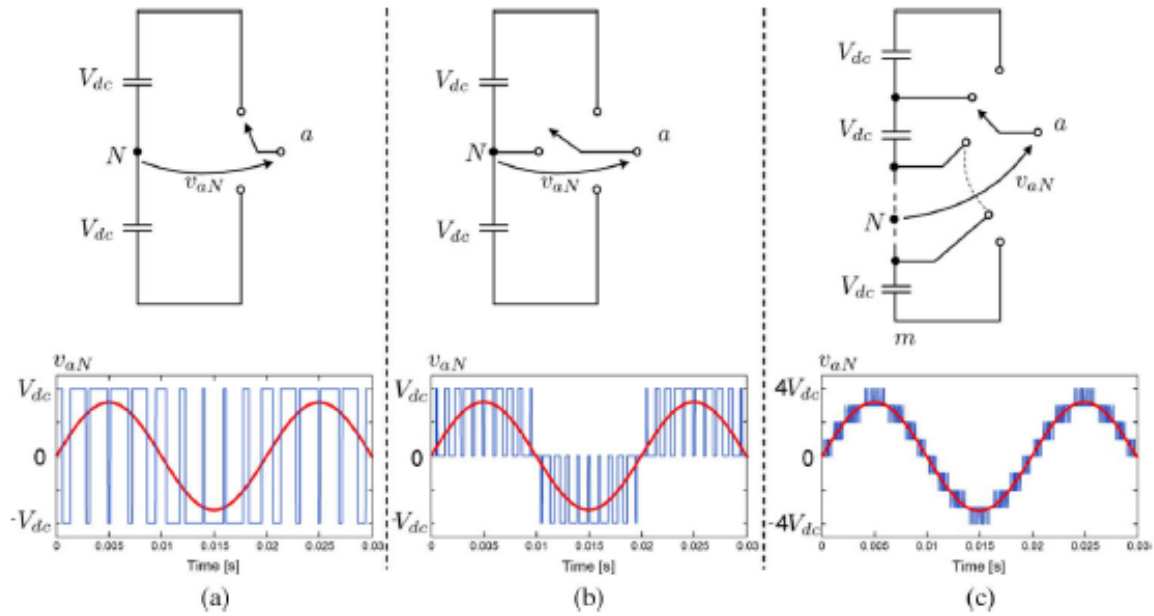


Fig. 45 Single phase converters and output waveforms (a) two level, (b) three level, (c) nine level [93].

The classification of different multilevel converter topologies is shown in Fig. 46. There are various types of multilevel topologies introduced in [92], [95]. The most popular topologies known for multilevel converters are the neutral point clamped or diode clamped, the flying capacitor or capacitor clamped, and the cascaded H-bridge [96]-[99]. Several multilevel converter topologies are discussed in Part III of this project.

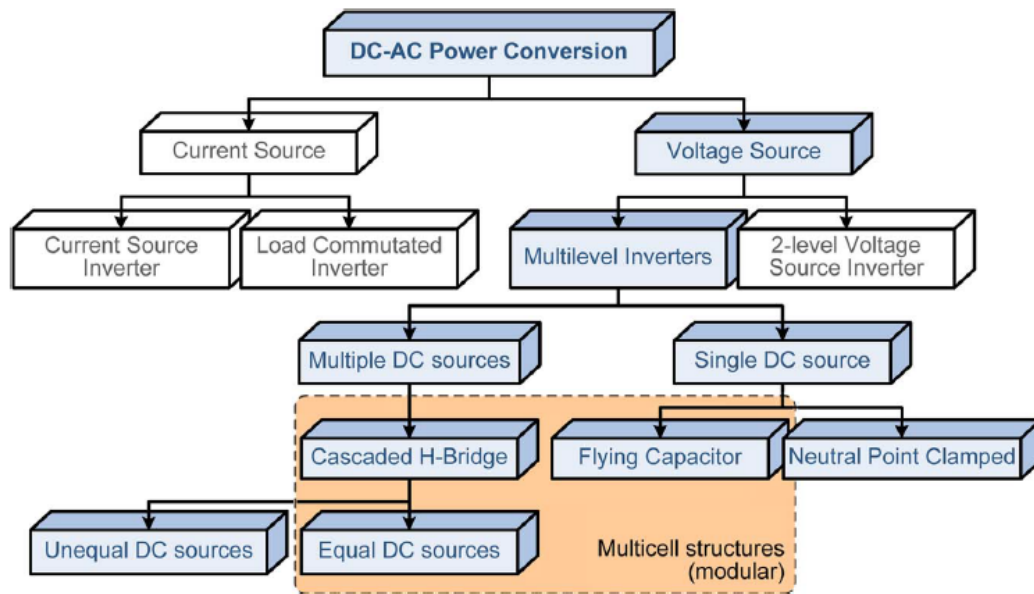


Fig. 46 Multilevel converter classification [93].

4. New and Commercial Applications

This chapter provides an overview of a few examples of new, possibly nonconventional applications of power electronics that are available as commercial solutions.

4.1 NR Electric DC De-icer

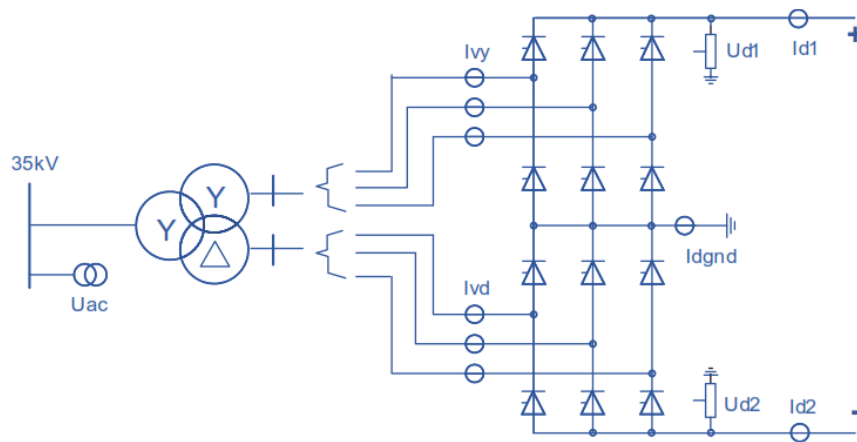
Exposure of the transmission lines to snow and rain in cold climates might cause formation of heaving ice coatings that can damage the lines and towers and ultimately causing a power outage. There are different de-icing technologies available on the market that work based on AC current. However, due to the inductive characteristics of the transmission lines, DC solutions can be more efficient and operate at lower voltages.

NR Electric PCS-9590 and PCS-9591 fixed and portable de-icers are the DC current based technologies available on the market. Fig. 47 shows the melting configuration with DC de-icers. The length and the diameter of the conductor used in the transmission line determines the voltage and current level of the de-icing device. This device can be utilized as an SVC when it is not used for de-icing.



Fig. 47 Melting configuration with DC de-icer [103].

The fixed de-icer technology is a good fit for high voltage long transmission lines. The fixed de-icer provided by NR Electric includes a 12-pulse conversion valve bank designed to convert AC to DC. The topology of the fixed DC de-icer is shown in Fig. 48.



A relocatable DC de-icer can be a good choice where there is a short transmission line with a low voltage level in a severe weather condition. The relocatable DC de-icers developed by NR Electric include a 6-pulse conversion valve for the AC to DC current conversion, unlike the fixed de-icer that has a 12-pulse valve. All the other components in the relocatable de-icer and the fixed de-icer are the same. Fig. 49 shows the topology of the relocatable DC de-icer by NR Electric.

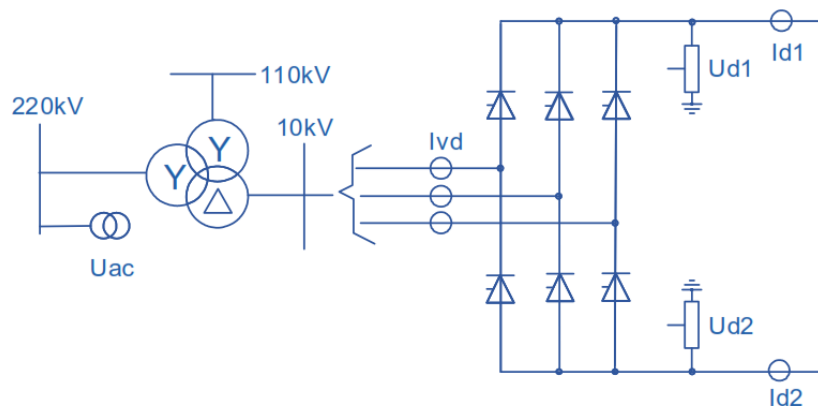


Fig. 49 Relocatable DC de-icer topology [103].

4.2 Siemens SVC Plus

SVC Plus, offered by Siemens, is a shunt FACTS device that is used for reactive power compensation and voltage profile control:

- SVC plus can improve the dynamic stability of the transmission system.
- SVC plus increases the power quality of the system and causes a decreased risk of voltage collapse and blackout.
- SVC plus can mitigate flickers in industrial applications.

- SVC plus benefits from the modular multilevel converter (MMC) topology that results in a lower harmonic content.

The use of MMC to design SVC Plus has several advantages:

- The ability to establish a sinusoidal output signal on the AC side and not needing a high frequency filter or a low pas filter for harmonics.
- The ability to have a low switching frequency and therefore a decreased power loss in the system.
- Increased design flexibility.

SVC Plus is designed such that the number of components is minimized. The reduced number of components and the modular design decreases the commissioning and installation time required for these systems. Fig. 50 compares the space requirement of a classic SVC with an SVC Plus. Where space is a concern, for example, in an existing substation within a megacity, SVC Plus can be an ideal solution. Also, the configuration of SVC Plus is such that it can be easily expanded or relocated. Moreover, the use of MMC in SVC Plus decreases the harmonics injected in the system, as seen in Fig. 51.

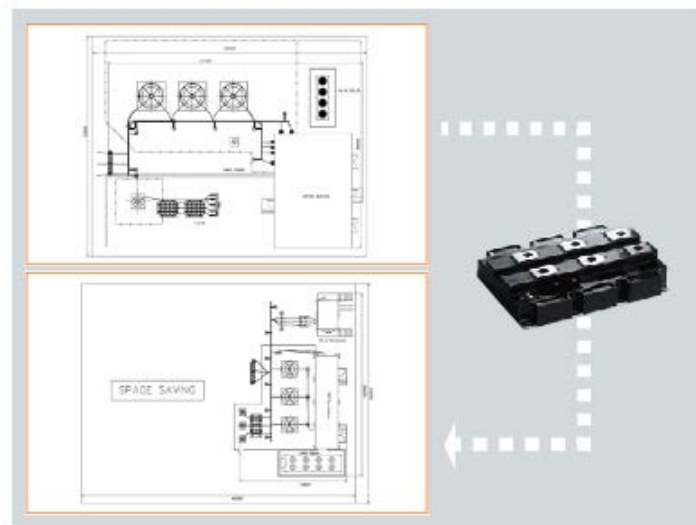


Fig. 50 Space requirement of an SVC plus compared with a classic SVC [104].

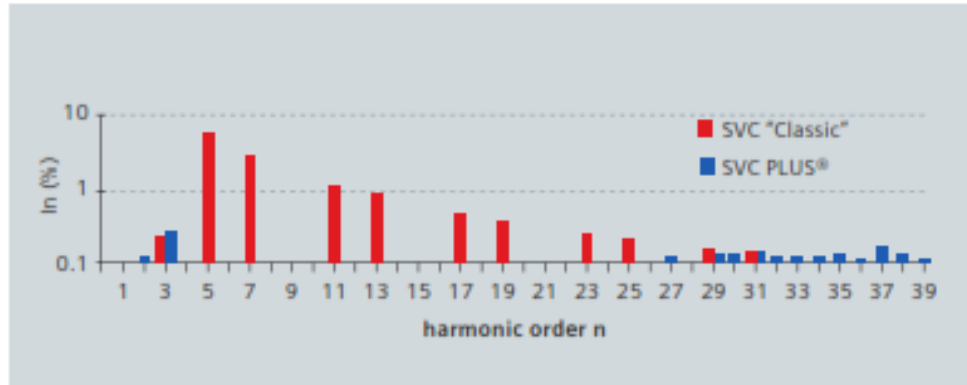


Fig. 51 Harmonics content of SVC plus versus SVC classic [104].

4.3 Mitsubishi HVDC Diamond

Mitsubishi has introduced an MMC-based HVDC interface system called HVDC-Diamond. There are several benefits and features listed for this technology that are as follows.

- Ability to control real and reactive powers at the same time.
- Minimum harmonic content.
- Ability to change the direction of the power flow without any change in the voltage.
- Ability to start easily after a black-out.
- Utilization of standard low frequency transformers.
- High reliability as a result of fast control and protection units.

HVDC Diamond is a VSC-based HVDC system, Fig. 52. The structure of HVDC-Diamond is shown in Fig. 53.

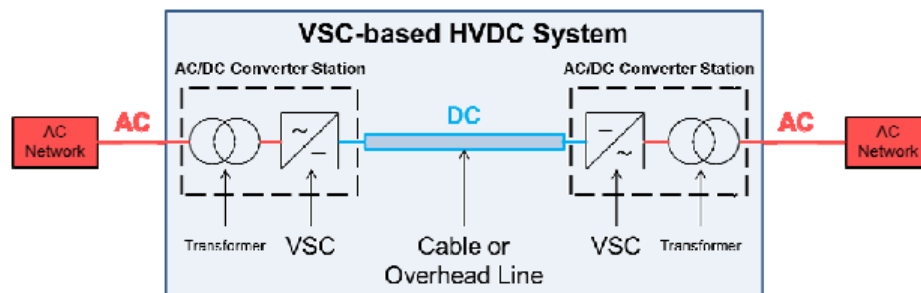


Fig. 52 A VSC-based HVDC configuration [104].

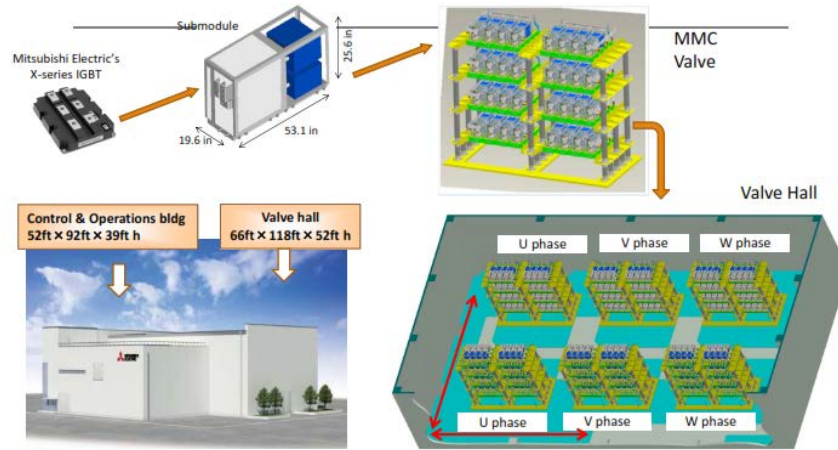


Fig. 53 The structure of Mitsubishi HVDC-Diamond [104].

4.4 ABB DC Circuit Breaker

ABB has recently introduced a new generation of DC circuit breakers in response to the fast growth of DC systems and power electronic devices, Fig. 54.

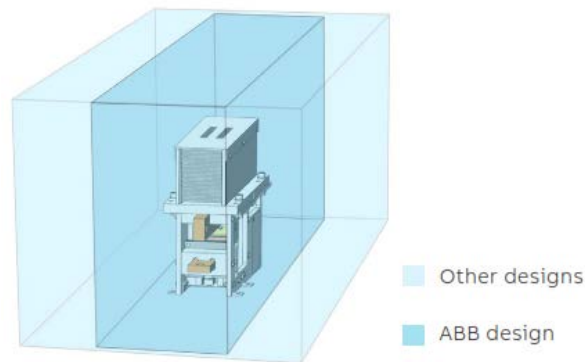


Fig. 54 ABB DC circuit breaker footprint compared to other technologies [105].

One of the features of this circuit breaker is that it complies with environmental standards related to the use of Cadmium in breaker contacts. Further, this circuit breaker has a much lighter design than the other products on the market. This results in a faster and easier installation. The ABB DC circuit breaker has a longer lifetime than the similar products with over 200,000 maintenance free operations.

4.5 ABB Plug and Play Microgrid

A modular and scalable plug and play microgrid solution (Fig. 55) is offered by ABB that can be a step forward towards flexible technologies in power distribution market. This is a containerized solution that includes a battery, a converter with a control system, and the ABB Microgrid Plus technology. The type of the input power source can be different based on the costumer's needs. It can be operated in both grid connected and islanded modes. Also, the containerized solution makes

the transportation and installation of this system faster and easier. Fig. 56 shows the detailed configuration of this technology.



Fig. 55 ABB modular microgrid [106].

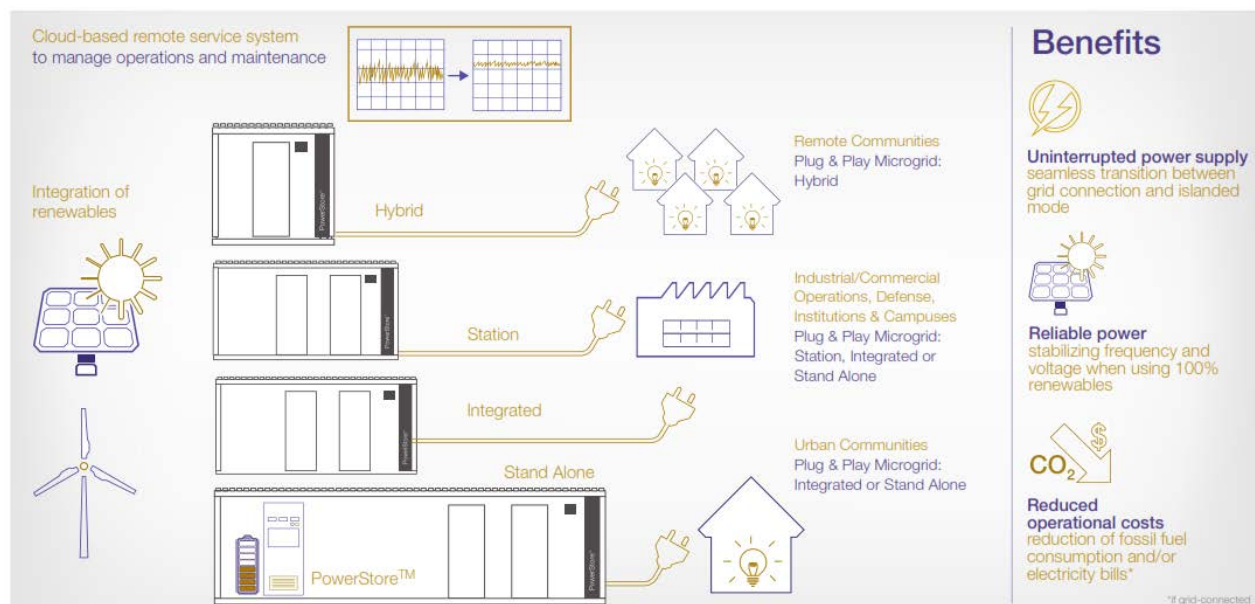


Fig. 56 Details on ABB Plug and Play microgrid [106].

4.6 Siemens Mobile STATCOM

Another power electronic based solution offered by Siemens is the mobile STATCOM, Fig. 57. This technology allows the fast relocation and installation of reactive power compensators when there is a need for voltage restoration and reactive power. All the equipment in this STATCOM is designed to be fit and transported within a container on a truck. This design is based on the plug and play configuration and minimizes the set up time.



Fig. 57 The Mobile STATCOM by Siemens [107].

5. Conclusions and Future Trends

This report provided a review of dominant power electronics applications for the power system and discussed the advantages and shortcomings. Emerging technologies such as wide bandgap (WBG) devices as well as niche and unconventional applications such as mobile and truck-mounted FACTS devices were also studied. Power electronics devices still have certain limitations despite the recent R&D efforts, several of which driven by large federally funded efforts, e.g., ARPA-E and DOE:

- Limited maximum blocking voltage
 - Possible solutions include series-connected devices and multilevel converters? WBG [Mainly Silicon Carbide (SiC) and Gallium Nitride (GaN)] also provide higher voltage ratings.
- Limited maximum switching frequency
 - Multilevel converter topologies can alleviate the need to higher frequencies by instead providing a higher resolution in voltage levels. Again, WBG devices have a higher frequency rating, lower losses, and higher temperature rating than conventional Si-based devices.
- Limited efficiency in certain applications
 - In one application that is considered in this project for voltage transformation, clearly magnetic conventional transformers have lower losses compared with a solid-state transformer. However, an SST can provide additional benefits, such as higher number of operations, ability to inject reactive power, and phase angle control. Moreover, if SST is used only as an add-on (that is, partially rated to provide the “tap changing” capability, many of these comparisons can be in favor of the SST-solution.
- High cost and limited experience of the personnel.

Despite these challenges, there are certain application areas in which power electronics devices are the only viable (or dominant) solution. These include:

- **Integration of renewables:** Nearly all modern converters (DC-DC and DC-AC) utilize power electronics, rather than machine-based solutions, because of their lower losses, higher speed, and minimal maintenance requirements. Existence of renewable portfolio standards/goals (US), organic need for increased power generation and availability of wind/solar resources (Australia and China), and environmental concerns (Europe) are drivers for integration of renewables which in turn increase the need for power electronics converters. As such, many countries now require fast transient simulations (electromagnetic type), e.g., in PSCAD, before they allow interconnection of new resources.
- **Power routing:** Power flows are determined by impedances, generator schedules, tap positions, and breaker statuses. While these can be coordinated to adjust and control power flow in a certain line, such solutions are mechanical and slow. Rather, power electronics devices known as FACTS can adjust the voltage or impedance of a line very fast: VSC-

based solutions (e.g., STATCOM and SSSC) in a cycle and thyristor-based devices (e.g., SVC) in a few cycles. Both of these times are much shorter than what is available with mechanical and conventional solutions. See the figure below for examples.

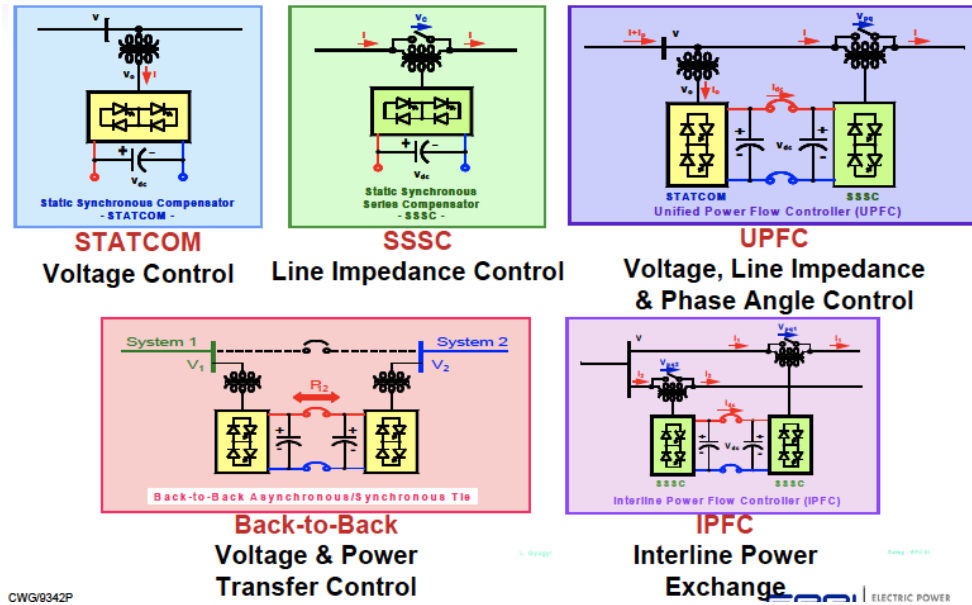


Figure 58. Example FACTS devices for power routing and control (from EPRI).

The high-penetration applications of power electronics, especially in light of increased renewable generation, can and will lead to system operational scenarios that challenge the existing paradigms of the power system. Two examples of such paradigms are reviewed below:

5.1 Notion of Inertia with Converter-Rich Power Systems

As the penetration of renewables increases in the power system, it is imperative to revisit the notion of inertia and its importance in for stability implications. A closely related concept is the relevance of frequency in such systems. Another consideration is the existence of motor loads (with inertia) in the system whose generation does not have mechanical inertia. In another project, we have worked on developing controllers for a system without any synchronous generators. The following figure shows some of the representative results demonstrating the viability of this concept. The studied scenario is load change when all system generators (IEEE 9-bus system) are replaced by VSC-based generation that need to share power among themselves.

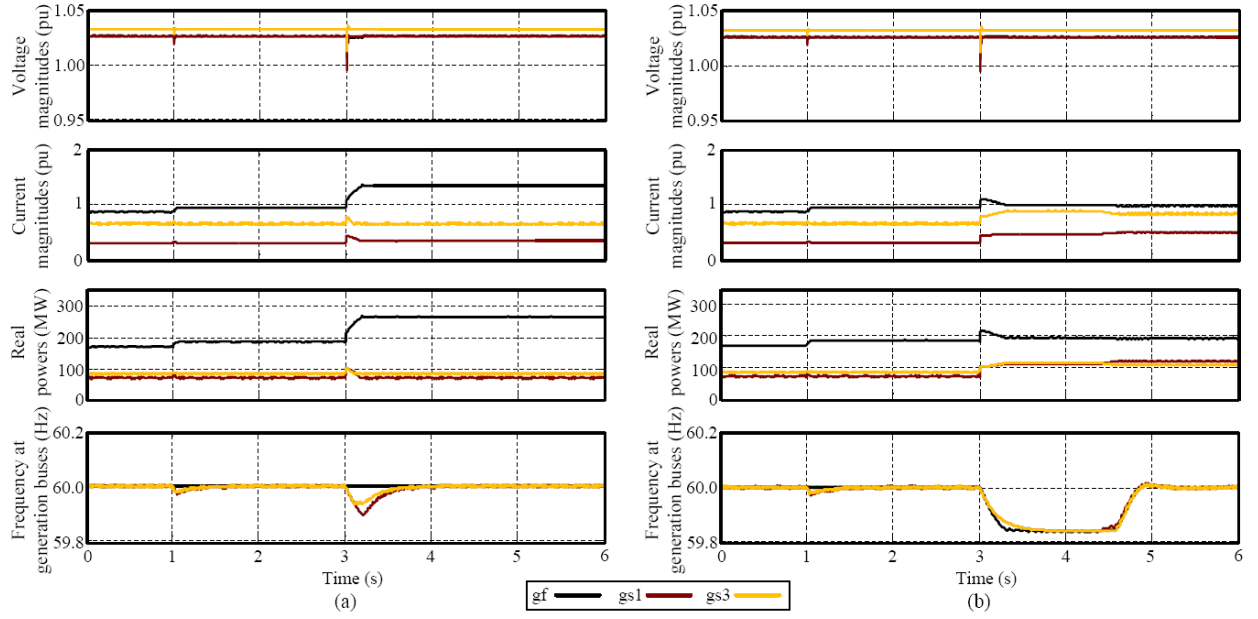


Figure 59. Unlimited grid-forming unit in the power system comprised of (a) all synchronous generators and (b) all VSC-based generation. In both systems, the load at bus 6 increases by 15 MW at $t = 1$ s and the load at bus 5 increases by 80 MW at $t = 3$ s.

5.2 Solid-State Transformers for Power Transfer Limit Improvement

In the conventional power system, load tap changers are utilized to increase power transfer limits by increasing the voltage. However, increasing the voltage also increases the impedance of the transformer which can reduce the effective increase in the power transfer. Solid-state transformers, however, can increase the voltage without a commensurate increase in the impedance and can hence be more effective in their function. Table 7 shows the preliminary results for increasing power transfer capability in a line in the IEEE 9-bus system. It is shown that with an SST, the increase in power for the same increase in voltage is 18.8% as opposed to 16.1% for a conventional transformer.

Table 7 Increased power transfer in the IEEE 9-bus system

Transformation tap (transformer-based or electronic) (%)	4.88%	9.54
Expected increase in power limit (%)	10	20
Achieved increase in power limit (transformer-based) (%)	8.39	16.11
Achieved increase in power limit (electronic) (%)	8.72	18.79
$\frac{L_{\text{leakage}}}{L_{\text{transmission}}}$	0.62	

References

- [1] Z. Chen, J. M. Guerrero, and F. Blaabjerg, "A review of the state of the art of power electronics for wind turbines," *IEEE Trans. Power Electron.*, vol. 24, no. 8, pp. 1859–1875, Aug. 2009.
- [2] F. Blaabjerg, Z. Chen, and S. B. Kjaer, "Power electronics as efficient interface in dispersed power generation systems," *IEEE Trans. Power Electron.*, vol. 19, no. 4, pp. 1184–1194, Sep. 2004.
- [3] D. Hansen, F. Iov, F. Blaabjerg, and L. H. Hansen, "Review of contemporary wind turbine concepts and their market penetration," *J. Wind Eng.*, vol. 28, no. 3, pp. 247–263, 2004.
- [4] M. P. Kazmierkowski, R. Krishnan, and F. Blaabjerg, *Control in Power Electronics-Selected Problems*. San Francisco, CA, USA: Academic, 2002.
- [5] F. Blaabjerg, M. Liserre, and K. Ma, "Power electronics converters for wind turbine systems," *IEEE Trans. Ind. Appl.*, vol. 48, no. 2, pp. 708–719, Mar-Apr. 2012.
- [6] R. Teodorescu, M. Liserre, and P. Rodriguez, *Grid Converters for Photovoltaic and Wind Power Systems*. New York, NY, USA: Wiley, 2011.
- [7] F. Blaabjerg, "Future on power electronics for wind turbine systems," *IEEE Journal of Emerging and Selected Topics in Power Electronics*, Vol. 1, No. 3, 2013.
- [8] *REN21—Renewables 2012 Global Status Report* [Online]. Available: <http://www.ren21.net>.
- [9] Green Energy—The Road to a Danish Energy System Without Fossil Fuels [Online]. Available: <http://www.klimakommissionen.dk/en-US/>
- [10] Vestas Wind Power, Aarhus, Denmark. (2011, Apr.). *Wind Turbines Overview* [Online]. Available: www.vestas.com
- [11] *Technical Regulation 3.2.5 for Wind Power Plants with a Power Output Greater than 11 kW*, Energinet, Fredericia, Denmark, Sep. 2010.
- [12] Requirements for Offshore Grid Connections in the E.ON Netz Network, E.ON-Netz, Bayreuth, Germany, Apr. 2008.
- [13] *Cost of Electricity by Source* [Online]. Available: http://en.wikipedia.org/wiki/Cost_of_electricity_by_source.
- [14] "Levelized cost of new generation resources in the annual energy outlook 2013," U.S. Dept. Energy, U.S. Energy Information Administration (EIA), Washington, DC, USA, 2013, [Online]. Available: <http://www.eia.gov/>
- [15] B. Hahn, M. Durstewitz, and K. Rohrig, "Reliability of wind turbines—Experience of 15 years with 1500 WTs," *Wind Energy*. Berlin, Germany:Springer-Verlag, 2007.
- [16] S. Yang, A. T. Bryant, P. A. Mawby, D. Xiang, L. Ran, and P. Tavner, "An industry-based survey of reliability in power electronic converters," *IEEE Trans. Ind. Appl.*, vol. 47, no. 3, pp. 1441–1451, May/Jun. 2011.
- [17] K. Ma, M. Liserre, and F. Blaabjerg, "Reactive power influence on the thermal cycling of multi-MW wind power inverter," *IEEE Trans. Ind. Appl.*, vol. 49, no. 2, pp. 922–930, Mar-Apr. 2013.
- [18] J. Friebe, M. Meinhardt, "Future challenges of power electronics for PV-inverter," *PCIM Europe*, May 2015, Nuremberg, Germany.
- [19] SMA Solar Tech. AG. "Sunny Boy 3600/5000 Smart energy – the perfect combination of PV inverter and battery," Niestetal, 2014.

- [20] T. Kaur, "Solar PV integration in smart grid-issues and challenges," *International Journal of Advanced Research in Electrical, Electronics and Instrumentation Engineering*, Vol. 4, Issue 7, 2015.
- [21] S. Kurtz, C. Deline, J. Wohlgemuth, et. al., "Opportunities and challenges for power electronics in PV modules," *ARPA Workshop*, Feb. 2011.
- [22] "Power Transformers Market - Global Industry Analysis, Size, Share, Growth, Trends and Forecast, 2013 – 2019," Transparency Market Research, November 2, 2013, [Online], Available: <http://www.prweb.com/releases/2013/11/prweb11294070.htm>
- [23] Wide bandgap power electronics technology assessment, *Government report*, 2015, [Online] Available: www.energy.gov
- [24] T. Meynard, H. Foch, P. Thomas, J. Courault, et. al., "Multicell converters: basic concepts and industry applications," *IEEE Transactions on Industrial Electronics*, Vol. 49, No. 5, 2002.
- [25] P. Shuai, J. Biela, "Influence of material properties and geometric shape of magnetic cores on acoustic noise emission of medium frequency transformers," *IEEE Transaction on Power Electronics*, under review, 2016.
- [26] J. W. Kolar and G. Ortiz, "Solid-State-Transformers: Key Components of Future Traction and Smart Grid Systems," in *Proc. of the International Power Electronics Conf. (IPEC)*, May 2014.
- [27] X. She, R. Burgos, G. Wang, F. Wang, and A. Q. Huang, "Review of solid state transformer in the distribution system: From components to field application," in *Proc. of the Energy Conversion Congr. And Expo. (ECCE)*, Sep. 2012, pp. 4077–4084.
- [28] A. Q. Huang, M. L. Crow, G. T. Heydt, J. P. Zheng, and S. J. Dale, "The Future Renewable Electric Energy Delivery and Management (FREEDM) System: The Energy Internet," *Proc. IEEE*, vol. 99, no. 1, pp. 133–148, Jan. 2011.
- [29] J. E. Huber and J. W. Kolar, "Volume/Weight/Cost Comparison of a 1MVA 10 kV/400 V Solid-State against a Conventional Low-Frequency Distribution Transformer," in *Proc. of the Energy Conversion Congr. and Expo. (ECCE)*, Sep. 2014, pp. 4545–4552.
- [30] D. Rothmund, G. Ortiz, and J. W. Kolar, "SiC-based Unidirectional Solid-State Transformer Concepts for Directly Interfacing 400V DC to Medium-Voltage AC Distribution Systems," in *Proc. of the Telecommunications Energy Conf. (INTELEC)*, Sep. 2014, pp. 1–9.
- [31] E. Huber and J. W. Kolar, "Optimum Number of Cascaded Cells for High-Power Medium-Voltage Multilevel Converters," in *Proc. of the Energy Conversion Congr. and Expo. (ECCE)*, Sep. 2013, pp. 359–366
- [32] D. Rothmund, J. E. Huber, and J. W. Kolar, "Operating Behavior and Design of the Half-Cycle Discontinuous-Conduction-Mode Series- Resonant-Converter with Small DC link Capacitors," in *Proc. of the Workshop on Control and Modeling for Power Electronics (COMPEL)*, Jun. 2013, pp. 1–9
- [33] T. Guillod, J. E. Huber, G. Ortiz, A. De, C. M. Franck, and J. W. Kolar, "Characterization of the Voltage and Electric Field Stresses in Multi-Cell Solid-State Transformers," in *Proc. of the Energy Conversion Congr. and Expo. (ECCE)*, Sep. 2014, pp. 4726–4734.
- [34] C. Zhao, D. Dujic, A. Mester, J. K. Steinke, M. Weiss, S. LewdeniSchmid, T. Chaudhuri, and P. Stefanutti, "Power Electronic Traction Transformer - Medium Voltage Prototype," *IEEE Trans. Ind. Electron.*, vol. 61, no. 7, pp. 3257–3268, Jul. 2014.

- [35] T. Guillod, F. Krismer, R. Farber, et. al., "Protection of MV/LV solid-state transformers in distribution grid," *High Voltage Laboratory Report, ETH Zurich*.
- [36] J. W. Kolar, "Research challenges and future perspectives of solid-state transformers," *ETH Zurich High Power Electronics Lab Report, 2015*.
- [37] Z. J. Shen, "Ultrafast solid-state circuit breakers: Protecting converter-based ac and dc microgrids against short circuit faults," *IEEE Electrification Magazine*, Vol. 4, Issue 2, 2016.
- [38] F. Tosato, "Voltage sags mitigation on distribution utilities," *Eur. Trans. Elect. Power*, Vol. 11, No. 1, Jan./Feb. 2001.
- [39] L. Klingbeil, W. Kalkner, and C. Heinrich, *Fast Acting Solid-State Circuit Breaker Using State-of-the-Art Power-Electronics Devices*. Graz, Austria: EPE, 2001.
- [40] C. Meyer, S. Scroder, R. De Doncker, "Solid-state circuit breakers and current limiters for medium voltage systems having distributed power systems," *IEEE Transactions on Power Electronics*, Vol. 19, No. 5, 2004.
- [41] A. Ekström, P. Bennich, M. De Oliveira, and A. Wilkström, *Design and Control of a Current-Controlled Current Limiting Device*. Graz, Austria: EPE, 2001.
- [42] R. Mehl, P. Meckler, "Comparison of advantages and disadvantages of electronic and mechanical protection systems for higher voltage DC 400 V," *Proceedings of 2013 35th International Telecommunications Energy Conference 'Smart Power and Efficiency'*, Germany 2013.
- [43] S. Whaite, B. Grainger, A. Kwasinski, "Power quality in DC power distribution systems and microgrids," *Journal of Energies*, 2015.
- [44] S. Vazquez, S. M. Lukic, E. Galvan, L. G. Franquelo, and J. M. Carrasco, "Energy storage systems for transport and grid applications," *IEEE Trans. Ind. Electron.*, vol. 57, no. 12, pp. 3881–3895, Dec. 2010.
- [45] G. Wang, G. Konstantinou, C. Townsen, et. al., "A review of power electronics for grid connection of utility-scale battery energy storage systems," *IEEE Transactions on Sustainable Energy*, Vol. 7, No. 4, 2016.
- [46] H. Akagi, "Classification, terminology, and application of the modular multilevel cascade converter (MMCC)," *IEEE Trans. Power Electron.*, vol. 26, no. 11, pp. 3119–3130, Nov. 2011.
- [47] N. Kawakami *et al.*, "Development of a 500-kW modular multilevel cascade converter for battery energy storage systems," *IEEE Trans. Ind. Appl.*, vol. 50, no. 6, pp. 3902–3910, Nov. 2014.
- [48] C. D. Townsend, T. J. Summers, and R. E. Betz, "Control and modulation scheme for a cascaded H-bridge multilevel converter in large scale photovoltaic systems," in *Proc. Energy Convers. Congr. Expo.*, Sep. 2012, pp. 3707–3714.
- [49] M. Hagiwara, R. Maeda, and H. Akagi, "Negative-sequence reactive power control by a PWM STATCOM based on a modular multilevel cascade converter (MMCC-SDBC)," *IEEE Trans. Ind. Appl.*, vol. 48, no. 2, pp. 720–729, Mar. 2012.
- [50] Y. Yu, G. Konstantinou, B. Hredzak, and V. G. Agelidis, "Power balance of cascaded H-bridge multilevel converters for large-scale photovoltaic integration," *IEEE Trans. Power Electron.*, vol. 31, no. 1, pp. 292–303, Jan. 2016.
- [51] L. Maharjan, S. Inoue, H. Akagi, and J. Asakura, "State-of-charge (SOC) balancing control of a battery energy storage system based on a cascade pwm converter," *IEEE Trans. Power Electron.*, vol. 24, no. 6, pp. 1628–1636, Jun. 2009.

- [52] ABB, DynaPeaQ SVC light with energy storage. [Online]. Available: [http://www02.abb.com/global/gad/gad02181.nsf/0/1c9442cf6083140ac1257a62003621b5/\\$file/DynaPeaQ](http://www02.abb.com/global/gad/gad02181.nsf/0/1c9442cf6083140ac1257a62003621b5/$file/DynaPeaQ).
- [53] US Department of Energy, Global energy storage database. [Online]. Available: <http://www.energystorageexchange.org/>
- [54] Global Wind Energy Council, Global wind report 2014: Annual market update. Mar. 2015 [Online]. Available: http://www.gwec.net/wpcontent/uploads/2015/03/GWEC_Global_Wind_2014_Report_LR.pdf.
- [55] V. Rudolf and K. D. Papastergiou, "Financial analysis of utility scale photovoltaic plants with battery energy storage," *Energy Policy*, vol. 63, pp. 139–146, 2013.
- [56] AES marks energy storage milestone with 400,000 MW-h of PJM service from Laurel Mountain. Apr. 11, 2013. [Online]. Available: <http://www.aesenergystorage.com/2013/04/11/aes-marksenergy-storage-milestone-with-400000-mw-h-of-pjm-service-fromlaurel-mountain>.
- [57] M. Bragard, N. Soltau, S. Thomas, and R. W. De Doncker, "The balance of renewable sources and user demands in grids: Power electronics for modular battery energy storage systems," *IEEE Trans. Power Electron.*, vol. 25, no. 12, pp. 3049–3056, Dec. 2010.
- [58] B. M. Grainger, G. F. Reed, A. R. Sparacino, and P. T. Lewis, "Power electronics for grid-scale energy storage," *Proc. IEEE*, vol. 102, no. 6, pp. 1000–1013, Jun. 2014.
- [59] H. Akagi, "Large static converters for industry and utility applications," *Proc. IEEE*, vol. 89, no. 6, pp. 976–983, Jun 2001.
- [60] N. Hingorani, "FACTS Technology-State of the art, current challenges and future prospects," *Power Engineering Society General Meeting*, 2007.
- [61] H. Tyll, F. Schettler, "Power system problems solved by FACTS devices," *2009 IEEE/PES Power Systems Conference and Exposition*, 2009.
- [62] R. Lasseter, "Smart distribution: Coupled microgrids," *IEEE Proc.*, Vol. 99, No. 6, pp. 1074-1082, Jun. 2011.
- [63] M. Barnes, J. Kondoh, H. Asano, J. Oyarzabal, G. Venkataramanan, R. Lasseter, N. Hatziargyriou, and T. Green, "Real-world microgrids – an overview," in *Proc. IEEE SoSE*, pp. 1-8, 2007.
- [64] N. Hatziargyriou, H. Asano, R. Iravani, and C. Marnay, "Microgrids," *IEEE Power Energy Mag.*, Vol. 6, No. 4, pp. 78-94, Jul./Aug. 2007.
- [65] D. Olivares, A. Mehrizi-Sani, A. Etemadi, et. al., "Trends in microgrid control," *IEEE Transactions on Smart Grid*, Vol. 5, No. 4, 2014.
- [66] S. Chakraborty and M. G. Simoes, "Advanced active filtering in a single high frequency AC microgrid," in *Proc. IEEE PESC*, pp. 191-197, 2005.
- [67] J. Driesen and F. Katiraei, "Design for distributed energy resources," *IEEE Power and Energy Mag.*, Vol. 6, No. 3, pp. 30-40, May/Jun. 2008.
- [68] X. Wang, J. Guerrero, F. Blaabjerg, "A review of power electronics based microgrids," *Journal of Power Electronics*, Vol. 12, No. 1, 2012.
- [69] K. Mizuguchi, S. Muroyama, Y. Kuwata, and Y. Ohashi, "A new decentralized dc power system for telecommunications systems," in *Proc. IEEE INTELEC*, pp. 55-62, 1990.
- [70] J. Ciezki and R. Ashton, "Selection and stability issues associated with a navy shipboard dc zonal electric distribution system," *IEEE Trans. Power Del.*, Vol. 15, No. 2, pp. 665-669, Apr. 2000.

- [71] A. Sannino, G. Postiglione, and M. Bollen, "Feasibility of a dc network for commercial facilities," *IEEE Trans. Ind. Appl.*, Vol. 39, No. 5, pp. 1499-1507, Sep./Oct., 2003.
- [72] S. Chakraborty, M. D. Weiss, and M. G. Simoes, "Distributed intelligent energy management system for a single-phase high-frequency ac microgrid," *IEEE Trans. Ind. Electron.*, Vol. 54, No. 1, pp. 1-13, Feb. 2007.
- [73] H. Kim, T. Yu, and S. Choi, "Indirect current control algorithm for utility interactive inverters in distributed generation systems," *IEEE Trans. Power Electron.*, Vol. 23, No. 3, pp.1342-1347, May 2008.
- [74] P. Roussel, "SiC market and industry update," presented at the Int. SiC Power Electron. Appl. Workshop, Kista, Sweden, 2011.
- [75] J. Millan, A. Perez, J. Rebollo, "A survey of wide bandgap power semiconductor devices," *IEEE Transactions on Power Electronics*," Vol. 29, No. 5, 2014.
- [76] J. Millan, "Wide band-gap power semiconductor devices," *IET Circuits, Devices & Systems*, Vol. 1, Issue 5, 2007.
- [77] M. Loboda, "SiC - Overcoming Cost and Materials Defects", *Power Electronic Technology*, Nov 2012.
- [78] P. Gammon, "Silicon and the wide bandgap semiconductors, shaping the future power electronic device market," *14th International Conference on Ultimate Integration on Silicon*, 2013.
- [79] e.F Huang, "Development of 4H-silicon carbide BJTs for power electronic applications", Ph.D. Dissertation, Purdue University, 2003.
- [80] S. Pearton, *CaN and 2nO-based Materials and Devices*, (Springer, Berlin, 2012.
- [81] N. Kaminski and O. Hilt, "SiC and CaN Devices Wide Band-Cap is not all the Same," *POWER2 Conference*, Warwick. 2012.
- [82] Isberg, J., Hammersberg, J., Johansson, E., Wikstro"m, T., Twitchen, D.J., Whitehead, A.J., Coe, S.E., and Scarsbrook, G.A.: 'High carrier mobility in single-crystal plasma-deposited diamond', *Science*, 2002, 297, pp. 1670–1672.
- [83] Twitchen, D.J., Whitehead, A.J., Coe, S.E., Isberg, J., Hammersberg, J., Wikstro"m, T., and Johansson, E.: 'High-voltage single-crystal diamond diodes', *IEEE Trans. Electron. Dev.*, 2004, 51, pp. 826–828.
- [84] Taniuchi, H., Umezawa, H., Arima, T., Tachiki, M., and Kawarada, H.: 'High-frequency performance of diamond field-effect transistor', *IEEE Electron Device Lett.*, 2001, 22, pp. 390–392.
- [85] Aleksov, A., Denisenko, A., Spitzberg, U., Jenkins, T., Ebert, W., and Kohn, E.: 'RF performance of surface channel diamond FETs with sub-micron gate length', *Diam. Relat. Mater.*, 2002, 11, pp. 382–38.
- [86] E. Van Brunt et. al, "27 kV, 20 A 4H-SiC n-IGBTs", *Mat. Sci. Forum*, Vol. 821-823, pp. 847-850, 2015.
- [87] Li Wang et.al. "A medium voltage bidirectional DC-DC converter combining resonant and dual active bridge converters," 2015 APEC, vol., no., pp.1104,1111, 15-19 March 2011.
- [88] A. Huang, "Wide bandgap power devices and their impacts on power delivery systems," *2016 IEEE International Electron Devices Meeting*, 2016.
- [89] A.P. Zhang, L.B. Rowland, E.B. Kaminsky, V. Tilak, J.C. Grande, J. Teetsov, A. Vertiatchikh, and L.F Eastman, *1. of Elec. Mat.* 32, 388, 2003.
- [90] B. J. Baliga, BEvolution of MOS-bipolar power semiconductor technology, *Proc. IEEE*, vol. 76, pp. 409–418, Apr. 1988.

- [91] L. M. Tolbert, F. Z. Peng, and T. G. Habetler, "Multilevel converters for large electric drives," *IEEE Trans. Ind. Appl.*, vol. 35, pp. 36–44, Jan./Feb. 1999.
- [92] L. G. Franquelo, J. Rodriguez, J. I. Leon, S. Kouro, R. Portillo, and M. A. M. Prats, "The age of multilevel converters arrives," *IEEE Ind. Electron. Mag.*, pp. 28–39, Jun. 2008.
- [93] J. Rodriguez, L. Franquelo, S. Kouro, et. al., "Multilevel converters: An enabling technology for high-power applications," *Proceedings of the IEEE*, Vol. 97, Issue 11, 2009.
- [94] J. Holtz, "Pulsewidth modulation for power converters," *Proc. IEEE*, vol. 82, pp. 1194–1214, Aug. 1994.
- [95] R. Teodorescu, F. Blaabjerg, J. K. Pedersen, E. Cengelci, S. Sulistijo, B. Woo, and P. Enjeti, "Multilevel converters a survey," in *Proc. Eur. Power Electron. Conf.*, Lausanne, Switzerland, 1999.
- [96] A. Nabae, I. Takahashi, and H. Akagi, "A neutral-point clamped PWM inverter," *IEEE Trans. Ind. Appl.*, vol. IA-17, pp. 518–523, Sep./Oct. 1981.
- [97] T. A. Meynard and H. Foch, "Multilevel choppers for high voltage applications," in *Proc. Eur. Conf. Power Electron. Appl.*, 1992, vol. 2, pp. 45–50.
- [98] M. Marchesoni, M. Mazzucchelli, and S. Tenconi, "A non-conventional power converter for plasma stabilization," in *Proc. Power Electron. Spec. Conf.*, 1988, pp. 122–129.
- [99] T. Bruckner, S. Bernet, and H. Guldner, "The active NPC converter and its loss balancing control," *IEEE Trans. Ind. Electron.*, vol. 52, pp. 855–868, Jun. 2005.
- [100] E. Villanueva, P. Correa, and J. Rodriguez, "Control of a single phase H-Bridge multilevel inverter for grid-connected PV applications," in *Proc. 13th Int. Power Electron. Motion Contr. Conf. (EPE-PEMC 2008)*, Poznan, Poland, Sep. 1–3, 2008, pp. 466–470.
- [101] J. Rodriguez, J. Pontt, N. Becker, and A. Weinstein, "Regenerative drives in the megawatt range for high-performance downhill belt conveyors," *IEEE Trans. Ind. Appl.*, vol. 38, no. 1, pp. 203–210, 2002.
- [102] J. R. Rodriguez, J. Pontt, R. Huerta, G. Alzamora, N. Becker, S. Kouro, P. Cortes, and P. Lezana, "Resonances in a high-power active-front-end rectifier system," *IEEE Trans. Ind. Electron.*, vol. 52, no. 2, pp. 482–488, 2005.
- [103] PCS-9590 Series DC De-Icer, NR-Electric Co., [Online] Available: <http://nrec.com/en/product/PCS-9590.html>
- [104] SVC Plus (VSC Technology), Siemens, [Online] Available: <https://www.energy.siemens.com/co/en/power-transmission/facts/static-var-compensator-plus/#content=Details>
- [105] DC Rolling Stock Circuit Breaker, ABB, [Online] Available: <http://new.abb.com/medium-voltage/apparatus/circuit-breakers/dc-circuit-breakers-for-railway/dc-railway-circuit-breaker-dcbreak>
- [106] ABB Launches Plug and Play Microgrid, ABB, [Online] Available: <http://www.abb.com/cawp/seitp202/BD6B7A09C76F6070C1258045004560AF.aspx>
- [107] Portable Power Solutions, Siemens, [Online] Available: <https://www.siemens.com/global/en/home/products/energy/high-voltage/substations/portable-power-solutions.html>
- [108] T. Luth, M. Merlin, T. Green, F. Hassan, C. Barker, "High-frequency operation of a DC/AC/DC System for HVDC applications," *IEEE Trans. Power. Elec.*, Vol. 29, Issue 8, 2014.

Part II

The Role of Basic Impulse Insulation Level in the Application of Power Electronics at the Distribution Level

Gerald Heydt

Arizona State University

For information about this project, contact:

Gerald Thomas Heydt
Arizona State University
School of Electrical, Computer, and Energy Engineering
P.O. BOX 875706
Tempe, AZ 85287-5706
Phone: 480-965-8307
Fax: 480-727-2052
heydt@asu.edu

Power Systems Engineering Research Center

The Power Systems Engineering Research Center (PSERC) is a multi-university Center conducting research on challenges facing the electric power industry and educating the next generation of power engineers. More information about PSERC can be found at the Center's website: <http://www.pserc.org>.

For additional information, contact:

Power Systems Engineering Research Center
Arizona State University
527 Engineering Research Center
Tempe, Arizona 85287-5706
Phone: 480-965-1643
Fax: 480-727-2052

Notice Concerning Copyright Material

PSERC members are given permission to copy without fee all or part of this publication for internal use if appropriate attribution is given to this document as the source material. This report is available for downloading from the PSERC website.

© 2018 Arizona State University. All rights reserved

Table of Contents

1. The Role of Basic Impulse Insulation Level in the Application of Power Electronics at the Distribution Level	1
1.1 Basic impulse insulation level	1
1.2 General discussion and literature survey	1
1.3 Organization of this report.....	4
2. BIL Formatting	5
2.1 A focus on IEC Standard 60071	5
2.2 A possible inconsistency in BIL specification at the 15 kV class	5
2.3 Main observations drawn from the literature search	6
2.4 Methods for providing for BIL requirements in power distribution circuits with electronic devices	9
3. Metal Oxide Varistors and Similar Surge Suppressors	10
3.1 Surge suppression devices	10
3.2 Ratings of MOVs and lightning arresters	10
3.3 Principal conclusions relating to MOVs and lightning arresters.....	14
4. Safety Issues.....	16
4.1 Safety in distribution class applications	16
4.2 Reduction of peak voltage	16
4.3 Failure of the MOVs.....	16
4.4 Speed of operation	16
References	17

List of Figures

Fig. 3.1 Lightning arrester and equipment insulation withstand in the time – voltage plane	14
Fig. 3.2 Lightning arrester characteristics (lower curve) and equipment withstand voltage (upper curve) for gapless MOV applications (taken directly from [12]).....	15

List of Tables

Table 2.1 Classes and shapes of overvoltages, standard voltage shapes, and standard withstand voltage tests, taken directly from IEC 60071.....	7
Table 2.2 Standard insulation levels for range I ($1 \text{ kV} \leq V_m \leq 245 \text{ kV}$), taken directly from IEC 60071	8
Table 3.1 Lightning arrester ratings for various types of technologies	11
Table 3.2 Arrester selection for ANSI lightning arresters Table agrees with IEEE standards	12
Table 3.3 Arrester selection for IEC lightning arresters Table agrees with IEC standards	13

Nomenclature

Abbreviations

<i>ANSI</i>	American National Standards Institute
<i>BIL</i>	Basic Impulse Insulation Level
<i>FCL</i>	Fault Current Limiter
<i>FREEDM</i>	Future Renewable Electric Energy Distribution Management (an NSF supported center)
<i>GTO</i>	Gate Turn Off
<i>HVDC</i>	High Voltage DC
<i>IEC</i>	International Electrotechnical Commission
<i>IEEE</i>	Institute of Electric and Electronic Engineers
<i>IGBT</i>	Insulated Gate Bipolar Transistor
<i>LIWL</i>	Lightning Impulse Withstand Level
<i>MCOV</i>	Maximum continuous operating voltage
<i>MMC</i>	Modular Multilevel Converter
<i>MOV</i>	Metal Oxide Varistor
<i>NSF</i>	National Science Foundation
<i>RMS</i>	Root Mean Square
<i>SSFCL</i>	Solid State Fault Current Limiter
<i>T1</i>	Rise time
<i>T2</i>	Fall time (i.e., peak to half voltage)
<i>Um</i>	Highest voltage applied to an asset (rms volts, phase to ground, European notation)
<i>Vm</i>	Highest voltage applied to an asset (rms volts, phase to ground)
<i>VSC</i>	Voltage Sourced Converter

1. The Role of Basic Impulse Insulation Level in the Application of Power Electronics at the Distribution Level

1.1 Basic impulse insulation level

Basic Impulse Insulation Level (BIL), also termed Lightning Impulse Withstand Level (LIWL) is discussed in this chapter. The application area is in power electronic controls and devices in power distribution systems (e.g., 15 kV class). The topical coverage of this volume includes the following:

- A literature survey of this topic
- Identification of the BIL requirements and the connection with the applicable codes and standards
- Methods to attain the BIL requirements
- A discussion of safety.

1.2 General discussion and literature survey

Several technical papers from the literature have addressed the subject of testing, application, and practical considerations for electronic controllers in power distribution systems. A sampling of the papers is shown in this section.

1.2.1 Testing of electronic components

The paper “Operational Tests for the MMC-Based VSC Valves” [1] discusses the operational testing of VSC valves. Basically the valve support to ground tested with a standard impulse. The test between the valve terminals also include impulse test for two level converters. However the Modular Multi– Level converter (MMC) is not tested directly by an impulse. One of the authors, Davidson Collin of ALSTOM, states (verbatim):

“The impulse test depends on the valve technology (2-level converter vs MMC) and on whether you are talking about the voltage between valve terminals or the voltage across the valve support. Tests across the valve support include a lightning impulse test but this is conventional, determined in the normal way as for any equipment, and doesn’t stress the active components (IGBTs).

For tests between valve terminals, a lightning impulse test is specified only for valves for 2-level converters – not for MMC valves. Note also that 2-level converter valves effectively experience a lightning impulse between their terminals every time they turn off, so this is an important test.

For MMC valves, impulse tests between terminals are not specified because the inbuilt capacitance is so large that it is impossible even to achieve a switching impulse, let alone a lightning impulse, without requiring so much current that

all the freewheel diodes would be destroyed instantly (just calculate how much current would be needed to charge a 10 mF capacitor to 3 kV in 250 μ s!).”

The use of distribution class STATCOMs has been proposed and applied in some distribution systems. The paper “STATCOM: a new era of reactive compensation” [2] discusses the dielectric test. The paper states:

“The dielectric tests were performed on a complete valve assembly when mounted in its cabin. The test comprised standard power frequency and lightning impulse test to the earth appropriate to 36 kV class plus special power frequency and switching impulse test between the valve terminals.”

“A voltage test between the terminals started with the power frequency tests which was followed by “three impulse of non-standard switching surge. The time to peak was 2.5 ms, and 100 ms time to half value. The peak amplitude was 53.9 kV, which is 10% higher than the valve surge arrester protective level. The nonstandard wave shape reflects the very slow natural response of the converter to an externally applied overvoltage”.

Various international groups have addressed the subject of electronic devices in power systems in general. For example, the CIGRE Working Group 33/14.05 [3] published a document that explains that valves and converters usually not stressed by lightning overvoltage because of shielding by the smoothing reactor and by the converter transformer. Unfortunately, a ground fault produces a steep front impulse similar to a lightning stroke. This suggests testing of the arrester with 1 / 2.5 microsecond or 4 / 10 microsecond impulses.

It is interesting that this document propose the testing of the valve with the arresters. This includes the determination of the residual voltage using:

- a) Steep current impulse (1/20 microsecond)
- b) Lightning current impulse (8/20 microsecond)
- c) Switching current impulse (30/100 microsecond)
- d) Slow front switching current impulse (front time 1 ms and half value 2-4 ms). An important consideration is the degradation of the arrester by the time of operation.

CIGRE publications

Referring for the CIGRE publications, Jonathan Danielsson of ABB provided the following explanation:

“I received your inquiry about BIL test voltages for HVDC Light converters. It is not a trivial question to answer since standard test levels for DC equipment does not exist in the same way as they do for AC equipment. For an HVDC installation an insulation coordination will be performed and it is based on a design philosophy achieved as the result of our extensive experience with

HVDC system and proven by our operational experience. The philosophy is also described in the CIGRE document “Guidelines, for the application of metal oxide arresters without gaps for HVDC converter stations”, and as well as in IEC 60071-5. For VSC valves IEC 62501 describes the electrical testing. But the standards only specify how the test levels should be calculated from the protective levels. The protective levels will however be defined by the arrester selected which is a result from the insulation coordination study”

IEEE Standard C57, 1303 and the IEC Standards 61954, 60071

The paper [4] discusses the stress subjected by HVDC converter transformers, presently only the line commutated inverters (thyristor valves) are considered. This document describes separately AC line winding and DC line winding tests. The AC winding test includes:

- a) Lightning Impulse test , including chopped impulse
- b) Switching impulse test
- c) AC short duration test
- d) AC long duration test.

These tests are similar to the test of every power transformer (IEEE C57). The valve winding tests include:

- a) Lightning Impulse test with standard 1.2/50 microsecond and chopped voltage test with 30% less amplitude. The untested terminals are grounded.
- b) Switching Impulse test. This test is performed with the test voltage simultaneously applied to both terminals.
- c) DC separate source voltage test. The test voltage is simultaneously applied both terminals. “The test voltage amplitude is 150% of the arithmetic sum of AC-voltage, and the average DC offset forms the test voltage.
- d) DC polarity reversal test.
- e) AC separate source voltage withstand test. The test voltage applied simultaneously on both terminals.

This standard also shows that the DC and AC winding stresses are different. The stress levels are determined by EMTDC simulations and actual system fault recordings were used to develop this information. The studies should investigate the effect DC polarity reversal, commutation failures and current harmonics.

Attention is called to the IEC 61954-1999 [5] standard on “Power electronics for electrical transmission system testing of thyristor valves for static VAR compensator”. This standard describes the recommended test procedure for a static VAR compensator but the standard does not refer to any impulse test or verification of transient behavior. It is expected that the dielectric tests are performed by the manufacturer.

IEEE 1303-1994 IEEE guide for Static var Compensator Field Tests [6] discusses each aspect of field testing for manufacturer supplied and tested equipment. This guide does not discuss insulation coordination or dielectric tests. However, Section 5.4.2 of the guide, “Dynamic Testing,” refers to transients and specifies tests included with tests for a transmission line switched into and out of service, and the energization of a capacitor bank and identification of possible resonance. The guide recommends the use of high resolution (kHz range) recorders.

The standard IEC 62501 2009 “Voltage sourced converter (VSC) valves for high-voltage direct current (HVDC) power transmission - Electrical testing” according a paper by Xu Tianning [1] describes all electrical tests needed for VSC valves. The tests include lightning impulse tests. This standard was updated in 2014 and applies to self-commutated converter valves for use in a three phase bridge voltage source converter (VSC). The VSC is intended for high voltage dc power transmission or as a back-to-back link. An important part of this publication is the lighting impulse test.

The IEC Standard 60071-5 2014 “Insulation Co-ordination Part 5 Procedures for High Voltage Direct Current (HVDC)” [8] presents a method for insulation coordination without specifying the test voltages. The standard is not applicable for industrial systems. The standard deals with study tools and modeling techniques. Typical examples are creepage distances and clearances. The standard is available from India which has now reproduced the original IEC standards and made these available free of charge. This all-encompassing, extensively illustrated guide explains how to apply IEC standards in testing high voltage equipment. It also draws on the author’s experience to sketch in some detail for future trends.

1.3 Organization of this report

This part of the final report on PSerc project T-58 has four chapters. The first chapter contains a literature summary, and the second chapter focuses on the BIL and how it is defined and specified. The project is mainly distribution oriented, and this is the focus. Chapter three focuses on metal oxide varistors, the main surge suppression device used in distribution circuits. Chapter four relates to safety issues with regard to power electronic applications in distribution circuits.

2. BIL Formatting

2.1 A focus on IEC Standard 60071

The main international standard for impulse testing of solid state components directly connected (ohmically, galvanically) to a high voltage power circuit appears in IEC 60071 [11]. The main parameters of the tests are shown in what is termed Tables 1 and 2 from these standards. These are reproduced here as Tables 2.1 and 2.2 verbatim.

2.2 A possible inconsistency in BIL specification at the 15 kV class

In the progress of the presently reported research, it has been discovered that a number of researchers quote variant values of BIL for equipment in the 15 kV distribution class. Of course, at higher voltages BIL specifications are governed by appropriate standards suited for transmission engineering. For example, Lambert in [16] cites a BIL of 650 kV for a 138 kV superconducting fault current limiter (FCL). This citation of BIL seems to be inconsistent with the IEC 60071 Standard. Instead, Lambert cites the IEEE C37.06 standard. It is worthwhile to caution readers that most standards cite the voltage class as a phase to neutral value (not phase – phase). Of course, rms values of voltage are used. Some citations, particularly embedded in the literature, use phase-phase voltage specifications (e.g., '15 kV class' – does this mean phase-phase or phase-neutral, and is an asset for 15.5 kV included?). With these potential pitfalls and inconsistencies in view, note that the following citations from the literature have been identified:

- The recommendation of a 95 kV BIL should be used for a 13.8 kV distribution primary, recommended for a solid state FCL in [17].
- A 1.2 / 50 μ s 'impulse' with peak 60 kV (instantaneous) be used for 4.76 kV circuit breakers as per IEEE C37.04, C37.06, and C37.09 in Bowen [18]. This reference also cites 95 kV BIL for 15 kV circuit breakers, and 125 kV BIL for 27 kV breakers.
- Relating to FCL testing, Marchionini, Fall and Steurer [19] quote a BIL of 95 kV for assets in the
- 17.5 kV class; and the same reference cites a BIL of 110 kV for 15 kV assets. The reference uses specifications from the "Zenergy power testing program" but there is no clear citation of an IEC or IEEE standard.

In private consultation with Adapa of EPRI [20], he states as follows:

"I have reviewed the information on the Solid State Fault Current Limiter (SSFCL) project. In fact, the line- to-line rms voltage for the SSFCL was 15.5 kV and the BIL level we used was 110 kV using IEEE Standard C37. If the SSFCL rating is 15 kV only, then the BIL is 95 kV which matches with your number from IEC standard." Adapa's reference is to the EPRI SSFCL project, and his reference to the IEC standard is to IEC 60071.

- It appears that most of the possible inconsistency in specification of BIL at the 15 kV

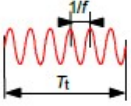
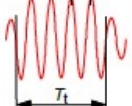
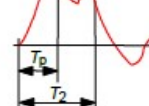
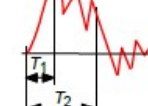
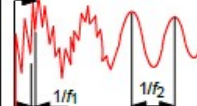
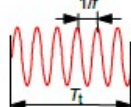
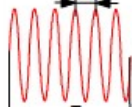
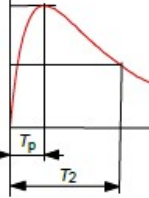
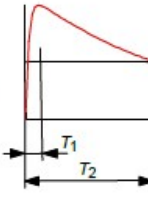
distribution class may be due to lack of care in specifying whether 15.5 kV is, in fact, in the 15 kV class. No judgement is made on this matter. Private conversations with researchers seems to indicate that there are other instances of inconsistencies exist between the IEC and IEEE standards.

2.3 Main observations drawn from the literature search

The following conclusions are drawn from the literature search reported above:

1. The IEC international standard 60071 deals with the impulse testing of low voltage VSC converters. Both voltage levels and the shape of impulses are specified in 60071.
2. However both voltage source (IGBT or GTO) and line commutated (thyristor) HVDC valves are subjected to 1.2/50 impulse tests. The test method is described in IEC 62501. These valves are directly subjected to lightning.
3. The consensus presented first by CIGRE and confirmed by ABB is that the converter and related network equipped with surge arresters must be simulated using advanced computer methods (EMTD or PSCAD).
4. The simulation based insulation coordination study will determine the type and amplitude of the impulses or switching surge that must be used for testing the electronic equipment, converters. Important that the tests should be performed converters equipped with protection surge arresters.

Table 2.1 Classes and shapes of overvoltages, standard voltage shapes, and standard withstand voltage tests, taken directly from IEC 60071

Class	Low frequency		Transient		
	Continuous	Temporary	Slow-front	Fast-front	Very-fast-front
Voltage or over-voltage shapes					
Range of voltage or over-voltage shapes	$f = 50 \text{ Hz or } 60 \text{ Hz}$ $T_t \geq 3 \text{ 600 s}$	$10 \text{ Hz} < f < 500 \text{ Hz}$ $0,02 \text{ s} \leq T_t \leq 3 \text{ 600 s}$	$20 \mu\text{s} < T_p \leq 5 \text{ 000 } \mu\text{s}$ $T_2 \leq 20 \text{ ms}$	$0,1 \mu\text{s} < T_1 \leq 20 \mu\text{s}$ $T_2 \leq 300 \mu\text{s}$	$T_f \leq 100 \text{ ns}$ $0,3 \text{ MHz} < f_1 < 100 \text{ MHz}$ $30 \text{ kHz} < f_2 < 300 \text{ kHz}$
Standard voltage shapes	 $f = 50 \text{ Hz or } 60 \text{ Hz}$ T_t^a	 $48 \text{ Hz} \leq f \leq 62 \text{ Hz}$ $T_t = 60 \text{ s}$	 $T_p = 250 \mu\text{s}$ $T_2 = 2 \text{ 500 } \mu\text{s}$	 $T_1 = 1,2 \mu\text{s}$ $T_2 = 50 \mu\text{s}$	a
Standard withstand voltage test	a	Short-duration power frequency test	Switching impulse test	Lightning impulse test	a

^a To be specified by the relevant apparatus committees.

The representative voltages and overvoltages may be characterized either by:

- an assumed maximum, or
- a set of peak values, or
- a complete statistical distribution of peak values.

NOTE In the last case additional characteristics of the overvoltage shapes may have to be considered.

Table 2.2 Standard insulation levels for range I ($1 \text{ kV} \leq V_m \leq 245 \text{ kV}$), taken directly from IEC 60071

Highest voltage for equipment (U_m) kV (r.m.s. value)	Standard rated short-duration power-frequency withstand voltage kV (r.m.s. value)	Standard rated lightning impulse withstand voltage kV (peak value)
3,6	10	20 40
7,2	20	40 60
12	28	60 75 95
17,5 ^a	38	75 95
24	50	95 125 145
36	70	145 170
52 ^a	95	250
72,5	140	325
100 ^b	(150)	(380)
	185	450
123	(185)	(450)
	230	550
145	(185)	(450)
	230	550
	275	650
170 ^a	(230)	(550)
	275	650
	325	750
245	(275)	(650)
	(325)	(750)
	360	850
	395	950
	460	1050
NOTE If values in brackets are considered insufficient to prove that the required phase-to-phase withstand voltages are met, additional phase-to-phase withstand voltage tests are needed.		
^a These U_m are non preferred values in IEC 60038 and thus no most frequently combinations standardized in apparatus standards are given.		
^b This U_m value is not mentioned in IEC 60038 but it has been introduced in range I in some apparatus standards.		

2.4 Methods for providing for BIL requirements in power distribution circuits with electronic devices

The main methods for providing for the BIL requirements in power electronic circuits in distribution systems are the following:

- Use of surge arresters
- Isolation of the circuits from sources of impulses
- Isolation of circuits from vulnerable components and from personnel. These are discussed in this section.

Placement of surge arresters in power electronic circuits connected directly to a high voltage circuit

Search of the literature has produced some results on the possibility of the use of a surge arrester for power electronic devices that are connected directly to a high voltage line. Conclusions and results of this investigation come mainly from the CIGRE T34 document and the salient conclusion is that surge arresters or MOV devices can be incorporated in devices such as a solid state transformer and a solid state fault interruption device.

Isolation methods

Isolation of circuits is a valid method for compliance with BIL and similar requirements. With regard to solid state switched components connected directly to the power distribution primaries, there are two salient issues: isolation afforded by an intermediate high frequency transformer and, secondly, isolation at semiconductor switching junctions. The latter are assumed to be not suitable for high voltage impulses, and therefore MOV and other measures must be taken to insure that the semiconductor junctions do not ‘see’ any high voltage impulses. Experience in the NSF supported center denominated as the Future Renewable Electric Energy Distribution Management (FREEDM) center indicates that it is very difficult to protect the semiconductor switches and therefore there is a serious safety issue. This remark comes from very preliminary testing of solid state transformers. Those preliminary tests showed that all first draft designs failed high voltage impulse tests. This does not imply that the problem is not solvable: at present testing is underway in the cited center to use MOVs to shunt impulse energy effectively to protect the semiconductor switches. The testing procedure and status of that work appears in [13]. In brief, laboratory facilities are presently being used to generate a 1.2 / 50 μ s 60 kV ‘impulse’ suitable for BIL compliance testing of solid state transformers and similar semiconductor switched components. It is believed that commercially available MOVs will allow compliance with the IEC standards – as predicted by PSCAD simulation testing. However, no conclusions are made on the safety of the MOV application.

Compliance of high frequency transformers via electrostatic isolation. At this point, it is believed that the combination of MOV protection and electrostatic screens between windings in high frequency transformers (e.g., as may appear in solid state transformers) may allow compliance with the IEC standards. No conclusion is made on the safety of these applications.

3. Metal Oxide Varistors and Similar Surge Suppressors

3.1 Surge suppression devices

In this section, a discussion is presented on the use of metal oxide varistors (MOVs) and other surge suppressors. The application area is in power distribution engineering. An MOV may be viewed as an anti-series connected pair of diodes which are designed to conduct and dissipate energy when the applied voltage exceeds a maximum peak voltage. The device ratings are generally:

- Maximum working voltage. This is the maximum steady-state, DC voltage. In this case, the value of the typical leakage current will be lesser than a specified value.
- Maximum clamping voltage which is obtained when a certain pulse current is applied to the component to obtain a maximum peak voltage.
- Surge current (maximum).
- Surge shift. This refers to the variation in voltage after a surge current is given.
- Energy absorption or energy discharge capability refers to the maximum energy that is dissipated for a certain waveform.
- Capacitance.
- Leakage current.
- Temporary overvoltage capability.
- Maximum continuous operating voltage (MCOV).
- Response time.
- Class.
- Operating duty cycle.
- Maximum AC RMS. This voltage refers to the maximum level of applied voltage as measured in RMS values that can be delivered to the MOV.
- Technology (SiC, gapless ZnO₂, and ‘with gap’ ZnO₂).

3.2 Ratings of MOVs and lightning arresters

Table 3.1 shows a summary of some commercially available MOVs and similar metal oxide lightning arresters. Table 3.2 shows a simple guide for the selection of arrester ratings in compliance with IEEE standards, and Table 3.3 is a similar table for IEC standards. Reference [10] gives a guide for lightning arrester specifications in the distribution primary voltages.

Table 3.1 Lightning arrester ratings for various types of technologies

<i>Type</i>	<i>Voltage ratings for commercially available units</i>	<i>Energy dissipation (maximum)</i>	<i>Comments and characteristics</i>
ZnO ₂ distribution secondary MOVs	440 – 1000 V	About 2.5 kJ	Designed and tested for secondary distribution
Polymer station arresters	3 to 144 kV readily available (RMS line-neutral voltage rating nominal, not the BIL)	Between 1.4 to 3.4 kJ / kV (the voltage is the MCOV)	Most units are available with the following maximum current ratings on breakdown for an 8 / 20 μ s impulse: 10 kA for 8.4 kV crest and 3 kV class unit; 16.7 kA for 6 kV crest; 27.8 kA for 10 kV rating.
Porcelain station arresters	3 to 144 kV readily available (RMS line-neutral voltage rating nominal, not the BIL)	4.9 kJ / kV (the voltage is the MCOV)	Most units are available with the following maximum current ratings on breakdown for an 8 / 20 μ s impulse: 10 kA for 8.4 kV crest and 3 kV class unit; 16.7 kA for 6 kV crest; 27.8 kA for 10 kV rating.

Table 3.2 Arrester selection for ANSI lightning arresters Table agrees with IEEE standards

Typical ANSI System Voltages				Suggested ANSI Arrester MCOV Rating			
Nom Line to Line Voltage	Max Line to Line Voltage	Max Line to Grnd Voltage		Solid Multi-grounded Systems (4 wire)	Uni-grounded Systems (3 wire)	Impedance grounded, Ungrounded and Delta Systems	Transmission Line Arresters for Lightning Protection Only
kV rms	kV rms	kV rms		MCOV	MCOV [*]	MCOV [*]	
2.40	2.52	1.46				2.55	
4.16	4.37	2.52		2.55	5.1	5.1	
4.80	5.04	2.91				5.1	
6.90	7.25	4.19				7.65	
8.32	8.74	5.05		5.1	7.65		
12.0	12.6	7.28		7.65	10.2		
12.5	13.1	7.57		7.65	12.7 [7.65]		
13.2	13.9	8.01		8.4	12.7 [8.4]		
13.8	14.5	8.38		8.4	12.7 [8.4]	15.3 [8.4]	15.3
20.8	21.8	12.6		12.7	15.3 [12.7]		21
22.9	24.0	13.9		15.3	19.5 [15.3]		22-24
23.0	24.2	14.0		15.3-17		24.4 [15.3]	22-24
24.9	26.2	15.1		15.3	22 [15.3]		24-29
27.6	29.0	16.8		17	24.4 [17]		24-29
34.5	36.2	20.9		22	29 [22]	36-39 [22]	29-36
46.0	48.3	27.9			29	39	29-39
69.0	72.5	41.9			42-48	53-67	48-67
115.0	121	69.8			70-76	84-98	76-98
138.0	145	83.8			84-98	106-115	98-115
161.0	169	98			98-115	115-131	115-131
230.0	242	140			140-152	182-190	152-190
345.0	362	209			209-245	230-289	245-289
500.0	525	303			318-452		>452
765.0	800	462			462-490		>490

[*] Cooper Power Systems Evolution Arrester Rating

Table 3.3 Arrester selection for IEC lightning arresters Table agrees with IEC standards

Typical IEC System Voltages			Suggested Uc for IEC Systems		
Nominal Line to Line Voltage	Typical Max Line to Line Voltage	Max Line to Grnd Voltage	Solidly Earthed Neutral at the Source Transformer	Impedance Earthed, Isolated and Delta Systems	Transmission Line Arresters for Lightning Protection Only
kV rms	kV rms	kV rms	Uc	Uc	
3.3	3.7	2.1	2.4	4.0	
6.6	7.3	4.2	4.8	7.2	
10.0	11.5	6.6	7.2	12	
11.0	12.0	6.9	9.6	12	12
16.4	18.0	10.4	12	18	18
22.0	24.0	13.9	16.8-24	24	24
33.0	36.3	21.0	24-36	36	36
47.0	52	30.1	33-43	53	43-53
66.0	72	41.6	43-58	72	58-72
91.0	100	57.8	66-77	102	77-102
110	123	71.1	77-86	125	86-125
132	145	83.8	96-115	145	115-145
155	170	98.3	110-125	170	125-170
220	245	142	154-188	245	188-245
275	300	173	182-192	300	192-300
330	362	209	221-230	360	230-360
400	420	243	269-288	420	288-420
500	550	318	420-440	550	440-550

3.3 Principal conclusions relating to MOVs and lightning arresters

Relating to the use and specification of MOVs and arresters, Fig. 3.1 is a guide. This configuration is the usual configuration for arrester specification, namely that the equipment insulation needs to be above the arrester characteristics. Typically, the BIL is located at about the one microsecond time interval and in the case of the FREEDM SST, at the 60 kV voltage level. In essence, the 1.0 μ s / 60 kV point is at the lowest possible point in Fig. 3.1. Fig. 3.2 shows the characteristics for a gapless MOV [12]. In Fig. 3.2, the steep front impulse characteristics are shown: this may be the main reason for not using lightning arresters to satisfy BIL requirements in the testing phase. That is, the test impulse voltages are too fast and too high a level to be accommodated by a lightning arrester. However, there is no apparent prohibition of the use of MOVs or lightning arresters to protect components (e.g., in parallel with semiconductor switches).

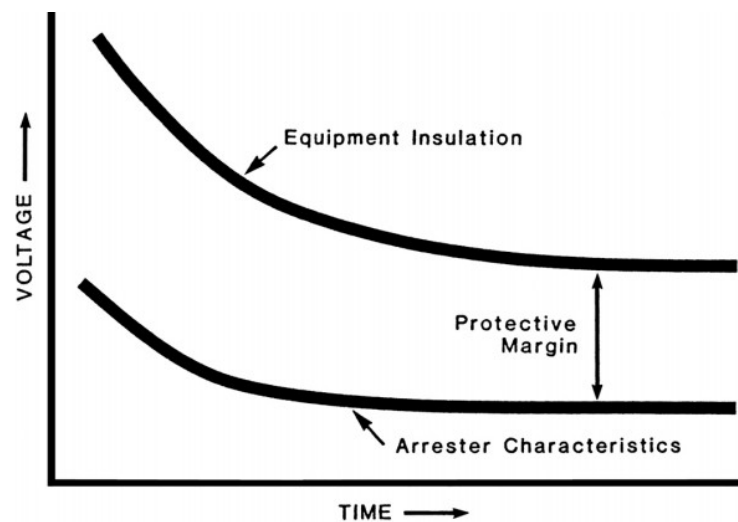


Fig. 3.1 Lightning arrester and equipment insulation withstand in the time – voltage plane

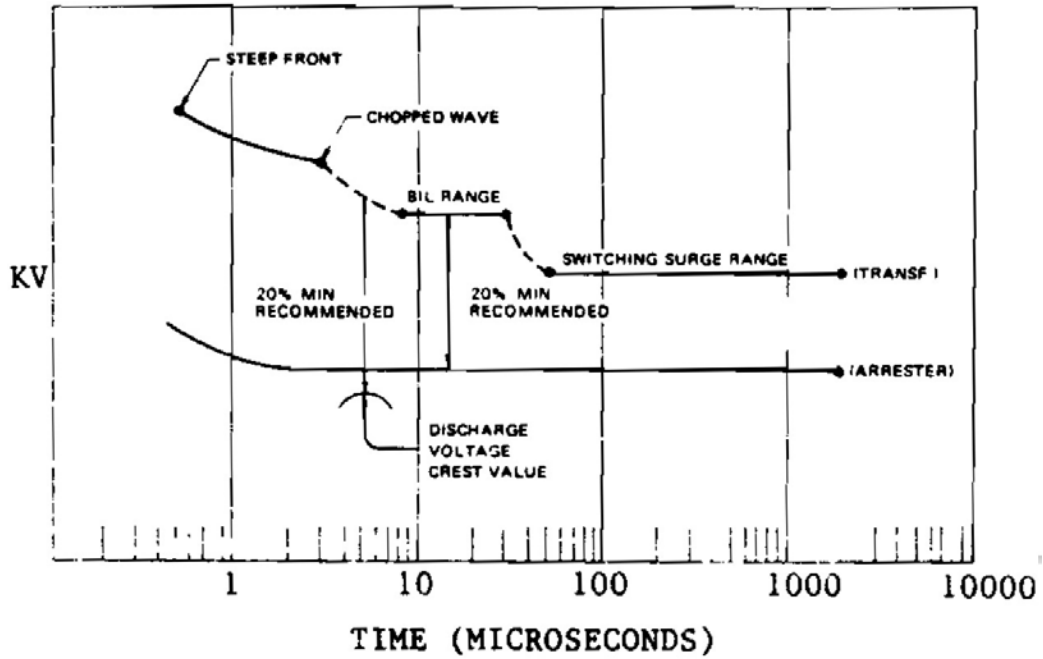


Fig. 3.2 Lightning arrester characteristics (lower curve) and equipment withstand voltage (upper curve) for gapless MOV applications (taken directly from [12]).

4. Safety Issues

4.1 Safety in distribution class applications

Safety may be the primary engineering factor in the application of MOV and other surge arresters in applications of power electronic device controlled devices that are directly connected to distribution primaries. Shock hazard and fire hazard are the main issues. In examining several representative applications in solid state transformers and machine drives operated directly from the distribution primaries, the following issues relating to safety are noted:

4.2 Reduction of peak voltage

The main function of MOV and other arresters is the reduction of peak voltage. The IEC standards require a 60 kV peak voltage limit for a 15 kV class distribution system. For this function, MOVs are effective. However, many MOVs do not have indicators that inform personnel that the device has operated (or that the device has failed). If the MOVs are placed 'downstream' from a fuse, the fuse may open when the MOV operates. It is assumed that the IEC standards are conservative, and if this is indeed the case, it may be deduced that peak voltages may not be a problem in semiconductor switched power devices in distribution systems. Further, the conservatism in the IEC peak voltage BIL levels are no different in the case of semiconductor controllers than in other passive devices. Nonetheless, it may be that it will be necessary to place a large number of these power electronic devices in service before making firm conclusions on the effectiveness of voltage clamping accessories.

4.3 Failure of the MOVs

As described in this chapter, the main safety enhancements come from the use of surge arresters. Most of these arresters have relatively high energy dissipation ratings (e.g., above 10 kJ). Simulations of 15 kV class applications indicate that MOV protective devices generally will be required to dissipate in the order of 3 kJ in a single lightning stroke instance. In many cases, if the arrester fails, the upstream fuse will open thus removing the device from service. Also, note that the MOVs as described in this chapter generally protect the semiconductor switches, and the failure of these switches usually do not present a safety hazard.

4.4 Speed of operation

The literature indicates that MOVs can operate in the microsecond range, and in some cases, the switching speed is so fast as to make measurement problematic. References [14] and [15] describe modern attempts to measure MOV switching speed. The results appear to be highly device dependent.

References

- [1] Tianning Xu, Colin C. Davidson, “Operational tests for the MMC-based VSC valves,” Proceedings of International Exhibition and Conference for Power Electronics, Intelligent Motion, Renewable Energy and Energy Management, 2014.
- [2] D. J. Hanson, M. L. Woodhouse, C. Horwill, M. M Osborn, “STATCOM: a new era of reactive compensation,” Power Engineering Journal, June 2002.
- [3] CIGRE, “T34 CIGRE Guidelines, for the application of metal oxide arresters without gaps for HVDC converter,” Paris, 2002.
- [4] CIGRE Working Group B4-51, “Study of Converter Transients Imposed on the HVDC converter transformers,” Paris, February 2015
- [5] International Electrotechnical Commission, “IEC 61954-1999 Power electronics for electrical transmission system testing of thyristor valves for static VAR compensator,” Geneva, Switzerland, 1999.
- [6] IEEE, “Standard 1303-1994 IEEE guide for static var compensator field tests,” Piscataway, NJ, 1994.
- [7] International Electrotechnical Commission, “IEC Standard 62501 2009. Voltage sourced converter (VSC) valves for high-voltage direct current (HVDC) power transmission - Electrical testing,” Geneva, Switzerland, 2009.
- [8] International Electrotechnical Commission, “IEC Standard IEC 60071-5. 2014 Insulation co- ordination Part 5 procedures for high voltage direct current (HVDC),” Geneva, Switzerland, 2014.
- [9] Wolfgang Hauschild, Eberhard Lemke, High-voltage measuring techniques, Berlin, Springer, 2014
- [10] Australian Rail Standard EP 21 00 00 01 SP “Insulation co-ordination and surge arrester selection,” Version 3.1, May 2013, NSW Rail Transport, Sydney, Australia.
- [11] International Electrotechnical Commission, “IS / IEC 60071-1 (2006): Insulation co-ordination, Part 1: definitions, principles and rules,” Geneva, Switzerland, 2006.
- [12] Cooper Power Systems, McGraw Edison Co., “Protective equipment update: metal oxide varistor technology,” Olean, NY, June 1987, No. 2.
- [13] G. T. Heydt, G. G. Karady, X. Rong, A. Q. Huang, M. Steurer, “The direct connection of electronic components to power distribution primaries,” Proc. North American Power Symposium, Morgantown, WV, September, 2017.
- [14] H. Shareef, S. Khalid, M. Mustafa, A. Mohamed, “Modeling and simulation of overvoltage surges in low voltage systems,” IEEE 2nd International Power and Energy Conference, 2008, pp. 357 – 361.
- [15] T. Ishida, T. Yumiba, Y. Kishimoto, K. Minakuchi, “Construction of lightning observing system and an example of its application,” 2001 Twenty-Third International Telecommunications Energy Conference INTELEC, 2001, pp. 469 – 473.
- [16] F. C. Lambert, “Presentation at the EPRI Superconductivity Conference,” Georgia Institute of Technology / NEETRAC, Atlanta, GA, September 21, 2007.
- [17] E. D. Johnson, “A silicon carbide based solid state fault current limiter for modern power distribution systems,” PhD. Thesis, University of Arkansas, Fayetteville, Arkansas, 2006
- [18] J. Bowen, “Medium voltage switchgear and circuit breaker ratings and applications,” undated, Aramco, Houston, Texas, available at:

- [19] <http://sites.ieee.org/houston/files/2016/01/7-MV-Switchgear-Mar-24-25.pdf>
- [20] B. Marchionini, N. K. Fall, M. Steurer, “An assessment of fault current limiter testing requirements,” United States Department of Energy, Office of Electricity Delivery and Energy Reliability, Washington, DC, February 2009.
- [21] R. Adapa, Electric Power Research Institute, private communication, Palo Alto, CA, March 6, 2018

Part III

Partially-Rated Solid-State Transformers Based on the Modular Multilevel Converter

Maryam Saeedifard
Qichen Yang, Graduate Student

Georgia Institute of Technology

For information about this project, contact:

Maryam Saeedifard
Georgia Institute of Technology
School of Electrical and Computer Engineering
Department Mail Code: 0250
777 Atlantic Dr NW
Atlanta, GA 30332
Phone: 404-894-4834
Email: maryam@ece.gatech.edu

Power Systems Engineering Research Center

The Power Systems Engineering Research Center (PSERC) is a multi-university Center conducting research on challenges facing the electric power industry and educating the next generation of power engineers. More information about PSERC can be found at the Center's website: <http://www.pserc.org>.

For additional information, contact:

Power Systems Engineering Research Center
Arizona State University
527 Engineering Research Center
Tempe, Arizona 85287-5706
Phone: 480-965-1643
Fax: 480-727-2052

Notice Concerning Copyright Material

PSERC members are given permission to copy without fee all or part of this publication for internal use if appropriate attribution is given to this document as the source material. This report is available for downloading from the PSERC website.

© 2018 Georgia Institute of Technology. All rights reserved

Table of Contents

1. Introduction.....	1
2. Functions of the AC-AC MMC-based PSST.....	3
3. The Proposed AC-AC MMC	4
3.1 Circuit Topology	4
3.2 Internal dynamics and current control of the proposed AC-AC MMC.....	4
3.3 Inter-subconverter energy adjustment strategy	5
3.4 Inner-subconverter energy balancing strategy.....	6
4. Application of the Proposed AC-AC MMC-based PSST in Scenario A.....	8
4.1 Power flow control strategy.....	8
4.2 Energy adjustment strategy for the s-subconverter	9
4.3 Compensation range of the output voltage	10
5. Application of the Proposed AC-AC MMC-based PSST in Scenario B	13
5.1 Control of the proposed PSST in Scenario B	13
5.2 Developed topology to absorb the zero-sequence component of the load currents	14
6. Simulation Results	16
6.1 Scenario A	16
6.2 Scenario B	17
Conclusion	20
References.....	21

List of Figures

Figure 1.1 Examples of the PSST used in the power system.	3
Figure 3.1 Circuit diagram of the proposed AC-AC MMC.....	4
Figure 4.1 Circuit diagram of the proposed MMC-based PSST in Scenario A.....	8
Figure 4.2 Phasor diagram of V_s and V_{pv} :	9
Figure 4.3 Output-side voltage compensation range of the PSST in Figure 4.1.	11
Figure 4.4 Control block diagrams of the proposed MMC-based PSST in Scenario A	12
Figure 5.1 Circuit diagram of the proposed MMC-based PSST in Scenario B.....	13
Figure 5.2 Phasor diagram of \tilde{V}_s^{pos} and of \tilde{V}_{pv}^{pos} based on Figure 5.1.	14
Figure 5.3 Control block diagrams of the proposed MMC-based PSST in Scenario B	14
Figure 5.4 Circuit diagram of the developed MMC-based PSST to absorb the zero-sequence component of the load currents in Scenario B.	15
Figure 6.1 Simulated waveforms of the proposed AC-AC MMC-based PSST (Figure 4.1) in Scenario A.....	17
Figure 6.2 Simulated waveforms of the proposed AC-AC MMC-based PSST (Figure 5.1) in Scenario B.....	19

List of Tables

Table 6.1 Parameters of the Study System for Scenario A (Figure 4.1).....	16
Table 6.2 Parameters of the Study System for Scenario B (Figure 5.1).....	18
Table 6.3 Magnitudes of the Current Components on the Load Side.....	18

1. Introduction

The increasing penetration rate of dynamic sources such as renewable energy resources together with the emergence of new dynamic loads such as electric vehicles, necessitate more flexible, efficient, and economical operation of the power grid. To maximize utilization of the power system infrastructure in an efficient and economical way, significant efforts have been made to actively control real and reactive power flows, compensate voltage sag/swell, and filter current harmonics based on power electronics. To this end, among the proposed power electronics-based solutions, solid-state transformer (SST) has become one of the emerging technologies [1], [2], [3]. However, the application/deployment of SST has been limited due to high cost and reliability issues. To combine the flexibility provided by the power electronics and reliability of the conventional magnetic transformer, an alternative method, i.e., partially-rated solid-state transformer (PSST), has emerged [4], in which a power electronics converter is integrated into the conventional magnetic transformer. Even if the power electronics part of the PSST fails, the conventional magnetic transformer is still able to transfer power, thereby preserving the reliability aspect. Furthermore, since the majority portion of power in a PSST is still transferred by the main magnetic part, the power electronics part does not need to be fully rated. The power electronics part of a PSST can be realized by a DC-AC or an AC-AC converter [5], [6]. Since the AC-AC converter, including the back-to-back connected AC-DC-AC converter, has two AC ports, it is capable of simultaneously adjusting the voltage and current of the grid. Therefore, an AC-AC converter-based PSST can provide most functionalities including power flow control, voltage sag/swell compensation, and current harmonics filtering.

In [5], various possible configurations of the PSST are discussed. An optimized design of a PSST is presented in [6], with an emphasis on differential mode filter design. The direct matrix converter and buck-boost matrix-reactance choppers are integrated for the PSST in [7] and [8]. A modular transformer converter-based power flow controller is proposed in [9]. In [10], the power electronics module is auto-connected to the secondary-side of the line frequency transformer to compensate the voltage sags and swells. Design considerations, evaluation criteria, and some candidate topologies are provided in [11].

Concomitantly, the modular multilevel converter (MMC) has become the most promising converter topology for medium- and high-power applications because of its high efficiency, scalability/modularity, redundancy, and excellent harmonic performance [12], [13], [14], [15], [16]. The direct AC-AC MMC topology, which has been derived based on the conventional MMC, inherits the salient features of the MMC to for AC-AC conversion. Nevertheless, one of the main challenges associated with the operation of the AC-AC MMC is the unbalanced DC power distribution among the submodule (SM) clusters when the input-side frequency is the same as the output-side frequency [17], [18]. This, particularly, hinders application of the AC-AC MMC in the context of the PSST where the input and output frequencies are the same. This paper aims at addressing this issue and enabling the application of the AC-AC MMC in the context of the PSSTs such that its salient features can be fully exploited.

In this report, MMC-based PSSTs along with their supporting control strategies are proposed and investigated for power flow control and active power filtering. The proposed PSSTs borrow the features of the MMC and combine them with new control strategies to enable the MMC-based

PSSTs. Simulation studies in the PSCAD/EMTDC software environment are carried out to validate the performance and effectiveness of the proposed MMC-based PSSTs and their supporting control methods.

2. Functions of the AC-AC MMC-based PSST

Figure 2.1 illustrates a simplified schematic of a power system along with its typical voltage ratings [19]. Since the MMC is targeted for use in medium-voltage (MV) and/or high-voltage (HV) applications, in this report, two potential application scenarios of the proposed AC-AC MMC-based PSST along with the corresponding functions are focused on.

- Scenario A: As illustrated in the red dashed blocks in Figure 2.1, the AC-AC MMC can be integrated into either the primary- or the secondary-side of the transformer to actively control the active and reactive power flows.
- Scenario B: As illustrated in the blue dotted blocks in Figure 2.1, the AC-AC MMC can be integrated into the MV side of a three-phase distribution transformer to compensate voltage sag/swell as well as unbalanced and/or distorted load current.

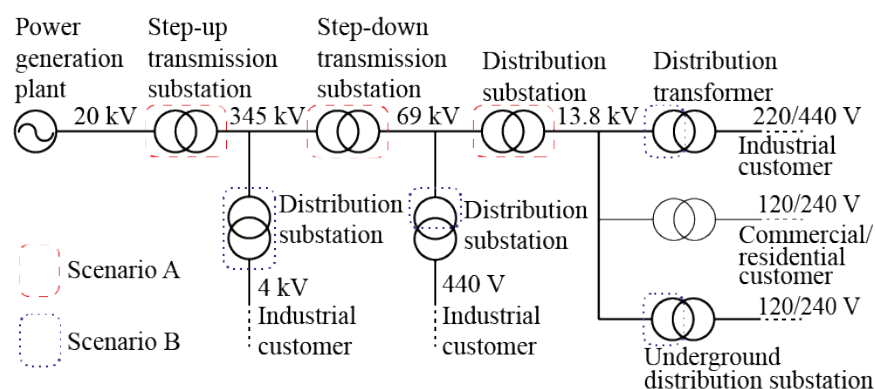


Figure 2.1 Examples of the PSST used in the power system.

3. The Proposed AC-AC MMC

3.1 Circuit Topology

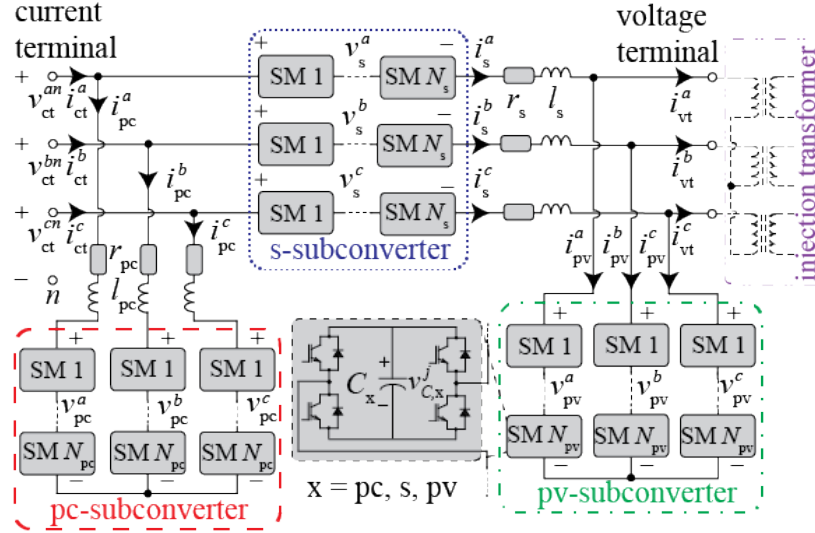


Figure 3.1 Circuit diagram of the proposed AC-AC MMC.

The circuit diagram of the proposed AC-AC MMC, i.e., the power electronics part of the PSST, is illustrated in Figure 3.1. The MMC consists of three subconverters, i.e., the parallel-voltage (pv-) subconverter, the series (s-) subconverter, and the parallel-current (pc-) subconverter, which are illustrated in the red dashed, blue dotted, and green dashed dotted blocks of Figure 3.1, respectively. Each subconverter consists of three SM clusters. The pc- and s-subconverters have series-connected inductors, while the pv-subconverter has no series-connected inductor. The terminal at the side of the pc-subconverter is termed current terminal (ct), which is connected in parallel with the conventional magnetic transformer to adjust the grid current. The virtual neutral point of the current terminal is illustrated by point “n” in Figure 3.1. The other terminal at the side of the pv-subconverter is termed voltage terminal (vt). The voltage terminal is connected in series with the main magnetic part of the PSST through an injection transformer. The injection transformer is illustrated in the purple dashed double-dotted block of Figure 3.1. Since the line-to-line primary-side voltage of the injection transformer is determined by v_{pv}^j , the secondary-side voltage of the injection transformer can be controlled to adjust the output voltage of the PSST.

3.2 Internal dynamics and current control of the proposed AC-AC MMC

Based on the averaged model, dynamics of i_{pc}^j and i_s^j in the AC-AC MMC can be summarized by

$$v_{ct}^{jn} - (v_{pc}^j - v_{pc}^z) = \left(r_{pc} + l_{pc} \frac{d}{dt} \right) i_{pc}^j, \quad (1a)$$

$$v_{ct}^{jn} + v_s^j - (v_{pv}^j - v_{pv}^z) = \left(r_s + l_s \frac{d}{dt} \right) i_s^j, \quad (1b)$$

where v_{ct}^{jn} is the voltage between phase j and the virtual neutral point “ n ” of the ct-terminal, v_x^j is the voltage across phase j cluster of x -subconverter ($x = pc, s, pv$), and v_{pc}^z is the zero-sequence component of v_x^j .

Based on (1a) and (1b), i_{pc}^j and i_s^j can be controlled by

$$v_{pc}^{j,\text{ref}} - v_{pc}^{z,\text{ref}} = -K_{p1}(i_{pc}^{j,\text{ref}} - i_{pc}^j) + v_{ct}^{jn}, \quad (2a)$$

$$v_s^{j,\text{ref}} = K_{p2}(i_s^{j,\text{ref}} - i_s^j) + (v_{pv}^{jn} - v_{pv}^{z,\text{ref}}) - v_{ct}^{jn}, \quad (2b)$$

where K_{p1} and K_{p2} are the gains of the proportional controllers, and the superscript “ref” denotes the references of the variables. In (2b), v_{pv}^{jn} is determined by the specific application scenarios. If $i_{pc}^{j,\text{ref}}$ and $i_s^{j,\text{ref}}$ only contains fundamental-frequency components (positive- and negative-sequence components), the proportional-integral (PI) controller can be applied to control i_{pc}^j and i_s^j [20]. In addition, since i_{vt}^j is determined by the load of the PSST, i_{pv}^j is regulated through controlling i_s^j .

3.3 Inter-subconverter energy adjustment strategy

To regulate the average SM capacitor voltages of the subconverters at their references, the power flows among the subconverters need to be controlled. The positive-sequence component of $i_{pc}^{j,\text{pos}}$ can be decomposed into the in-phase and quadrature components with respect to the phase angle of $v_{ct}^{j,\text{pos}}$. The in-phase component, i.e., $i_{pc}^{q,\text{pos}}$, is regulated to adjust $\bar{v}_{C,pc}$, based on:

$$i_{pc}^{q,\text{pos},\text{ref}} = \left(K_{p3} + \frac{K_{i3}}{s}\right)(V_{C,pc}^{\text{ref}} - \bar{v}_{C,pc}). \quad (3)$$

where K_{p3} is the proportional coefficient of the PI controller, K_{i3} is the integral coefficient of the PI controller, the superscript “pos” indicates the positive-sequence component, and $V_{C,pc}^{\text{ref}}$ is the reference of $\bar{v}_{C,pc}$. The quadrature component, i.e., $i_{pc}^{d,\text{pos}}$, is regulated to control i^d based on:

$$i_{pc}^{d,\text{pos},\text{ref}} = i_{ct}^{d,\text{ref}} - i_s^{d,\text{ref}}, \quad (4)$$

where i_{ct}^d can be used to control reactive power at the current terminal.

Similar to i_{pc}^j , the three-phase balanced set of i_s^j can be decomposed into the in-phase and quadrature components with respect to the phase angle of $v_{pv}^{j,\text{pos}}$. The in-phase component, i.e., $i_s^{q,\text{pos}}$, is regulated to adjust $\bar{v}_{C,pv}$, based on:

$$i_s^{q,\text{pos},\text{ref}} = \left(K_{p4} + \frac{K_{i4}}{s}\right)(V_{C,pv}^{\text{ref}} - \bar{v}_{C,pv}), \quad (5)$$

where K_{p4} is the proportional coefficient of the PI controller, K_{i4} is the integral coefficient of the PI controller, and $V_{C,pv}^{\text{ref}}$ is the reference of $\bar{v}_{C,pv}$.

The quadrature component, i.e., $i_s^{d,\text{pos}}$, is regulated to adjust $\bar{v}_{C,s}$ based on:

$$i_s^{d,\text{pos,ref}} = \text{sgn} \left(\cos \left(\phi_{v,pv}^{\text{pos}} - \phi_{v,s}^{\text{pos}} - \frac{\pi}{2} \right) \right) \left(K_{p5} + \frac{K_{i5}}{s} \right) (V_{C,s}^{\text{ref}} - \bar{v}_{C,s}), \quad (6)$$

where $\text{sgn}(\cdot)$ is the sign function, K_{p5} is the proportional coefficient of the PI controller, K_{i5} is the integral coefficient of the PI controller, $\phi_{v,pv}^{\text{pos}}$ is the initial phase angle of $v_{pv}^{j,\text{pos}}$, $\phi_{v,s}^{\text{pos}}$ is the initial phase angle of $v_s^{j,\text{pos}}$, and $V_{C,s}^{\text{ref}}$ is the reference of $\bar{v}_{C,s}$.

The validity condition of (6) is that the phase difference between $\phi_{v,pv}^{\text{pos}}$ and $\phi_{v,s}^{\text{pos}}$ should be between 45° and 135° . To obtain the safety margin, the phase difference between $\phi_{v,pv}^{\text{pos}}$ and $\phi_{v,s}^{\text{pos}}$ should be between γ_{\min} and $\pi - \gamma_{\min}$, where γ_{\min} must be between 45° and 90° . In addition, to decrease the reactive power in both the s- and pv-subconverters, $|\phi_{v,pv}^{\text{pos}} - \phi_{v,s}^{\text{pos}}|$ should be as close as possible to 90° .

3.4 Inner-subconverter energy balancing strategy

To main the SM capacitor voltages balanced within each subconverter, the dynamics of each subconverter are transferred to the $\alpha\beta$ -frame by using the $\alpha\beta$ -transformation:

$$\begin{bmatrix} f_x^\alpha \\ f_x^\beta \\ f_x^z \end{bmatrix} = \sqrt{\frac{2}{3}} \begin{bmatrix} 1 & -\frac{1}{2} & -\frac{1}{2} \\ 0 & \frac{\sqrt{3}}{2} & -\frac{\sqrt{3}}{2} \\ \frac{1}{\sqrt{2}} & \frac{1}{\sqrt{2}} & \frac{1}{\sqrt{2}} \end{bmatrix} \begin{bmatrix} f_x^a \\ f_x^b \\ f_x^c \end{bmatrix} \quad (7)$$

where the subscript “x” indicates pv, s, and pc and f_x^j denotes v_x^j , i_x^j , and $\bar{v}_{C,x}^j$. For the pv- and pc-subconverters, the zero-sequence component of v_x^j , i.e., v_z^j is used to maintain the energy of the three-phase clusters balanced within each subconverter, i.e.,

$$v_x^{z,\text{ref}} = -K_{p6} \left(\bar{v}_{C,x}^\alpha \cos(\theta_{i,x}^{\text{pos}}) + \bar{v}_{C,x}^\beta \sin(\theta_{i,x}^{\text{pos}}) \right), \quad (8)$$

where K_{p6} is the gain of the proportional controller and $\theta_{i,x}^{\text{pos}}$ is the phase angle of i_x^{pos} , i.e., $\omega t + \phi_{i,x}^{\text{pos}}$.

For the s-subconverter, the negative-sequence component of i_s^j is regulated to maintain energy of the three clusters balanced based on:

$$\begin{aligned} i_s^{\alpha,\text{neg,ref}} &= -K_{p7} \bar{v}_{C,s}^\alpha \cos(\theta_{v,s}^{\text{pos}}) + K_{p7} \bar{v}_{C,s}^\beta \sin(\theta_{v,s}^{\text{pos}}), \\ i_s^{\beta,\text{neg,ref}} &= K_{p7} \bar{v}_{C,s}^\alpha \sin(\theta_{v,s}^{\text{pos}}) + K_{p7} \bar{v}_{C,s}^\beta \cos(\theta_{v,s}^{\text{pos}}). \end{aligned} \quad (9)$$

where K_{p7} is the gain of the proportional controllers, the superscript “neg” indicates the negative-sequence component, and $\theta_{v,s}^{\text{pos}}$ is the phase angle of $v_s^{j,\text{pos}}$, i.e., $\omega t + \phi_{v,s}^{\text{pos}}$. To prevent the injected negative-sequence current components from flowing into the grid, $i_{\text{pc}}^{\alpha,\text{neg,ref}}$ and $i_{\text{pc}}^{\beta,\text{neg,ref}}$ should be added to $i_{\text{pc}}^{j,\text{ref}}$.

4. Application of the Proposed AC-AC MMC-based PSST in Scenario A

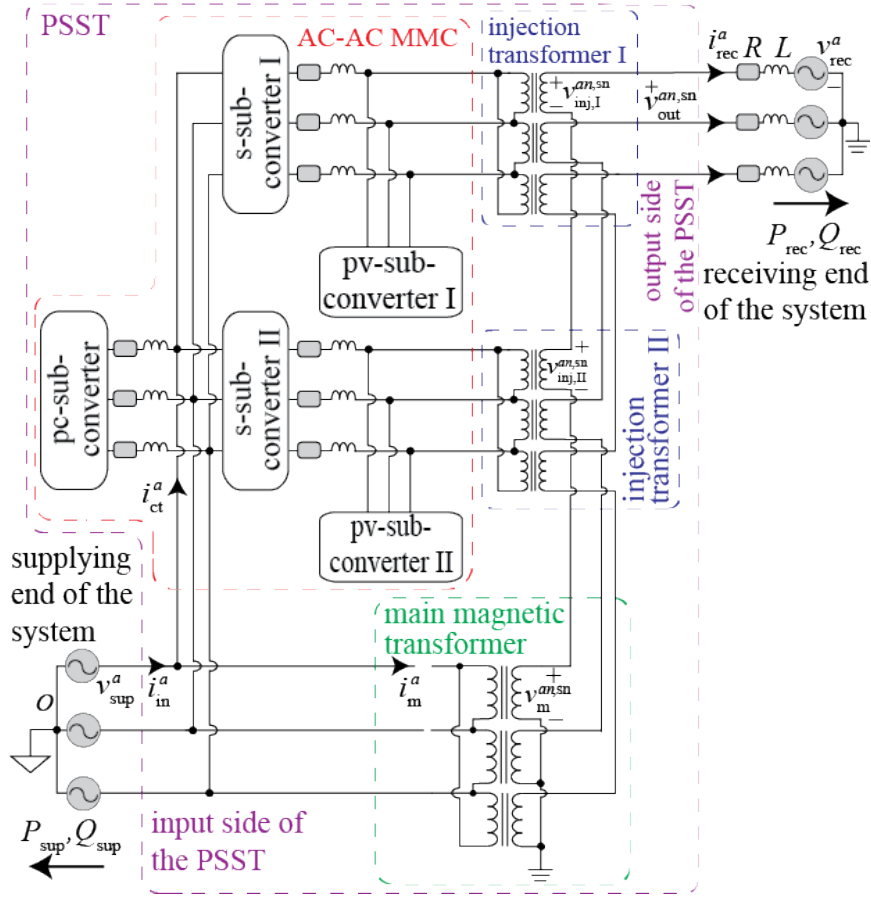


Figure 4.1 Circuit diagram of the proposed MMC-based PSST in Scenario A.

Figure 4.1 illustrates the proposed MMC-based PSST in Scenario A, where the PSST should be able to adjust real and reactive power flows. The AC-AC MMC in Figure 4.1 is developed based on the AC-AC MMC in Figure 3.1, where another pair of s- and pv-subconverters is added. As illustrated in Figure 4.1, the two pairs of the s- and pv-subconverters are connected in parallel at the common current terminal and in series through two injection transformers. The two series-connected injection transformers are connected in series with the secondary side of the main magnetic transformer to constitute the output side of the PSST. The output side of the PSST is connected to the receiving end of the system through series connected inductor and resistor. The current terminal of the AC-AC MMC and the primary side of the conventional magnetic transformer are connected in parallel to form the input side of the PSST. The input side of the PSST is directly connected to the supplying end of the system.

4.1 Power flow control

To adjust the receiving-end real and reactive powers, v_{pv}^j is controlled to regulate the receiving-end currents. Based on Figure 4.1, the references of the secondary-side voltage of the injection transformers are generated by

$$\begin{aligned}
v_{\text{inj,I}}^{q,\text{sn,ref}} + v_{\text{inj,II}}^{q,\text{sn,ref}} &= \left(K_{\text{p8}} + \frac{K_{\text{i8}}}{s} \right) (i_{\text{rec}}^{q,\text{ref}} - i_{\text{rec}}^q) - \omega L i_{\text{rec}}^d - v_{\text{m}}^{q,\text{sn}}, \\
v_{\text{inj,I}}^{d,\text{sn,ref}} + v_{\text{inj,II}}^{d,\text{sn,ref}} &= \left(K_{\text{p8}} + \frac{K_{\text{i8}}}{s} \right) (i_{\text{rec}}^{d,\text{ref}} - i_{\text{rec}}^d) + \omega L i_{\text{rec}}^q - v_{\text{m}}^{d,\text{sn}},
\end{aligned} \tag{10}$$

where the superscript “sn” indicates secondary-side of the transformers, $v_{\text{pv,I}}^{\xi,\text{sn,ref}}$ and $v_{\text{pv,II}}^{\xi,\text{sn,ref}}$ are the references of the ξ -axis components of the three-phase secondary-side voltages of injection transformer I and II ($\xi = q, d$), $v_{\text{m}}^{\xi,\text{sn}}$ is the ξ -axis component of the three-phase secondary-side voltages of the main magnetic transformer, K_{p8} is the proportional coefficient of the PI controllers, K_{i8} is the integral coefficient of the PI controllers, and v_{rec}^{ξ} is the ξ -axis current component of the receiving end. For the supplying end, i_{ct}^d of the AC-AC MMC is controlled to adjust the reactive power based on

$$i_{\text{ct}}^{d,\text{ref}} = -\frac{Q_{\text{sup}}^{\text{ref}}}{V_{\text{sup}}^q} - i_{\text{m}}^d, \tag{11}$$

where $i_{\text{ct}}^{d,\text{ref}}$ is the reference of the d -axis current of the current terminal of the MMC, the subscript “sup” indicates the supplying side, $Q_{\text{sup}}^{\text{ref}}$ is the reference of the reactive power of the supplying end, V_{sup}^q is the q -axis voltage component of the supplying end, and i_{m}^d is the d -axis component of the three-phase primary-side current of the main magnetic transformer.

4.2 Energy adjustment strategy for the s-subconverter

As presented in Section 3.3, the validity condition for (6) is that the phase angle difference between $\varphi_{v,\text{pv}}^{\text{pos}}$ and $\varphi_{v,s}^{\text{pos}}$ should be between γ_{min} and $\pi - \gamma_{\text{min}}$. However, if the AC-AC MMC has only one pair of s- and pv-subconverters, as illustrated in Figure 3.1, both $\varphi_{v,\text{pv}}^{\text{pos}}$ and $\varphi_{v,s}^{\text{pos}}$ are determined by the references of the receiving-end real and reactive powers. Therefore, the validity condition may not be satisfied under certain conditions, e.g., the condition in Figure 4.2(a). To solve the problem, as illustrated in Figure 4.1, two pairs of s- and pv-subconverters are integrated. For the condition in Figure 4.2(a), the phasor diagram can be modified into (b). Therefore, the validity condition can be guaranteed in each pair of s- and pv-subconverters.

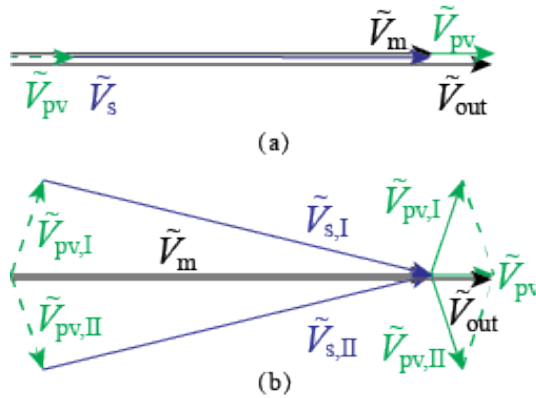


Figure 4.2 Phasor diagram of \tilde{V}_s and \tilde{V}_{pv} : (a) an example of invalid energy adjustment strategy for the s-subconverter, (b) solution to the problem shown in Figure 4.2(a).

4.3 Compensation range of the output voltage

To simplify expressions, in Section 4.3, the ratio and configuration of the main magnetic transformer is assumed to be the same as those of the injection transformers. Based on Figure 4.1 and the s-subconverter energy adjustment strategy in Section 4.2, the output-side voltage compensation range of the PSST is illustrated by the shaded and striped areas in Figure 4.3. In Figure 4.3, the critical angles are

$$\begin{aligned}\delta_1 &= \arcsin(y_1 \sin(\gamma_{\min})), \\ \delta_2 &= \pi - \arcsin(y_2 \sin(\gamma_{\min})),\end{aligned}\tag{12}$$

where

$$\begin{aligned}y_1 &= -\cos(\gamma_{\min})\eta + \sqrt{1 - \sin^2(\gamma_{\min})\eta^2}, \\ y_2 &= \cos(\gamma_{\min})\eta + \sqrt{1 - \sin^2(\gamma_{\min})\eta^2},\end{aligned}\tag{13}$$

and η is the ratio of the maximum $|v_{pv}^{j,pos}|$ to $|v_m^{jn,pm}|$. Based on Figure 4.3, the compensation range contains two sectors, i.e., shaded area X in Figure 4.3, and two rhombuses, i.e., striped area Y in Figure 4.3. The radius of the sectors is twice the maximum $|v_{pv}^{j,pos}|$ while the side length of the rhombuses is the maximum $|v_{pv}^{j,pos}|$. If the phasor reference of the sum of the two pv-subconverters, i.e., $\tilde{V}_{pv}^{\text{ref}}$ is in the shaded area X, each pair of s- and pv-subconverters can individually achieve a valid energy adjustment strategy. Therefore, $\tilde{V}_{pv}^{\text{ref}}$ can be distributed into the two pv-subconverters evenly, i.e.,

$$\tilde{V}_{pv,I}^{\text{ref}} = \tilde{V}_{pv,II}^{\text{ref}} = \frac{1}{2} \tilde{V}_{pv}^{\text{ref}}.\tag{14}$$

If $\tilde{V}_{pv}^{\text{ref}}$ is in the striped area Y, based on the parallelogram law, $\tilde{V}_{pv}^{\text{ref}}$ needs to be formed by $\tilde{V}_{pv,I}^{\text{ref}}$ and $\tilde{V}_{pv,II}^{\text{ref}}$. The minimum distance from the neutral to the boundary of the shaded area, i.e., $|\tilde{V}_{pv,\min}|$ in Figure 4.3, is

$$|\tilde{V}_{pv,\min}| = \sin(2\delta_2 - \pi)\eta|\tilde{V}_m|.\tag{15}$$

The overall control strategy for the PSST in Scenario A is summarized in (c)

Figure 4.4.

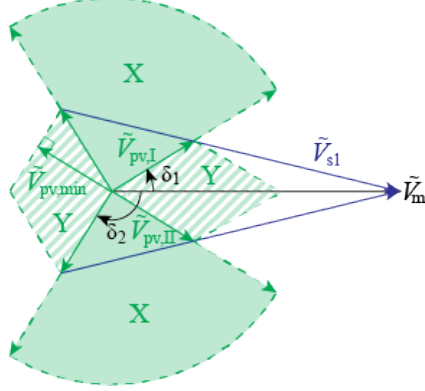
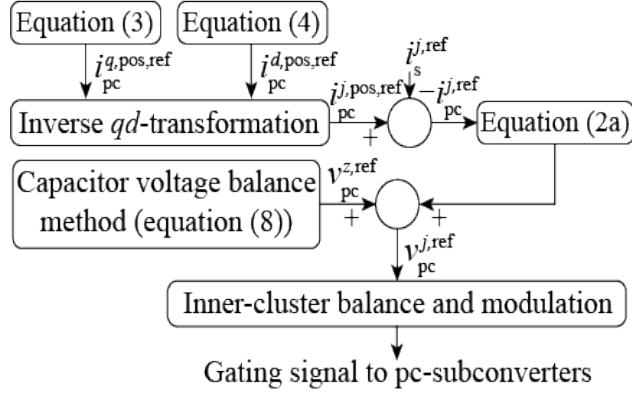
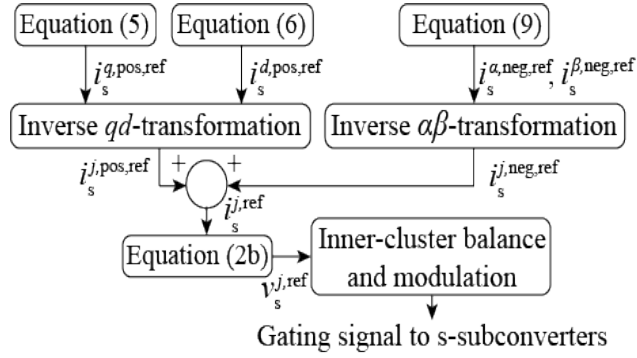


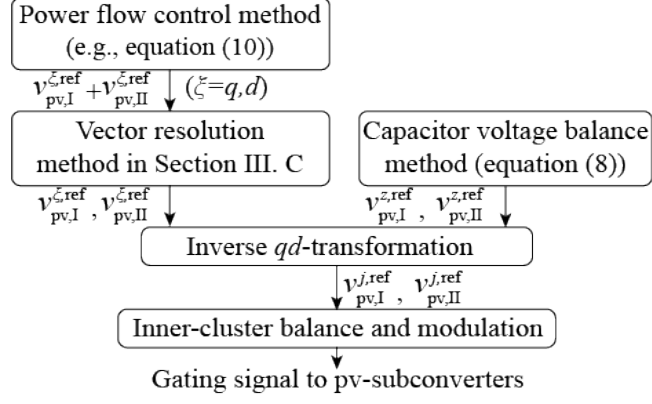
Figure 4.3 Output-side voltage compensation range of the PSST in Figure 4.1.



(a)



(b)



(c)

Figure 4.4 Control block diagrams of the proposed MMC-based PSST in Scenario A (Figure 4.1): (a) control of the pc-subconverter, (b) control of the s-subconverters, and (c) control of the pv-subconverters.

5. Application of the Proposed AC-AC MMC-based PSST in Scenario B

5.1 Control of the proposed PSST in Scenario B

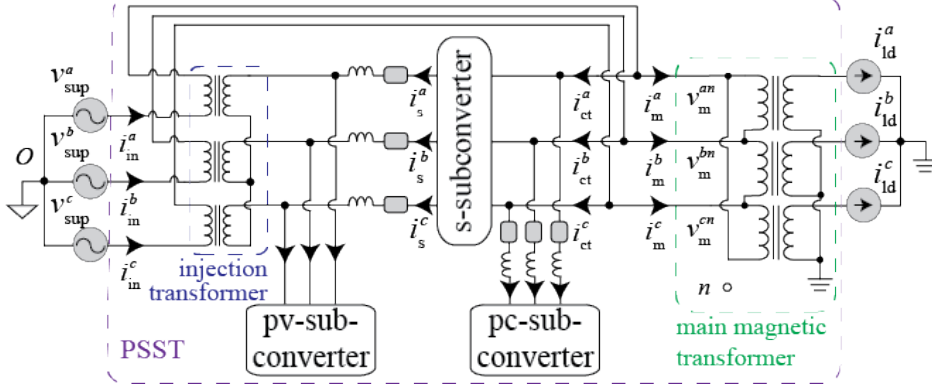


Figure 5.1 Circuit diagram of the proposed MMC-based PSST in Scenario B.

In the application of distribution transformer (Scenario B), the primary function of the MMC-based PSST is to compensate the supply-side voltage sag/swell and to absorb unbalanced components and/or harmonics of the load currents. Figure 5.1 illustrates the configuration of the proposed MMC-based PSST in this scenario. Based on Figure 5.1, the zero-sequence component of the supply voltage cannot pass the conventional Δ/Y_g main magnetic transformer. Meanwhile, the zero-sequence component of the load current cannot flow through the main magnetic transformer. Based on Figure 5.1, to compensate the undesired non-zero-sequence components, $v_{vt}^{j,ref}$ and $i_{pc}^{j,ref}$ are generated by

$$v_{vt}^{jn,ref} = v_m^{jn,ref} - v_{sup}^j, \quad (16a)$$

$$i_{pc}^{j,ref} = i_{in}^{j,ref} - i_m^{j,pm} - i_s^{j,ref} + i_{pc,vC}^{j,ref}, \quad (16b)$$

where the superscript “pm” indicates the primary-side of the transformers, $i_{pc,vC}^{j,ref}$ is generated by (3) to adjust the energy of the pc-subconverter.

The current control strategies for the i_s^j and i_{pc}^j and the inner-subconverter energy balancing strategy in Scenario B are exactly the same as those in Scenario A. In addition, the inter-subconverter energy adjustment strategy for the pc- and pv-subconverters in Scenario B is identical with those in Scenario B while the inter-subconverter energy adjustment strategy for the s-subconverter in Scenario B is different from that in Scenario A. In Scenario A, the phase angle of $v_{pv,I}^j + v_{pv,II}^j$ depends on the real and reactive power references. However, in Scenario B, since the load is not sensitive to the phase angle of the output voltage of the distribution transformer, the phase angle of $v_{pv}^{j,pos}$ can be fixed. The fixed $\phi_{v,pv}^{pos}$ can guarantee that the difference between $\phi_{v,pv}^{pos}$ and $\phi_{v,s}^{pos}$ is between 45° and 135° .

If the magnitude of $v_{pv}^{j,pos}$ is 20% of the magnitude of $v_m^{jn,ref}$, the phase angle of $v_{pv}^{j,pos}$ can be set as -95.74° to maintain the magnitude of the output voltage unchanged. The phasor diagram is illustrated in Figure 5.2. Under such conditions, the difference between $\phi_{v,pv}^{pos}$ and $\phi_{v,s}^{pos}$ is fixed at 84.26° . Subsequent to obtaining proper $\phi_{v,pv}^{pos}$ and $\phi_{v,s}^{pos}$, the following control strategy for the s-subconverter in Scenario B is the same as that in Scenario A, which is illustrated in Fig. 6(b). The control strategies for the pv- and pc-subconverter in Scenario B are summarized in Figure 5.3.

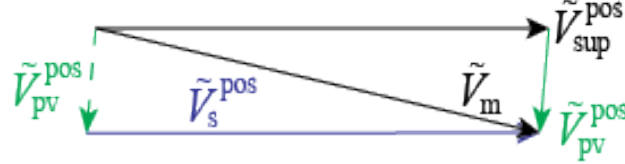


Figure 5.2 Phasor diagram of \tilde{V}_s^{pos} and \tilde{V}_{pv}^{pos} based on Figure 5.1.

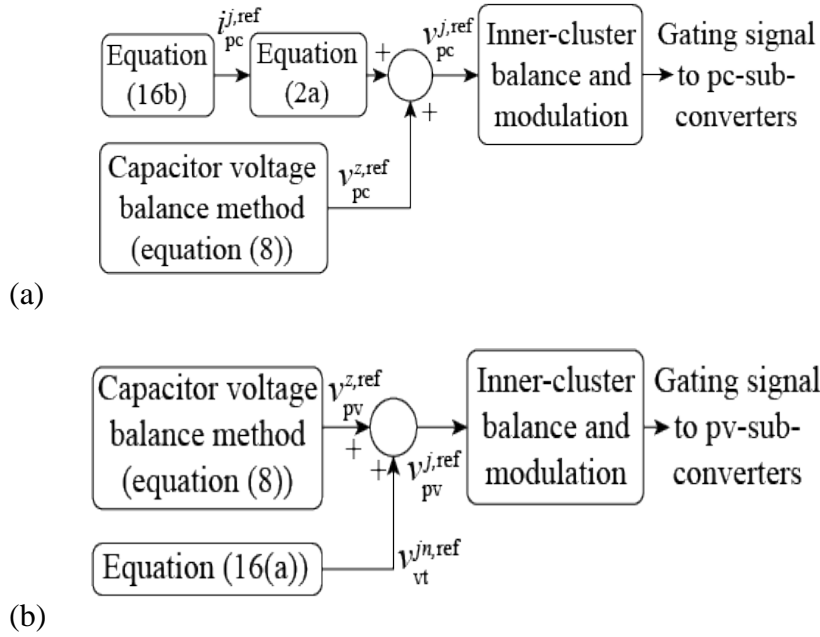


Figure 5.3 Control block diagrams of the proposed MMC-based PSST in Scenario B (Figure 5.1): (a) control of the pc-subconverter, (b) control of the pv-subconverter.

5.2 Developed topology to absorb the zero-sequence component of the load currents

Although the zero-sequence component of the load current in Figure 5.1 is trapped by the primary-side Δ winding, it is still undesired from the main transformer perspective. Figure 5.4 presents a modified version of Figure 5.1, where a parallel-zero (pz-) subconverter is added. The pz-subconverter is able to absorb the zero-sequence fundamental-frequency component and low-frequency harmonics at the secondary side of the main transformer. The neutral point of the pz-subconverter is grounded and i_{pz}^j is generated by

$$i_{pz}^{j,\text{ref}} = -(i_{ld,\text{fund}}^z + i_{ld,\text{har}}^j), \quad (17)$$

where $i_{ld,\text{fund}}^z$ is the zero-sequence component of the fundamental frequency component of the load current and $i_{ld,\text{har}}^j$ is the harmonics of the load current of phase j .

The positive-sequence component of i_{pz}^j is regulated to adjust the average capacitor voltage of the pz-subconverter based on

$$i_{pz}^{q,\text{ref}} = \left(K_{p9} + \frac{K_{i9}}{s}\right) (V_{C,pz}^{\text{ref}} - \bar{v}_{C,pz}), \quad (18)$$

where K_{p9} is the proportional coefficient of the PI controller, K_{i9} is the integral coefficient of the PI controller, and $V_{C,pz}^{\text{ref}}$ is the reference of $\bar{v}_{C,pz}$.

If needed, $i_{pz}^{d,\text{ref}}$ can be used to adjust the reactive power of the load side together with $i_{pc}^{d,\text{ref}}$. The negative-sequence component of i_{pz}^j is regulated to maintain energy among different clusters balanced based on:

$$\begin{aligned} i_{pz}^{\alpha,\text{neg},\text{ref}} &= -K_{p10} \bar{v}_{C,pz}^\alpha \cos(\theta_{v,\text{in}}) + K_{p10} \bar{v}_{C,pz}^\beta \sin(\theta_{v,\text{in}}), \\ i_{pz}^{\beta,\text{neg},\text{ref}} &= K_{p10} \bar{v}_{C,pz}^\alpha \sin(\theta_{v,\text{in}}) + K_{p10} \bar{v}_{C,pz}^\beta \cos(\theta_{v,\text{in}}), \end{aligned} \quad (19)$$

where K_{p10} is the proportional coefficient of the PI controllers, K_{i10} is the integral coefficient of the PI controllers, and $\theta_{v,\text{in}}^{\text{pos}}$ is the phase angle of v_{in}^j .

The negative-sequence component is provided by the pc-subconverter, which prevents the injected negative-sequence component from flowing into the grid. For the low-voltage applications, only one SM is needed in each cluster of the pz-subconverter.

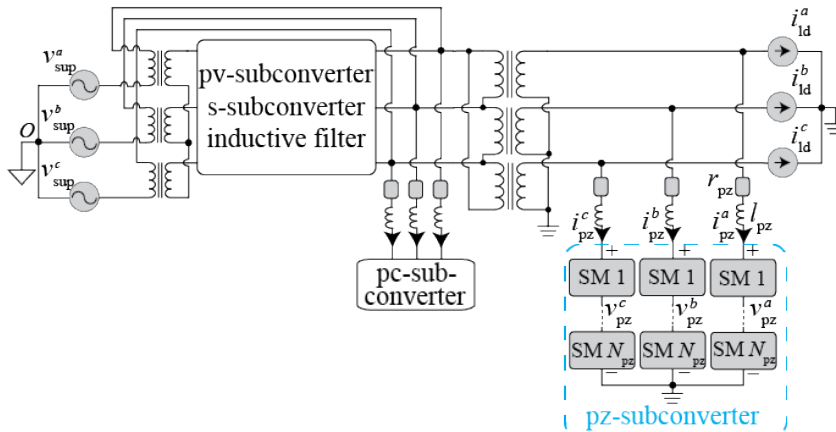


Figure 5.4 Circuit diagram of the developed MMC-based PSST to absorb the zero-sequence component of the load currents in Scenario B.

6. Simulation Results

6.1 Scenario A

To demonstrate the performance and effectiveness of the proposed control strategies in Scenario A, the proposed MMC-based PSST illustrated in Figure 4.1, is simulated in the PSCAD/EMTDC software environment. Parameters of the study system are listed in Table 6.1. The setpoint of the receiving-end real power is ramped down from 40 MW to 10 MW. The setpoints of the reactive powers of the receiving and supplying ends are 10 MVar and 30 MVar, respectively.

Table 6.1 Parameters of the Study System for Scenario A (Figure 4.1)

main transformer	Value	pv-subconverter	Value
capacity	50 MVA	N_{pv}	4
primary-winding voltage	34.5 kV	C_{pv}	10000 μ F
secondary-winding voltage	6.9 kV	s-subconverter	Value
leakage reactance	0.03 pu	N_s	12
basic operation frequency	60 Hz	C_s	1000 μ F
injection transformer (1-ph)	Value	l_s	2.5 mH
capacity	1.7 MVA	r_s	0.5 m Ω
primary-winding voltage	2.0 kV	pc-subconverter	Value
secondary-winding voltage	400 V	N_{pc}	12
leakage reactance	0.03 pu	C_{pc}	3000 μ F
basic operation frequency	60 Hz	l_{pc}	5.0 mH
receive end	Value	r_{pc}	1.0 m Ω
V_{rcv}	6.9 kV	supply end	Value
L	2.5 mH	V_{sup}	34.5 kV
R	1.2 m Ω		

As illustrated in Figure 6.1(a), the transferred real power is well-regulated to follow its reference. Figure 6.1(b) illustrates reactive powers of the supplying and receiving ends, which are controlled at their references. Figure 6.1(c) shows the secondary-side voltage of the magnetic transformer, the sum of the secondary-side voltages of the two injection transformers, and the output voltage of the MMC-based PSST. As illustrated in Figure 6.1(c), the output voltage of the PSST is actively adjusted by controlling the AC-AC MMC. Figure 6.1(d) shows the primary-side current of the magnetic transformer, the current-terminal current of the MMC, and the input current of the PSST. As illustrated, the input current of the PSST is actively regulated by controlling the AC-AC MMC. Figure 6.1(e)-(g) illustrate the average SM capacitor voltages of the pv-, s-, and pc-subconverters, respectively. As shown, all the SM capacitor voltages are maintained balanced during the real power ramping process.

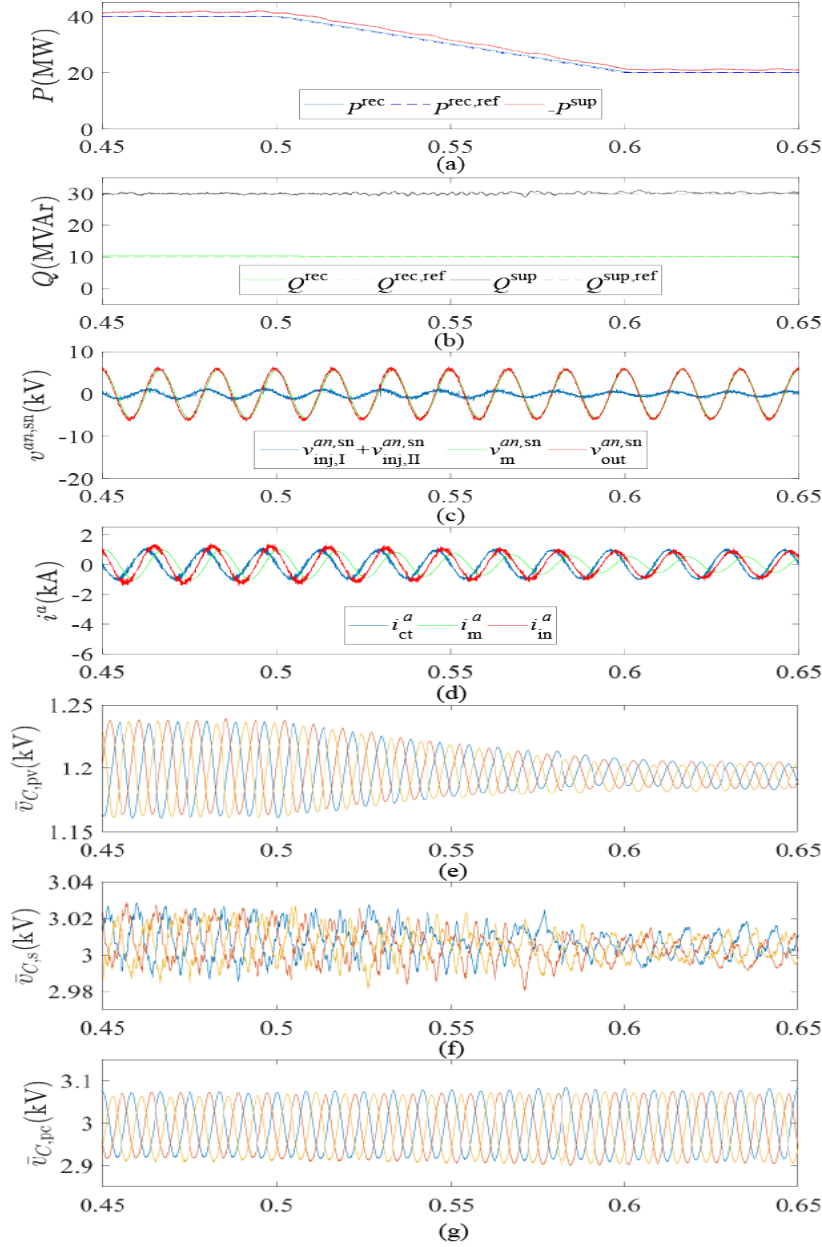


Figure 6.1 Simulated waveforms of the proposed AC-AC MMC-based PSST (Figure 4.1) in Scenario A: (a) supplying- and receiving-end real powers, (b) supplying- and receiving-end reactive powers, (c) output-side voltages of the proposed PSST (phase a), (d) input-side currents of the proposed PSST (phase a), (e) average SM capacitor voltages of phases a , b , and c in the pv-subconverter, (f) average SM capacitor voltages of phases a , b , and c in the s-subconverter, and (g) average SM capacitor voltages of phases a , b , and c in the pc-subconverter.

6.2 Scenario B

To demonstrate the performance and effectiveness of the proposed control strategies in Scenario B, the proposed MMC-based PSST illustrated in Figure 5.1, is simulated in the PSCAD/EMTDC software environment. Parameters of the study system are listed in Table 6.2. As illustrated in

Figure 6.2(a), 20% voltage sag and swell are imposed on phases a and c of the supply voltages from $t = 0.67$ s to $t = 0.73$ s, respectively. The load currents contain negative-sequence fundamental-frequency and the fifth- and seventh-order harmonic components. The RMS values of the components are provided in

Table 6.3.

Table 6.2 Parameters of the Study System for Scenario B (Figure 5.1)

main transformer	Value	pv-subconverter	Value
capacity	5 MVA	N_{pv}	3
primary-winding voltage	13.8 kV	C_{pv}	3000 μ F
secondary-winding voltage	440 V	s-subconverter	Value
leakage reactance	0.03 pu	N_s	6
basic operation frequency	60 Hz	C_s	3000 μ F
injection transformer (1-ph)	Value	l_s	10 mH
capacity	700 kVA	r_s	2 m Ω
primary-winding voltage	3 kV	pc-subconverter	Value
secondary-winding voltage	3 kV	N_{pc}	6
leakage reactance	0.03 pu	C_{pc}	1000 μ F
basic operation frequency	60 Hz	l_{pc}	12 mH
supply end	Value	r_{pc}	2.4 m Ω
nominal voltage	13.8 kV		

Table 6.3 Magnitudes of the Current Components on the Load Side

Component	Value
fundamental (positive sequence)	5 kA
fundamental (negative sequence)	0.5 kA
fifth-order harmonic (negative sequence)	1.25 kA
Seventh-order harmonic (positive sequence)	1.0 kA

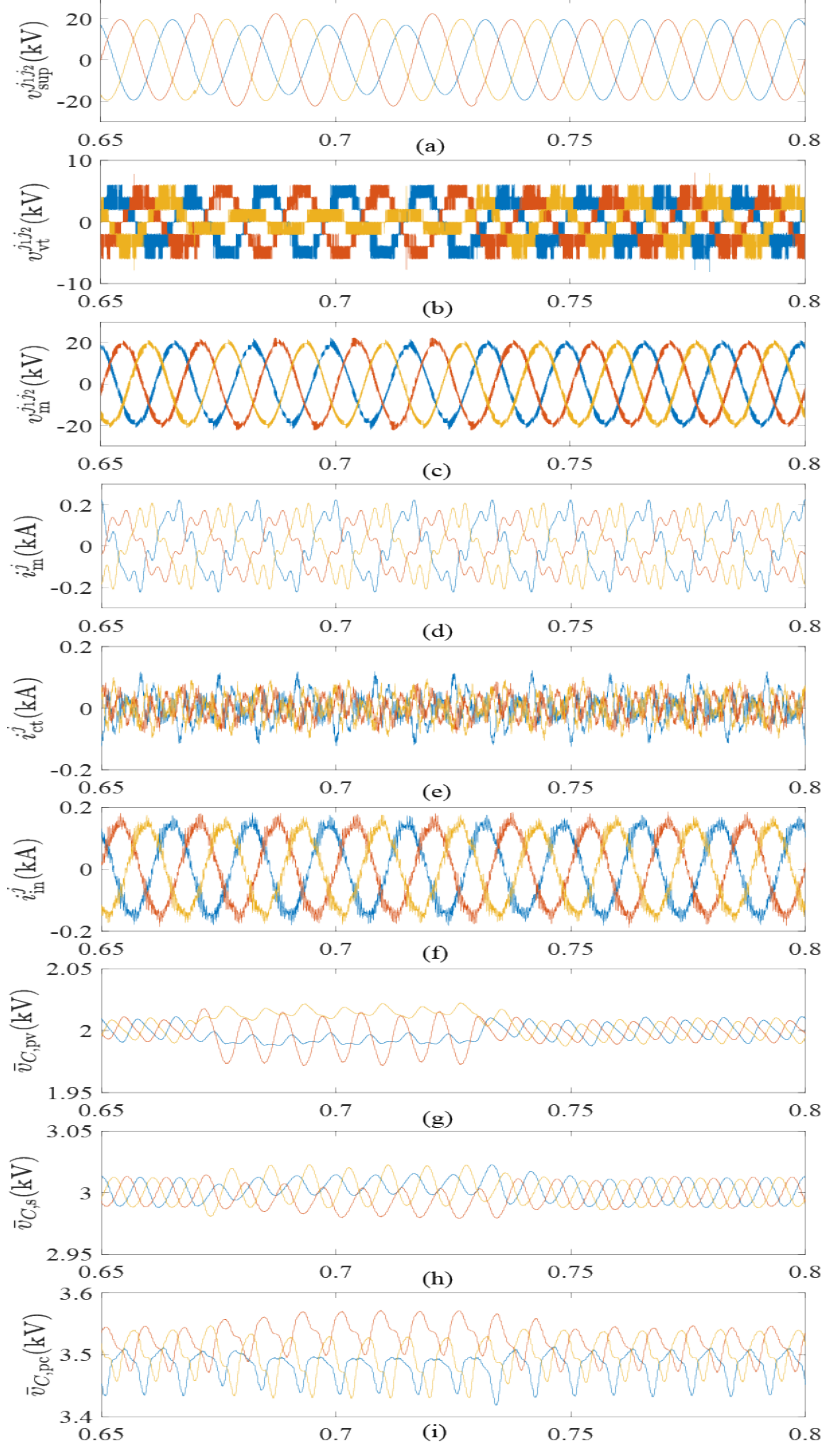


Figure 6.2 Simulated waveforms of the proposed AC-AC MMC-based PSST (Figure 5.1) in Scenario B: (a) line-to-line supply-end voltages of the system, (b) line-to-line voltage-terminal voltages of the AC-AC MMC, (c) line-to-line primary-side voltages of the main magnetic transformer, (d) three-phase primary-side currents of the main magnetic transformer, (e) three-phase current-terminal currents of the AC-AC MMC, (f) three-phase supply-side currents of the system, and (g-i) average SM capacitor voltages of the pv-, s-, and pc-subconverters.

Conclusion

In this report, new PSST configurations based on the AC-AC MMC along with their supporting control strategies are proposed, which borrow the features of the MMC and introduce them into the PSSTs. The PSSTs is capable of controlling power flow, compensating voltage sag/swell, filtering the current harmonics, and removing unbalanced current components in the grid. Simulation studies in the PSCAD/EMTDC software environment are carried out to validate the performance and effectiveness of the proposed MMC-based PSSTs and the supporting control methods for different applications.

References

- [1] E. R. Ronan, S. D. Sudhoff, S. F. Glover, and D. L. Galloway, "A power electronic-based distribution transformer," *IEEE Trans. Power Del.*, vol. 17, no. 2, pp. 537–543, Apr 2002.
- [2] T. Zhao, G. Wang, S. Bhattacharya, and A. Q. Huang, "Voltage and power balance control for a cascaded h-bridge converter-based solid-state transformer," *IEEE Trans. Power Electron.*, vol. 28, no. 4, pp. 1523–1532, April 2013.
- [3] J. E. Huber and J. W. Kolar, "Applicability of solid-state transformers in todays and future distribution grids," *IEEE Trans. Smart Grid*, pp. 1–1, 2017.
- [4] E. C. Aeloiza, P. N. Enjeti, L. A. Moran, and I. Pitel, "Next generation distribution transformer: to address power quality for critical loads," in *Proc. IEEE PESC*, vol. 3, June 2003, pp. 1266–1271.
- [5] S. Bala, D. Das, E. Aeloiza, A. Maitra, and S. Rajagopalan, "Hybrid distribution transformer: Concept development and field demonstration," in *Proc. IEEE ECCE*, Sept 2012, pp. 4061–4068.
- [6] J. Burkard and J. Biela, "Evaluation of topologies and optimal design of a hybrid distribution transformer," in *Proc. IEEE EPE*, Sept 2015, pp. 1–10.
- [7] J. Kaniewski, Z. Fedyczak, and G. Benysek, "Ac voltage sag/swell compensator based on three-phase hybrid transformer with buck-boost matrix-reactance chopper," *IEEE Trans. Ind. Electron.*, vol. 61, no. 8, pp. 3835–3846, Aug 2014.
- [8] P. Szczeniak and J. Kaniewski, "Hybrid transformer with matrix converter," *IEEE Trans. Power Del.*, vol. 31, no. 3, pp. 1388–1396, June 2016.
- [9] N. Yousefpour, B. Parkhideh, A. Azidehak, S. Bhattacharya, and B. Fardanesh, "Modular transformer converter-based convertible static transmission controller for transmission grid management," *IEEE Trans. Power Electron.*, vol. 29, no. 12, pp. 6293–6306, Dec 2014.
- [10] T. Kang, S. Choi, A. S. Morsy, and P. N. Enjeti, "Series voltage regulator for a distribution transformer to compensate voltage sag/swell," *IEEE Trans. Industrial Electron.*, vol. 64, no. 6, pp. 4501–4510, June 2017.
- [11] J. Sastry and S. Bala, "Considerations for the design of power electronic modules for hybrid distribution transformers," in *Proc. IEEE ECCE*, Sept 2013, pp. 1422–1428.
- [12] S. Debnath, J. Qin, B. Bahrani, M. Saeedifard, and P. Barbosa, "Operation, control, and applications of the modular multilevel converter: A review," *IEEE Trans. Power Electron.*, vol. 30, no. 1, pp. 37–53, Jan 2015.
- [13] M. A. Perez, S. Bernet, J. Rodriguez, S. Kouro, and R. Lizana, "Circuit topologies, modeling, control schemes, and applications of modular multilevel converters," *IEEE Trans. Power Electron.*, vol. 30, no. 1, pp. 4–17, Jan 2015.
- [14] S. Allebrod, R. Hamerski, and R. Marquardt, "New transformerless, scalable modular multilevel converters for HVDC-transmission," in *Proc. IEEE PESC*, pp. 174–179, June 2008.
- [15] J. Dorn, H. Huang, and D. Retzmann, "A new multilevel voltage-sourced converter topology for HVDC applications," in *Cigre Session*, pp. B4–304, 2008.
- [16] G. Kish, M. Ranjram, and P. Lehn, "A modular multilevel DC/DC converter with fault blocking capability for HVDC interconnects," *IEEE Trans. Power Electron.*, vol. 30, no. 1, pp. 148–162, Jan 2015.
- [17] A. Korn, M. Winkelkemper, P. Steimer, and J. Kolar, "Direct modular multi-level converter for gearless low-speed drives," in *Proc. IEEE EPE*, pp. 1–7, Aug 2011.

- [18] W. Kawamura, Y. Chiba, M. Hagiwara, and H. Akagi, "Experimental verification of TSBC-based electrical drives when the motor frequency is passing through, or equal to, the supply frequency," in *Proc. IEEE ECCE*, pp. 5490–5497, Sept 2015.
- [19] "United states electricity industry primer," *Office of Electricity Delivery and Energy Reliability, U.S. Department of Energy, Tech. Rep.*, 2015.
- [20] A. Yazdani and R. Iravani, "A unified dynamic model and control for the voltage-sourced converter under unbalanced grid conditions," *IEEE Trans. Power Del.*, vol. 21, no. 3, pp. 1620–1629, July 2006.